Evaluating the Performance of Activated Carbon, Polymeric, and Zeolite Adsorbents for Volatile Organic Compounds Control

by

Biniyam Tefera Amdebrhan

A thesis submitted in partial fulfillment of the requirements for the degree of

Master of Science

in

Environmental Engineering

Department of Civil and Environmental Engineering

University of Alberta

ABSTRACT

Activated carbon, zeolites, and polymeric adsorbents are commonly used adsorbents to remove Volatile organic compounds (VOCs) from industrial gas streams. To better understand of adsorbents performance for the removal of VOCs, adsorption capacity, cumulative heel and the influence of water vapor on VOCs uptake were investigated. For this purpose, five-cycle adsorption/desorption tests were completed for a single VOC, 1,2,4-Trimethylbenzene (TMB) and a mixture of VOCs (OAC-SST) using a fixed-bed of Optipore V503, BAC, ZEOcat Z700, ZEOcat F603, and ZEOcat Z400. To assess the effect of humidity on the performance of aforementioned adsorbents during the adsorption of TMB, adsorption experiments were conducted at 0% and 75% relative humidity (RH). The effect of water vapor on the adsorption of polar and non-polar VOCs on ZEOcat Z700 and ZEOcat F603 were measured, and the adsorption experiments were completed for TMB (non-polar) and 2-butoxyethanol (polar) adsorbate, at 0%, 45% and 75% RH. TMB adsorption capacities on Optipore V503 and BAC were 51% and 48%, respectively. Adsorption of OAC-SST on the same adsorbents show adsorption capacities of 45% and 43%, respectively. In case of zeolite, the adsorption capacities of ZEOcat Z700, ZEOcat F603, and Z400 were 16.4%, 10.2% and 2.1% for TMB and 16%, 14%, and 10% for OAC-SST, respectively, demonstrating a lower adsorption performance of zeolites compared to Optipore V503 and BAC. Moreover, cumulative heel buildup with Optipore V503 was noticeably lower compared to the other adsorbents used in this study although V503 was regenerated at 200ºC while BAC and zeolites were regenerated at 288ºC. A maximum of 3% impact of RH on TMB adsorption on BAC and Optipore V503 can be observed at 75% RH due to water vapor's low affinity towards BAC and Optipore V503. However, there were 31% and

51% decrease in TMB adsorption on ZEOcat Z700 and ZEOcat F603, respectively at 75% RH. Moreover, the adsorption capacity of 2-butoxyethanol on ZEO F603 decreased by 7.5% and 18.0% at 45% RH and 75% RH, respectively. However, the adsorption capacity of 2-butoxyethanol on ZEOcat Z700 decreased by 15.6% and 20.8% at 45 % RH and 75% RH, respectively. The results of this study are helpful for understanding the adsorption performance of adsorbents and their capacities for VOC uptake under different humidity conditions.

DEDICATION

I dedicate this dissertation to my beloved parents, Tefera and Eskedar, my dearest wife, Mekdes, and my adorable daughters, Rediet and Mariyamawit. They have been a constant source of support, motivation, and determination for me throughout my life.

ACKNOWLEDGMENT

TABLE OF CONTENTS

LIST OF TABLES

LIST OF FIGURES

LIST OF ACRONYMS

TMB	1,2,4-Trimethylbenzene
AC	Activated carbon
BAC	Beaded activated carbon
BET	Brunauer-Emmett-Teller
DAC	Data acquisition and control
DTG	Derivative thermo-gravimetric
EPA	Environmental protection agency
FID	Flame ionization detector
HPA	Hypercrosslinked polymer
LP	Lead-time percentage
MFC	Mass flow controller
MTZ	Mass transfer zone
PSD	Pore size distribution
QSDFT	Quenched solid density functional theory
RH	Relative humidity
SCCM	Standard cubic centimeter per minute
SLPM	Standard liter per minute
TGA	Thermo-gravimetric analysis
TPR	Throughput ratio
TSA	Temperature swing adsorption
VOCs	Volatile organic compounds

1. CHAPTER ONE: INTRODUCTION

1.1. Introduction

1.1.1. Volatile organic compound

The United States Environmental Protection Agency defines volatile organic compounds (VOCs) as "any compounds of carbon, excluding carbon monoxide, carbon dioxide, carbonic acid, metallic carbides or carbonates, and ammonium carbonate, which participates in atmospheric photochemical reactions" (US EPA, 2017). Similarly, Environment and Climate Change Canada describes VOCs as "organic compounds containing one or more carbon atoms that have high vapor pressures and evaporate readily to the atmosphere". This definition focuses only on the 50 to 150 most abundant compounds containing two to twelve carbon atoms and excludes the photochemically non-reactive compounds such as methane, ethane and the chlorofluorocarbons (Environment and Climate Change Canada, 2016).

1.1.2. VOCs emission from automotive painting

VOCs are emitted by the chemical process industries and the use of chemical cleaners, paint, varnishes, solvents, lubricants, and liquid fuels (Khan & Ghoshal, 2000; Kolade et al., 2009; Monneyron et al., 2003; Nevskaia et al., 2003). In the automotive industry, painting operations consume large amounts of organic solvents in both solvent-based and water-borne coating processes (Kamravaei et al., 2017). Paint booths, in the auto manufacturing sectors, are a major source of VOCs emission during the painting of automotive parts for decoration, weatherproofing, and corrosion resistance (Chang & Lee, 2002). The contribution of these painting operations can be as high as 85% of the total emitted VOCs from automotive industries (Kim et al., 2000)., about 6.58 kg of VOCs is emitted per vehicle in a typical automotive painting

operation in North America from the use of paint solvents (Kim, 2011). Therefore, compliance with their environmental responsibilities, primarily in terms of VOC emissions, is the paramount operational consideration for commercial paint shops (Anand & Howarth, 2013; Chang & Lee, 2002). The emitted VOCs consist of aromatic and aliphatic hydrocarbons, esters, ketones, alcohols, and glycol ethers (Kim, 2011). VOCs are classified into hydrophobic and hydrophilic categories according to their Henry's law constant. The hydrophobic group consists of aromatic hydrocarbons (e.g. toluene, xylenes, ethyl-benzene, 1,2,4-trimethylbenzene, and naphthalene), aliphatic hydrocarbons (e.g. n-heptane and naphtha), and other hydrocarbon mixtures (e.g. mineral spirits). Whereas, the hydrophilic group consists of ketones (acetone, methyl ethyl ketone, methyl isobutyl ketone, methyl amyl ketone, di-isobutyl ketone etc.), esters (ethyl acetate, n-butyl acetate, ethyl propionate, isobutyl isobutyrate etc.), alcohols (methanol, ethanol, propanol, butanol etc.), and glycol ethers (such as butyl cellosolve acetate and butyl carbitol) (Kim et al., 2000).

1.1.3. Health and environmental impacts

VOCs are challenging pollutants in gaseous and aqueous streams (wastewater) due to their health and environmental hazards (Monneyron et al., 2003). VOCs are toxic and can cause various health impacts including but not limited to headache, irritations of eyes, nose, and throat, nausea, dizziness, memory impairment, and damage to liver, nervous system and lungs (Environment and Climate Change, 2016; Kampa & Castanas, 2008). Some of the VOCs are also suspected to have carcinogenic effects (Lodewyckx, 2014; Parisellia et al., 2009).

VOCs also get converted to other hazardous compounds such as ground-level ozone. Ground-level ozone is the primary component of smog and is formed by the photochemical reaction of VOCs and oxides of nitrogen (NOx) (Environment and Climate Change, 2016; Kim,

2011). Additionally, oxidized organic compounds are also produced during the reaction of VOCs with ozone in the presence of sunlight. The oxidized organic compounds get mixed with other compounds, leading to photochemical smog and formation of small particles in the air (Atkinson, 2000; Lodewyckx, 2014; Sullivan et al., 2004).

Because of their health and environmental hazards, government and intergovernmental organizations worldwide have set standards and regulations to reduce the emission of VOCs and to limit their exposure (Khan & Ghoshal, 2000). The concerns about VOCs health and environmental impacts triggered many treatment techniques for controlling their emissions.

1.1.4. VOCs abatement techniques

Selection of the most effective technique for VOC abatement depends on several parameters such as pollutant type, source, concentration, flow rate, presence of compounds other than VOCs, reusability of captured compounds, other operational and ambient conditions, regulation limits, safety, location, cost, and operative possibility (Cooper & Alley, 2002; Parmar & Rao, 2009). In general, treatment techniques are classified as destructive and recovery methods (Khan & Ghoshal, 2000; Parmar & Rao, 2009). Parmar and Rao (20009) illustrated different destruction and recovery techniques for VOCs abatement (Figure 1). Destructive techniques are often used when the recovery of the removed compounds is neither necessary nor economical. As the name suggests, destruction techniques lead to the knocking down of VOCs into other non-hazardous chemical compounds such as CO_2 and H_2O. The most commonly employed destruction techniques are biofiltration and oxidative treatment techniques such as chemical treatment, photocatalysis, and thermal and catalytic oxidation (Berenjian et al., 2012). Contrarily, in recovery methods, pollutants are removed from effluents to preserve their nature and properties and allow their reuse. The commonly used recovery methods are absorption,

adsorption, condensation, and membrane separation for gaseous and liquid streams (Khan & Ghoshal, 2000; Parmar & Rao, 2009). The suitability of each treatment technique differs on the basis of their advantages and disadvantages under different physical conditions. The following section describes various treatment techniques used for removal of VOCs.
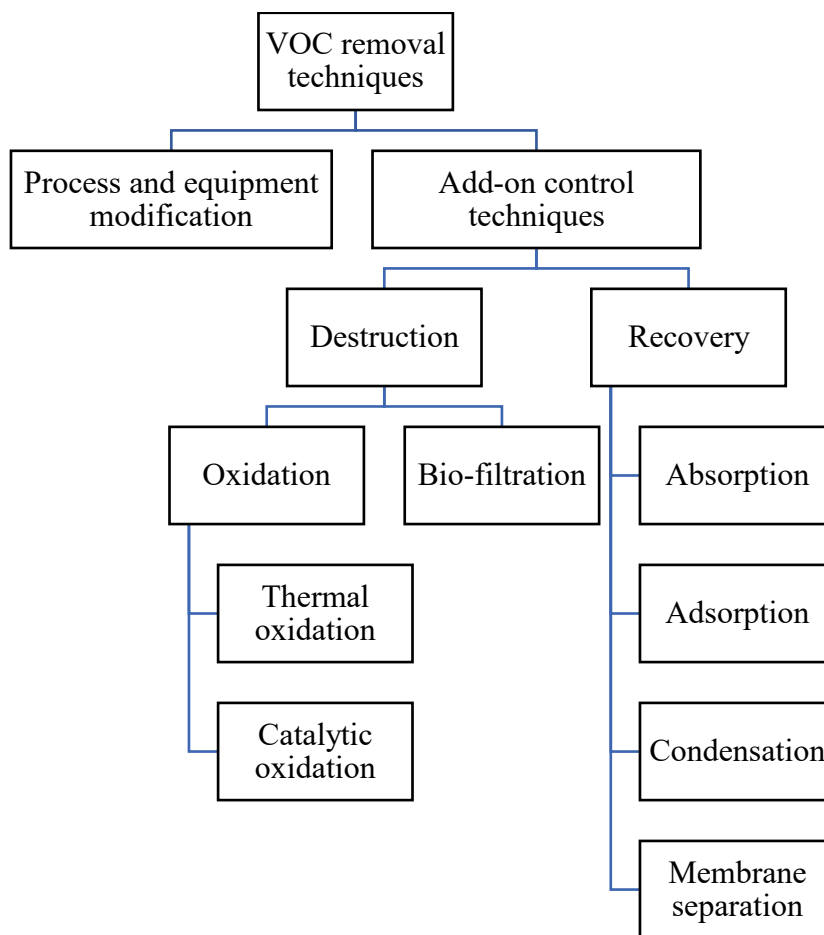
Figure 1.1: Classification of VOCs treatment techniques. " Adapted from Khan & Ghoshal, 2000".

In the destruction methods, oxidation could be thermal or catalytic. **Thermal oxidation** is considered to be suitable for streams with a high concentration of VOCs and facilitates high energy recovery from the exhaust heat (Kim, 2011). Its application is restricted, as the outlet

stream usually needs to be treated before releasing to the atmosphere, due to the production of few noxious products (Khan & Ghoshal, 2000). **Catalytic oxidation** is used when the catalyst is compatible with the pollutant-laden stream to prevent catalyst poisoning (Khan & Ghoshal, 2000). **Biofiltration** is used for low VOC concentration streams although sluggishness, inability to tolerate high and fluctuating concentrations of pollutants, sensitivity to operating conditions, and selective destruction limit its commercial application (Khan & Ghoshal, 2000; Kim et al., 2000) cannot tolerate high and fluctuating concentrations of pollutants (Hashisho et al., 2008). In recovery methods, **condensation** may be a feasible treatment for streams with high VOCs' concentration and low boiling point (Khan & Ghoshal, 2000). However, due to its low efficiency for removal of the pollutants (Khan & Ghoshal, 2000), it is not an economical method for low VOC concentration streams (Mohan et al., 2009). **Absorption** process can be used for removal of a wide range of VOCs from gas streams. Moreover, its process is simple with good recovery efficiency. However, it has limited application due to the requirement of post-treatments (distillation or extraction) to remove pollutants from the liquid phase, high initial investment, and design difficulties (Khan & Ghoshal, 2000). **Adsorption** is one of the promising techniques for the removal VOCs from gaseous streams with a potential to recover valuable vapors (Long et al., 2009). Adsorption is low cost, has high removal efficiency, and can be used for high/low concentration feed streams even for unsteady input concentration, and contaminants with a wide range of boiling point (Huang et al., 2002; Parmar & Rao, 2009).

1.1.5. Adsorption process

Adsorption can be defined as the interaction between the field of forces of the solid surface and fluid phase (Lodewyckx, 2014). The resultant forces from the field of forces attract and retains molecules, atoms, or ions of a fluid on the solid surface. Adsorption of gases and

vapors by microporous solids has attracted much attention because of its practical importance in the fields of gas separation, gas purification, and environmental problems (Khan & Ghoshal, 2000). Physisorption and chemisorption are the two types of adsorption (Gregg & Sing, 1982). This classification is based on adsorbates and adsorbent interactions during adsorption. Physisorption is a result of dipole moments, polarization forces, dispersive forces, or short-range repulsive interactions whereas, chemisorption involves specific forces, such as those that are operative in the formation of chemical bonds (Yahia et al., 2013).

1.1.6. Activated carbon, polymeric and zeolites

Adsorption onto activated carbon (AC) is commonly used for removal of VOCs (Long, 2012; Parmar & Rao, 2009). Large surface area, high porosity, and sustainability are some of the properties which make AC preferable in adsorption (Parmar & Rao, 2009; Albero et al., 2009). ACs is available in many different forms such as fibers, beads, powders, monoliths, and granules (Nevskaia et al., 2003). Although ACs are commonly used adsorbents, they have some limitations such as regeneration difficulties for high boiling solvents (> 150°C), hygroscopicity, possibility of polymerization or oxidation of some solvents, and risk of fire (Blocki, 1993; Parmar & Rao, 2009; Albero et al., 2009). These limitations encourage developing new adsorbent materials to separate and recover VOCs from industrial gas streams (Liu et al., 2009).

Recently, polymeric adsorbents have attracted interests as an alternative to the ACs for removal of organic pollutants from waste streams because of their controllable pore structure, stable physical-chemical properties, and, more importantly, easier regeneration (Choung et al., 2001; Long et al., 2009; Tsyurupa & Davankov, 2006). Particularly, a hypercrosslinked polymer which is produced by crosslinking polymers of microporous resin has gained increasing interest because of its narrow pore size distribution (PSD) (Baya et al., 2000), ability to control pore

structure, and the ability to vary internal surface area by varying the polymerization conditions (Choung et al., 2001).

Zeolite is a rock composed of aluminum, silicon, and oxygen that is found naturally or can be synthesized (Blocki, 1993). It has a crystal structure with fixed pore size, described as windows, cages, and supercages (Parmar & Rao, 2009). Zeolites are sometimes called molecular sieves because their fixed pore size excludes larger molecules and hence can selectively adsorb the target molecules (Blocki, 1993). Research has been focused on developing zeolites for VOC separation by targeting efficient material with high adsorption capacity and stable performance (Y. Wang et al., 2017).

1.1.7. Relative humidity

Adsorbents such as zeolites, activated carbon, and silica gel have often been used to remove VOCs emitted from industrial gas streams. However, the presence of moisture in the gas stream can significantly influence the performance of adsorbents (Long et al., 2012; Qi et al., 2006; Tao et al., 2004). The relationship between water vapor content and VOCs removed is difficult to describe, though different studies have reported the effect of high humidity (RH, RH>50%) at low VOC concentration on the breakthrough time and capacity of adsorption of the activated carbon (Blocki, 1993; Jonas et al., 1985; Tao et al., 2004).

Okazaki et al. (1978) suggested the formation of a liquid film on activated carbon due to the presence of humidity that is responsible for the enhanced adsorption of water-soluble vapors. An increase in RH results in an earlier breakthrough and broaden the breakthrough curve of activated carbon, but when VOC concentration exceeds $20g/m^3$, adsorption capacity is not reduced even if the air is saturated with water. Biron and his colleagues (1998) reported that

molecules with strong affinity to the carbon surface were less influenced by the presence of water. Their study showed solubility is not the only factor which affects the adsorption on a wet carbon surface, though it might be more important when small molecules with low affinity to the surface are involved.

1.2. Objectives

The goal of this research is to evaluate the performance for adsorption and desorption of organic vapors on commercial activated carbon, hypercrosslinked polymer, and zeolites. Beaded activated carbon (BAC), Optipore V503, ZEOCAT Z700, ZEOCAT F603 and ZEOcat Z400 were uesd as adosrbents. 1,2,4 TMB, 2-butoxyethanol and OAC SST were used as adsorbates. Therefore, the main objectives of this research are:

1. To investigate the performance (adsorption capacity and heel build up) of commercial activated carbon, hypercrosslinked polymer, and zeolites during adsorption of VOCs, and

2. To explore the effect of water vapor on breakthrough time and VOC uptake during adsorption of polar and non-polar VOCs on commercial activated carbon, hypercrosslinked polymer, and zeolites.

Many industries use adsorption to reduce their VOC emissions to the atmosphere, and many investigations have been completed to improve adsorption and desorption processes. However, there is a knowledge gap regarding the effects of high relative humidity on adsorbents. The result of this study is helpful for understanding the adsorption performance of adsorbents and their capacity for VOC adsorption under different humidity conditions

1.3. Thesis outline

The thesis contains five chapters that contribute towards the fulfillment of the overall objective of this research. Chapter 1, as already described, outlines the background and goal of the present research. General literature review on adsorbates, adsorption of VOCs on different adsorbents (activated carbon, zeolite, and polymeric adsorbent), adsorption conditions, and regeneration processes are described in Chapter 2. The materials and methodology used for completion of the research are reported in Chapter 3. The experimental results obtained, followed by a discussion are presented in Chapter 4. Lastly, the conclusions derived from this research and future perspective are presented in Chapter 5.

2. CHAPTER TWO: LITERATURE REVIEW

2.1 Adsorption

This chapter includes a review of the literature on adsorption, which serves as a common technique for capturing organic compounds from gaseous streams. Adsorption typically represents a phenomenon of attracting and retaining adsorbate molecules on the surface of a solid, resulting into a higher concentration of the molecules on the surface (Tchobanoglous et al, 2003). In adsorption, the molecules form a weak or strong interactions with the solid surface through electrostatic, dispersive or stronger forces (Suzukthe, 1990). Usually, the term adsorbent is used to designate the solid that provides a surface for adsorption and the term adsorbate designates the gas or liquid substances which are to be adsorbed on to the adsorbent (Thommes et al., 2015). Adsorption is categorized into two types: physisorption (physical adsorption) and chemisorption (chemical adsorption) (Bansal & Goyal, 2005; Thommes et al., 2015).

Based on the operation of the adsorption process, physical adsorption is categorized into two: Temperature Swing Adsorption (TSA) and Pressure Swing Adsorption (PSA) (Khan and Ghoshal, 2000). Physisorption is the formation of weak and low energy forces of Van der Waals, field-dipole interactions between the adsorbent and adsorbate (Thommes et al., 2015). In physisorption, the process can be readily reversed during desorption (Lodewyckx, 2014; Singh et al., 2002). On the other hand, chemisorption involves strong interaction forces, usually covalent bond. The electron exchange between the adsorbate and the adsorbent in chemisorption leads to the formation of chemical bonds (Thommes et al., 2015). The strength of the bond depends on the functional groups present on the surface of the adsorbent and type of adsorbate (Yang, 1987). Higher temperature during adsorption can favor chemisorption as it provides the activation

energy needed for the formation of adsorbate−adsorbent complex (Schnelle & Brown, 2002). Other factors promoting chemisorption include the presence of adsorbates with electron-donating functional groups such as amine (−NH$_2$) and hydroxyl (−OH) (Tamon et al., 1996), and π−π electron donor-acceptor interaction between the aromatic ring and unsaturated bond on the carbon (Jahandar Lashaki et al., 2012; Villacañas et al., 2006). The reversibility of chemisorption becomes difficult due to rearrangement of the electrons that leads to transformation on the adsorbent surface (Suzukthe, 1990). The heat of adsorption for physisorption is from 10 to 20 kJ.mol^{-1}, whereas in chemisorption it ranges between 40 to 400 kJ.mol^{-1} (Bansal & Goyal, 2005).

2.2 Adsorption isotherms

Adsorption isotherm demonstrate the amount of adsorbate that gets adsorbed onto a solid surface, which is a function of the adsorbate partial pressure or concentration at a constant temperature (Cooper & Alley, 2002; Gregg & Sing, 1982; Peter Lodewyckx, 2014). Adsorption isotherms for some VOCs on different adsorbents (e.g., activated carbon, polymeric adsorbent, or zeolite) could be obtained using multiple techniques such as the dynamic column method (Popescu et al., 2003), the static volumetric method (Yun et al., 1998), and the gravimetric method (Cal et al., 1997). Using adsorption isotherm, the maximum adsorption capacity of a selected adsorbent can be determined.

There are six types of adsorption isotherms according to the International Union of Pure and Applied Chemistry (IUPAC) classification, as shown in Figure 2.1. Each of the six isotherms shapes depict unique adsorbent-adsorbate interaction as described below (Thommes et al., 2015):

Type I isotherms are obtained with microporous adsorbents where the pore size does not exceed a few adsorbate molecular diameters and monolayer adsorption occurs at low pressure.

At a low relative pressure, a gaseous molecule inside one of the pores of these small dimensions encounters the overlapping potential near the pore walls, enhancing the quantity adsorbed due to a strong adsorbate-adsorbent interaction. However, at a higher pressure, the pores are filled by adsorbed or condensed adsorbates leading to the plateau, indicating little or no additional adsorption after the micropores have been filled (Abril et al., 2009; Gregg & Sing, 1982).

Type II isotherms are seen when adsorption occurs on adsorbents with pore diameters larger than micropores. The inflection point of the isotherm usually occurs near the completion of the first adsorbed monolayer and with increasing relative pressure, second and higher layers are completed until saturated. **Type III isotherms** represent heat of adsorption lesser than the adsorbate heat of liquefaction. Thus, as adsorption proceeds, additional adsorption is facilitated because the adsorbate interaction with an adsorbed layer is greater than the interaction with the adsorbent surface (Gregg & Sing, 1982).

Type IV and Type V isotherms are shown with porous adsorbents having pores in the radius range of 15-1000 Angstroms (Å) and are characterized by mono and multilayer adsorption and capillary condensation (Bansal & Goyal, 2005). **Type VI** are the rare ones and are usually encountered during multi-layer adsorption (IUPAC-Recommendation, 1985; Lowell & Shields, 1984). The slop of each step is system and temperature dependent (Yahia et al., 2013).
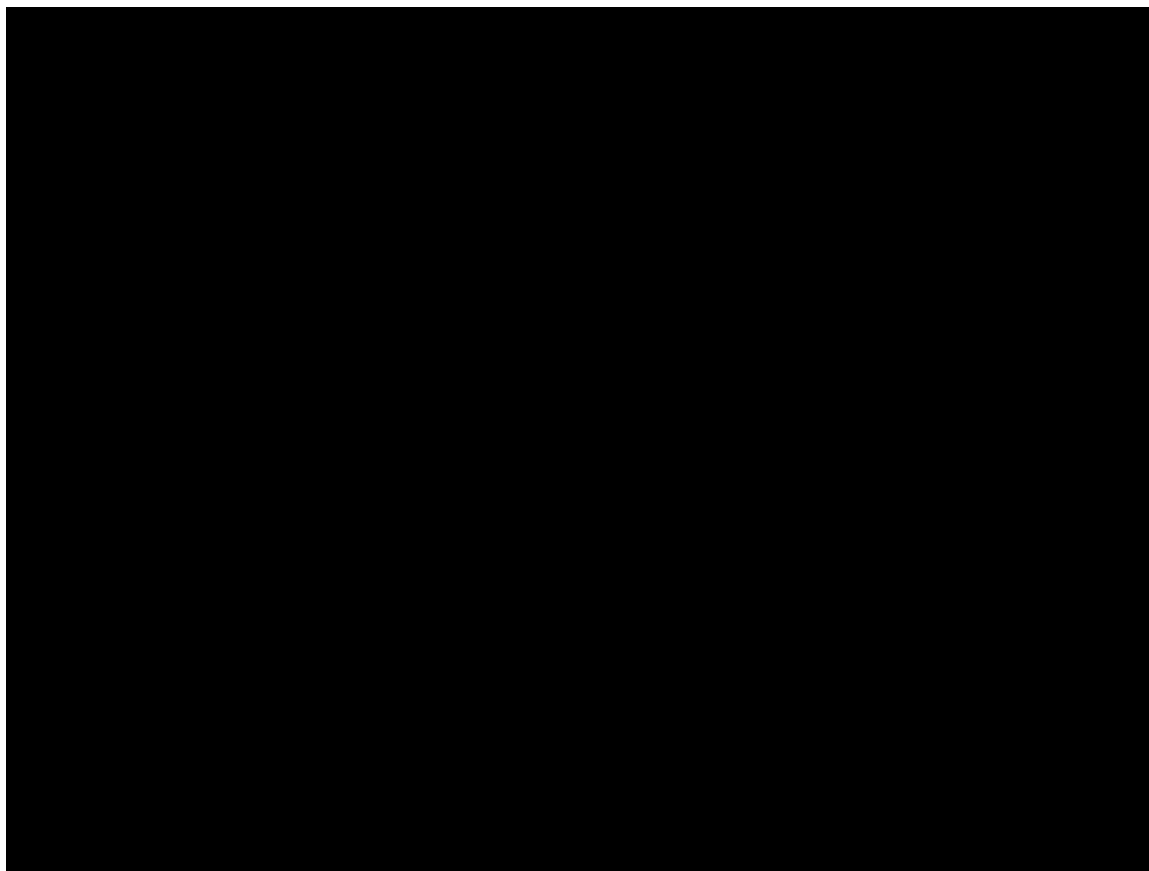
Figure 2.1 Types of adsorption isotherms (IUPAC-Recommendation, 1985).

(IUPAC-Recommendation 1994, Donohue and Aranovich 1998, Sing 1998)

2.3 Desorption

After adsorption, recovery of the loaded adsorbents are conducted by desorption, also named as regeneration. Desorption restores the adsorption capacity of the adsorbent and recovers the valuable adsorbates to reduce the costs and to avoid secondary solid hazardous waste (Suzukthe, 1990). Adsorption can be categorized into reversible adsorption and irreversible adsorption. Adsorption is a reversible process when adsorbate and adsorbent are held together by van der waals forces (Suzukthe, 1990). When the entire quantity of molecules adsorbed is recovered, the regeneration is said to be completely achieved. On the other hand, irreversible

adsorption is a stronger interaction between the adsorbate and the adsorbent. The term heel build-up is the unwanted accumulation of adsorbate in an adsorbent pores or adsorbent surface after regeneration under specified conditions (temperature and time) (Niknaddaf et al., 2016). It is a challenge associated with adsorbents for VOC adsorption because heel decreases the adsorbent's capacity and lifespan, increasing operation and maintenance costs (Jahandar Lashaki et al., 2016; Lashaki et al., 2012). There are three possible mechanisms leading to irreversible adsorption. a) chemisorption or chemical bonding between adsorbent and adsorbate b) oligomerization or oxidative coupling of adsorbate molecules inside the narrow pores, c) decomposition of adsorbates during desorption (Aktaş & Çeçen, 2006; Leng & Pinto, 1997; Vidic et al., 1993; Vidic et al., 1997).

Desorption is typically carried out by increasing the temperature (temperature swing regeneration, TSR) such as steam regeneration (Kim et al., 2001), microwave regeneration (Ania et al., 2005), or reducing the pressure (pressure swing regeneration, PSR) of the adsorbent. Other spent adsorbent regeneration techniques that are commonly used are biological methods for biodegradation of previously adsorbed organic matter for further adsorption, which are slow processes (Scholz & Martin, 1998), chemical methods such as acid–base ionization and solvent extraction, or by introducing a stronger adsorbate that is able to displace the adsorbed VOCs. (Tipnis & Harriott, 1986; Yang et al., 1987), catalytic oxidation, which requires lower temperature and residence time (Sheintuch, 1999), electrochemical methods (Wang & Balasubramanian, 2009), and extraction with supercritical fluids (F. Salvador & Jiménez, 1996), electrothermal heating (Hashisho et al., 2008; Sullivan et al., & Hay, 2004)

The selection of a particular regeneration technique mainly depends on the type of the adsorbent and adsorbent-adsorbate interaction, which can be obtained by the adsorption

isotherm. For example, TSR is a more favorable technique for Type I isotherms, while PSR is more suitable for regeneration of adsorbents with Type II and III isotherms (Kulkarni and Kaware 2014, Joss et al. 2015). The type of adsorbent should also be considered during the selection of regeneration technique. For instance, thermal and chemical instabilities of activated carbon regeneration cause significant safety concerns (Blocki, 1993).

Desorption isotherms and reversibility of the adsorption depend on the concentration of the adsorbate (Suzuki et al., 1978), type of adsorbate and adsorbent, adsorbent pore structure and functional groups based on its activation method (Aktaş & Çeçen, 2006), and operational conditions such as temperature and carrier gas velocity (Ramalingam et al., 2012). The irreversibility of the adsorption is evident in the difference of adsorption - desorption isotherm as hysteresis (Tamon et al., 1996).

2.4 Adsorption parameters

Various factors affect the adsorption capacity, adsorption kinetics, and adsorbent regeneration. Identification of these parameters and deciphering their effects on the process of adsorption helps in improving the process in a more efficient and economical way. Many studies have been accomplished to investigate the important factors and their optimization to improve the treatment techniques for capturing VOCs from polluted air streams. These factors can be classified as adsorbent's physical and chemical properties, adsorbate characteristics, and adsorption operating conditions (Huang et al., 2002; Huang et al., 2003).

Adsorption capacity expressed as the adsorbed species per mass of adsorbent. Adsorption isotherm provides the adsorption capacity as a function of the adsorbate partial pressure or concentration at a constant temperature (Vidic & Suidan, 1991).The adsorption capacity can be

calculated through the integration of the breakthrough curve. The breakthrough curve shows the concentration of the adsorbate leaving the adsorption column. In most of the literature, breakthrough time is defined as the time during which the adsorbate outlet concentration is 5% of the inlet concentration and the saturation time is when the outlet concentration reaches 95% of the inlet concentration (Carratalá-Abril et al., 2009). The shape and slope of the breakthrough curves depend on the mass transfer zone (MTZ). When the MTZ reaches the end of the adsorbent bed, the breakthrough begins and when it leaves, the adsorbent is saturated. Longer MTZ length depicts slower adsorption kinetic (Mohan et al., 2009).

2.4.1 Adsorbent properties

Adsorption ability of the adsorbents depends on various factors such as surface area, pore volume, pore size distribution, surface accessibility, diffusion resistance, hydrophilicity/hydrophobicity, metal content, and surface functional groups (Aktaş & Çeçen, 2006; Chakma & Meisen, 1989; Huang et al., 2002; Leng & Pinto, 1997).

Typically, higher surface area corresponds to the greater number of adsorption sites for VOCs and higher adsorption capacity (Chiang et al., 2002). In addition to the surface area of adsorbents, pore size distribution also has a significant influence on adsorption process. Lillo-Ró et al., (2005) studied the effect of porosity on adsorption of toluene and benzene and reported that the volume of narrow micropores governs adsorption at low VOCs concentration. Huang et al., (2002) have also studied the effect of pore size distribution on the adsorption of acetone and n-hexane and postulated that the difference in adsorption characteristics and diffusion of adsorbate were attributed to the pore size distribution of adsorbent.

Although, mesopores have more significant effect on adsorption capacity of VOCs at higher concentration, it has been recognized that the volume of narrow micropores (<0.7 nm) is a governing factor in adsorption capacity and saturation time at lower concentrations (Abril et al., 2009; Lillo-Ró Denas et al., 2005). Aktaş & Çeçen (2006) had studied the effect of the type of activated carbon on the extent of adsorption of phenol and the reversibility of adsorption. It was observed that the type of carbon activation plays a significant role in the adsorbability of phenol and its reversibility as compared to the type of physical form of the activated carbon. Leng and Pin (1997) studied the effect of metal impurity on physisorption and surface polymerization of activated carbon and reported that the higher concentration of metal reduced adsorption capacity but promoted polymerization of phenol on activated carbon. Activated carbon with high microporosity, low oxygen content, and high purity showed better adsorption capacity for VOCs (Lashaki et al., 2012; Wang et al., 2012).

Aktaş & Çeçen, (2006) and Huang et al., (2002) showed that the surface accessibility, diffusion path, and chemical surface characteristics of the adsorbents are more important factors than the total surface area, for determining the adsorption performance. However, other studies have found that the adsorbent physical properties are of greater relevance for determining the adsorption capacity (Díaz, 2005; Tsai, 2008).

Similarly, effects of adsorbent properties have also been studied for zeolites. Ferreira et al., (2013) studied the influence of the aluminum content on the adsorption of hexane isomers on MFI type zeolites. It was observed that the Si/Al ratio strongly influences the adsorption equilibrium properties of MFI. Ejka et al., (2004) studied the effect of the structure of large pore zeolites of Mordenite, beta, L, and Y types of zeolites for diffusion. Their study suggested that the values of measured diffusion coefficients on these zeolites were decreasing in the following

order m-xylene >1,2,4-TMB > 1,3,5-TMB; which supports the importance of transport. Therefore, while selecting an adsorbent it is important to consider the physical and chemical properties of the adsorbate.

2.4.2 Adsorbate properties

Physical and chemical properties of adsorbate such as molecular weight, size, structure, functional groups, polarity and boiling point are the most important characteristics affecting adsorption and regeneration (Tipnis & Harriott, 1986).

As diffusion in the adsorbent affects adsorption rate, adsorbates with large diameters are unable to enter narrow pores resulting in lower adsorption capacity (Canet et al., 2007). They also have lower regeneration efficiency as they exhibit low diffusion rates and may get trapped inside pores (Lashaki et al., 2012). Some adsorbents with narrow pore size distribution can only adsorb molecules with specific range of kinetic diameters from a mixture. For a given pore size, the size and shape of adsorbate determine the amount adsorbed during competitive adsorption (Lu & Sorial, 2009). Ferreira et al., (2013) compared three hexane isomers adsorption on a hydrophobic adsorbent. They found that the effect of kinetic diameter limits diffusion of molecules inside the adsorbent pore.

Chiang et al. (2001) reported that the surface area and pore volume are more critical for the adsorption capacity than adsorbate polarity and adsorbent functionality. However, Lee et. al. (2008) compared acetone (polar) and toluene (non–polar) adsorption on silica-alumina adsorbent, and found that the polar compounds exhibited higher affinity for hydrophilic adsorbent sites. Similarly, for polymeric adsorbent, Long and his colleagues (2009) found that

the order of adsorption affinity of benzene was greater than trichloroethylene due to benzene's non-polar nature. So, adsorbate polarity is an important factor for adsorption.

Kawasaki et al. (2004) studied the effect of boiling point and molecular weight on adsorption behavior of toluene, benzene, and xylene on activated carbon. They reported that the adsorption rate of benzene is the fastest compared to toluene and xylene. Li et al. (2012) used toluene, acetone, and xylene to study the effect of different functional groups. They reported that the adsorption capacity increased linearly with the increase in the molecular weight, dynamic diameter, boiling point, and density of the adsorbate. However, adsorption capacity decreased as the polarity index and vapor pressure of the adsorbate increased.

2.4.3 Adsorption conditions
2.4.3.1 Temperature

Since adsorption is an exothermic process, higher temperature would have an inverse effect on adsorption efficiency (Huang et al., 2003). Increasing adsorption temperature increases diffusion rate that results in faster adsorption kinetics (Jahandar et al., 2012). Hence, the breakthrough time and MTZ are shorter at a higher temperature (Chuang et al., 2003). Cheng et al., (2013) research indicated that the breakthrough time and the adsorption capacity of toluene decreased with increasing adsorption temperature. Higher temperature increases the motion of the molecules, resulting in easier diffusion of the adsorbate into the narrow micropores. However, the adsorption capacity decreases at high temperature (Jahandar et al., 2012). Thermal hazard (e.g. fire) is also another crucial problem with high adsorption temperature of high concentration VOC stream (Delage et al., 1999).

Moreover, higher temperature enhances the interactions between the adsorbate and adsorbent which can enhance chemisorption and decrease regeneration efficiency (Chiang et al., 2001; Jahandar et al., 2012).

2.4.3.2   Humidity

Humidity exists in many industrial gas streams and may reduce the adsorption capacity due to competitive adsorption between the water vapor and VOCs (Brennan et al., 2001; Meng et al., 2014). Water vapor is the most common polar molecule which can be adsorbed by physisorption or chemical interactions (e.g., hydrogen bonding) with surface functional groups (Biron, 1998). Activated carbon surface is nonpolar or slightly polar as a result of surface oxide groups and inorganic impurities (Ralph Yang, 1987a). Activated carbon that has adsorbed water vapor can lose this water vapor by replacement with organic and non-polar or weakly polar compounds which adsorb preferentially on its surface than water does. However, humidity levels exceeding 60% relative humidity are not desirable (Parmar & Rao, 2009). Polar adsorbents such as zeolites, porous alumina, silica gel, or silica-alumina are hydrophilic (Suzukthe, 1990). The surface polarity of these adsorbents is responsible for attracting polar substances including water.

Therefore, adsorbents having hydrophilic surface properties have lower removal efficiency of VOCs in presence of water vapor (Abiko 2016; Park 2017). Gong & Keener (1993) showed effects of water vapors on binary vapor adsorption of toluene and methylene chloride on activated carbon with different adsorbate concentration ranging from 400 to 1200 ppmv at three levels of relative humidity (15%,65% and 90%). They found that the shape of breakthrough curves was asymmetrically distorted and the width of the curves was broadened for toluene and steepened for methylene chloride with an increase in relative humidity from 15% to 90%.

In competitive adsorption, adsorption of water molecules could hinder adsorption of VOCs through clustering and clogging of micropore entrances (Jia 2017; Zoraida 2015). When the adsorbate have higher affinity to the adsorbent than water, it can substitute water molecules by competitive adsorption and eliminate the humidity influence on adsorption efficiency. In other words, adsorbates with higher adsorption energy than water could displace water molecules during adsorption (Biron & Evans, 1998). Therefore, molecules with high affinity to the adsorbent surface, whether soluble or not, are less influenced by the presence of water vapor.

Many studies have investigated the effect of humidity during adsorption of VOCs. However, the adsorption mechanism of water vapor in VOCs streams is still not clear. One of the practical solutions to eliminate the effect of humidity is using hydrophobic adsorbents. There are no entirely hydrophobic adsorbents as most surfaces contain a nonzero quantity of hydrophilic adsorption sites (Burtch, 2014). However, increased research focused on developing a hydrophobic adsorbent to maintain VOCs adsorption capacity under practical conditions where some moisture usually exists in a process stream. Typically, carbonaceous materials with no surface oxygen groups and some of the synthesized non-carbon based materials such as zeolite and polymeric adsorbents can be used for low concentration VOC adsorption from humid gas streams (Delage, 1999).

2.5 Adsorbents

Adsorbents are porous materials having capacity for gas purification and separation (Yang, 1987). Porous materials have the ability to adsorb due to their large internal surface area (Parmar and Rao, 2009). IUPAC has classified the adsorbents' pores with respect to their diameters into three groups: micropores (less than 2 nm), mesopores (between 2 to 50 nm), and macropores (more than 50 nm) (Bansal and Goyal, 2005).

The adsorption process is mostly completed in micropores and mesopores. Micropores create a shorter diffusion path thus, higher adsorption capacity and faster adsorption kinetics. On the other hand, the different functional groups on the surface of adsorbents can influence their adsorptive behavior (Yang, 1987). Various porous adsorbents were introduced in literature with varied physical and chemical properties depending on adsorption conditions and adsorbate properties. Adsorbents used for VOCs capturing were generally classified as carbonaceous and non-carbonaceous materials. The following section highlights common adsorbents used for capturing of VOCs.

2.5.1 Activated carbon

Carbon based adsorption is a very common method of VOCs emission control. Activated carbon (AC) exists in several physical forms including fibers, powders, beads, monoliths, and granules which make them usable in nearly every kind of reactors (Jahandar Lashaki, et al., 2012). Besides, they can be modified to have desirable physical and chemical properties and also exhibit good tolerance in both acidic and basic conditions. These properties make activated carbon useful in different applications such as decolorization, deodorization, purification, and separation to remove or modify harmful constituents from gases and liquid solutions (Bansal & Goyal, 2005).

Activated carbon preparation involves two main steps: carbonization of carbonaceous raw material and activation of the carbonized product (Bansal & Goyal, 2005).Different carbonaceous raw materials such as coal, wood, nutshells, bamboo, coconut shell, lignite, sawdust, petroleum coke, peat, synthetic polymers, biomass materials, and agricultural by-products through carbonization process (Abiko et al., 2016; Chun et al., 2001). During carbonization process, most of the non-carbon elements such as oxygen, hydrogen, and nitrogen

are detached by pyrolytic decomposition of raw materials at temperatures below 800ºC. The residual carbon atoms group together into stacks of aromatic sheets that are randomly cross-linked This type of structure provides a porous network which is occupied with tarry matter or products from decomposition and are partially blocked (Bansal & Goyal, 2005). Then, activation can be done in air, CO_2 and or steam at 800-1000ºC to increase the number of pores and enlarge them. The macropores contribution to the surface area does not typically exceed 0.5 m^2/g. They usually act as a pathway and conduct adsorbate molecules into the micro- and mesopores. The AC prepared with different methods and treatment shows significantly different adsorption properties even though, they have a similar surface area (Bansal & Goyal, 2005).

In general, the AC adsorption has been frequently applied to remove VOCs from a gaseous stream (Long, 2011). Excellent adsorption capacities are one of the many reasons to consider AC as a preferable adsorbent in separation. Others being larger surface area and pore volume (Huang et al., 2002), a microporous structure which provides a highly developed porosity, and a high degree of surface reactivity (Bansal & Goyal, 2005).

Although, activated carbons are commonly used adsorbents for VOCs, they also have some drawbacks such as pore blocking, inefficiently desorption of high-boiling adsorbates, risk of fire (Kamravaei et al., 2017; Lashaki et al., 2016), and polymerization or oxidation of adsorbates to toxic or insoluble compounds (Khan and Ghoshal, 2000; Stelzeret al., 1998). These limitations of AC have prompted research to develop polymeric and zeolite adsorbents (Liu et al., 2009; Parmar & Rao, 2009; Stelzer et al., 1998).

2.5.2 Polymeric adsorbents

Polymeric adsorbents have been studied for removal of organic pollutants from waste streams (DAVANKOV & TSYURUPA, 2011). They have emerged as a potential alternative to AC because of their controllable pore structure, easy regeneration, and stable physical and chemical properties (Jia et al., 2017; Long, 2009; Tsyurupa & Davankov, 2006). In particular, one of the main advantages of polymeric adsorbents is that the adsorption can occur by weak adsorption affinity in opposition to other adsorbents such as activated carbons. Therefore, it is expected that the polymeric adsorbents are useful for treating solvent vapors by pressure swing adsorption (Choung et al., 2001). Several application of polymeric adsorbents include adsorption of organic pollutants, namely phenolic compounds, organic acids, aromatic and polyaromatic hydrocarbons, alkane and their derivatives (Bingjun Pan et al., 2009; Deosarkar & Pangarkar, 2004). More recently, the hypercrosslinked polymers (produced by crosslinking polymers of microporous resin) have gained more attention due to their characteristic narrow pore size distribution (PSD) (Baya et al., 2000). Hypercrosslinked polymeric adsorbents represent a class of predominantly microporous organic materials with the larger specific surface area and high micropore volume (Long, 2012).

Recently, some studies have investigated using hypercrosslinked polymeric adsorbents for removing the VOCs from gas streams. Liu et al. investigated the effect of temperature and polarity on hyper-crosslinked polymeric resin NDA201, and showed higher temperature reduces the adsorption capacity of trichloroethylene and benzene. It was also found that the adsorption affinity of benzene was greater than trichloroethylene (2009). A hydrophobic hypercrosslinked polymer, LC-1, prepared by Long et al., (2011) resulted in better adsorption capacity for three chlorinated VOCs than commercial hypercrosslinked polymer (NDA-201), due to its abundant

micropore structure. Wang et al., (2015) recently discovered highly efficient hypercrosslinked polymers with high surface area (1394 m^2/g), large pore volume (1.55 m^3/g), and controllable average pore size for adsorbing organic pollutants from dry and humid air streams. Long et al., (2010) studied the adsorption characteristics of benzene–chlorobenzene vapors on hypercrosslinked polystyrene adsorbent, in lab-scale and pilot-scale application.

Adsorption of VOCs using Optipore V503 (a commercial hypercrosslinked hydrophobic polymer adsorbent) showed high adsorption capacity for benzene but low desorption efficiency using microwave-assisted desorption. After sulfonation, Optipore V503 led to an increase in the desorption efficiency and decrease in the adsorption capacity due to adsorption of water (Meng et al., 2013). Some of the major findings of polymeric adsorbents for VOCs adsorption are shown in Table 2.1.

Table 2.1: Polymeric adsorbents for adsorption of VOCs

Polymeric type	Adsorbate	Summary of result	Reference(s)
Hypercrosslinked polymeric (HPA) and granular activated carbon (GAC)	Water vapors	With increasing relative pressure of water vapor, the decrease in effective pore width and micropore filling leads to the development of barriers for surface diffusion into porous structure of HPA probably associated with the formation of water clusters	(Jia et al., 2017)
Hypercrosslinked polymers	Benzene and Water vapors	The existence of water vapor had little effect on the dynamic	(Nguyen et al., 2014)

		adsorption capacity of benzene	
Highly porous hypercrosslinked adsorbents	Benzene and Water vapors	Desorption efficiency was increased.	(Meng et al., 2013)
Ambersorb 600 Sp 850 and Dowex Optipore V493	Toluene	Isosteric heat of adsorption varied with surface loading.	(Choung et al., 2001)
Hypercrosslinked polymer	Trichloroethylene, trichloromethane, 1, 2-dichloroethane, and Water vapors	Breakthrough time decreased by less than 11% when the moisture content was above 90% RH	(Long et al., 2011)
Hypercrosslinked polymeric resin (NDA201)	Trichloroethylene (TCE) and Benzene	Adsorption affinity of benzene was higher than trichloroethylene	(Liu et al., 2009)
Macroporous and hypercrosslinked polymeric adsorbent (NDA-150)	Naphthalene	The adsorption capacity of hypercrosslinked adsorbent was higher due to its larger micropore volume	(Long et al., 2009)
Hypersol-Macronet (MN-200)	Alkanes, cyclohexane, toluene, methanol, and Dichloromethane	Required low desorption temperatures	(Baya et al., 2000)
hypercrosslinked polymeric adsorbent (HY-1), microporous activated carbon (m-	Benzene and Water	HY-1 would be particularly efficient and competitive adsorbent for VOCs	(Long et al., 2012)

GAC), and activated carbon fiber (ACF)			
Hydrophobic polydivinylbenzene–silica (PDVB)	Toluene and Water	High humidity had no effect on PDVB after 10 adsorptions–desorption cycles, continued exhibiting excellent adsorption	(Lu et al., 2013)

2.5.3 Zeolites

Zeolites are porous alumina silicates that exist naturally as different minerals. These can also be synthesized artificially for different applications such as to act as a catalyst and for the adsorption process (Ejka et al., 2004). Zeolites sometimes are also referred as molecular sieves because of their crystalline framework with channels (pores) and interconnecting voids (Blocki, 1993). The structure of a zeolite crystal is based on a tetrahedron formed by four oxygen atoms, which are joined to silicon/aluminum atom by its four valence electrons. They consist of a crystalline structure built from $[AlO_4]^{5-}$ and $[AlO_4]^{4-}$ bonded together in such a way that all four oxygen atoms located at corners of each tetrahedron are shared with adjacent tetrahedral crystals (Jha & Singh, 2016).

In general, zeolite pore sizes fall into the microporous size and with ring size between 8-20 nm (Guth & Kessler, 1999). Among several types of molecular sieve materials, zeolites are a well-known category which has already been synthesized in laboratories and industries due to their unique catalytic, adsorptive, and separation properties (Dĕdeček et al., 2009). Zeolites based on Si/Al molar ratio can be graded as low silica ($\leq$ 2), intermediate silica (2-5) and high silica ($\geq$ 5). The Si/Al ratio can significantly affect (increase or decrease) parameters like acid resistivity, thermal stability, hydrophobicity, acidic site density, and cation concentration.

Several factors affect the adsorption performance of zeolites including, adsorbate, pore volume, active site, and hydrophobicity (Blocki, 1993). Daems and his colleagues (2006) studied the adsorption of alkanes, alkenes, and aromatics on zeolites NaX (Si:Al 1.23) and NaY (Si:Al 2.55). Their results showed that the separation potential decreases with the increase in alkane chain length on both zeolites. Lee et al., (2008) studied adsorption characteristics of acetone and toluene vapors of different concentrations on silica alumina (pore volume was 0.44 cm^3/g, average pore diameter was 27 A°, BET specific surface area was 641 m^2/g). They reported that the adsorption capacity increased and breakthrough time decreased by increasing the inlet concentration and linear velocity of acetone and toluene vapors. Herná et al., (2005) found that the uptake degree of these aromatic hydrocarbons on dealuminated clinoptilolites was temperature dependent. Wang and his collogues (2007) found that the presence of Al can significantly affect the adsorption of butene-1 than that of n-butane on ZSM-5 zeolites, which have different Si/Al ratios. Some of the other studies are tabulated in Table 2.2.

Table 2.2: VOCs adsorption on Zeolites

Zeolite type	Adsorbate	Summary of result	Reference(s)
NaZSM-5 and HZSM-5	Benzene, Toluene, Ethylbenzene, and Xylene	H-ZSM-5 was found to be a useful adsorbent in comparison to the synthesized Na- ZSM-5 zeolite material	(Azizet al., 2017)
LiLSX, NaLSX, KLSX, NaX, and two NaY	Alkanes and Aromatic compound	Henry constant increases with rising Si/Al ratio	(Canet et al., 2007)
Beta zeolites (beta-trans, beta- DA,	Acetone, n-Hexane, Benzene,	Adsorption capacity of each adsorbent decreased with the	(Zhu et al., 2017)

beta-OH, beta-F, beta-F, beta-trans, beta-OH, beta- DA)	and Toluene	increase of adsorbate molecular diameter from acetone to toluene	
ZSM-5	Toluene	After four successive cycles of adsorption/ozonation, the adsorption efficiency was not affected	(Zaitan et al., 2015)
Silica–alumina	Acetone and Toluene	Rollover effect (the more strongly adsorbed adsorbate (acetone) displaces the weaker adsorbate (toluene))	(Lee et al., 2008)
USY Zeolite	1,3,5-TMB	Diffusion limitations were observed for 1,3,5-TMB	(Tukur & Khattaf, 2007)
Beta Zeolites (beta-F, beta-trans, beta-OH, beta-DA	Acetone, n-hexane, benzene, toluene, and water	Beta-DA adsorbed larger volume of water due to the presence of many silanol nests	(Zhu et al., 2017)
All silica Zeolite beta	Water, toluene, and methylcyclohexane	Significantly smaller amount of defect was shown	(Stelzer et al., 1998)
Modified ZSM-5 particles	Water	Increasing alkyl chain increased the hydrophobicity. However, with an increase in pretreatment temperature, the hydrophobicity decreased	(Han et al., 2011)

As zeolites are inorganic-based adsorbents, they are capable of withstanding very high temperatures. This thermal stability was also found to increase with an increase in SiO_2/Al_2O_3 ratio of zeolites. In general, zeolites are non-flammable and therefore, will not

contribute to fire in a solvent-laden atmosphere (Blocki, 1993; Parmar & Rao, 2009). Except for honeycomb structure, hydrophobic zeolite can withstand temperatures as high as 1000°C (Blocki, 1993).

2.6 Hydrophobicity

During the removal of VOCs from gas streams, water vapor is typically present and can degrade the performance of adsorbent because it competes with the VOCs (Jia et al., 2017). Water vapor leads to decrease in kinetics and selectivity of a given adsorbent towards a mixture of adsorbates (Qi, 2006; Zhao et al., 2015). In general, there are no perfectly hydrophobic adsorbents as most surfaces will contain a nonzero quantity of hydrophilic adsorption sites. These sites are introduced from defects, impurities, or dopants, and are present in various forms in both zeolites and AC (Burtch et al., 2014).

Activated carbon that have hydroxyl groups on the carbon surface establishes hydrogen bond with water vapor molecules, which can produce clusters that may block the passage of the adsorptive molecules into the micropores (Villacañas et al., 2006). Halogenated compounds are strongly affected by increased relative humidity, whereas aromatic compounds are only weakly affected. However, because water vapor competes with the VOCs in gas streams for adsorption sites on the carbon surface, relative humidity levels exceeding 60% are not desirable (Khan and. Ghoshal, 2000).

Most zeolites are hydrophilic hence, are not well suited for removing VOCs in a humid atmosphere. However; recent advancements have made it possible to manufacture a hydrophobic zeolite with extended physical characteristics (Blocki, 1993). Hydrophobic zeolites have gained considerable attention due to their ability of selectively removing organic pollutants from humid

air streams (Tao et al., 2004). In general, hydrophobicity increases with an increase in SiO_2/Al_2O_3 ratio of zeolites (Marcus, 1999). Zeolites have the advantages of thermal stability, precise pore size distribution, selective adsorption and non-flammability (Blocki, 1993; Khan & Ghoshal, 2000; Parmar & Rao, 2009).

Zeolites with high Si/Al ratio such as in USY, ZSM-5 type, dealuminated faujasites, and beta zeolites, are effective in removing VOCs from the humid stream (Marcus et al.,, 1999). It has been demonstrated that hydrophobic all-silica beta zeolite exhibits superior performance in competitive adsorption of toluene/water or methylcyclohexane/water vapor mixtures in comparison to other siliceous materials, such as dealuminated beta zeolites, FAU- and EMT-type zeolites (Stelzer et al., 1998). In general, zeolites commonly have the following properties including non-flammable material (withstand temperatures up to l000ºC), can handle a wide variety of solvents, efficient adsorption at a wide range of concentrations, does not promote solvent polymerization or reaction, and repels moisture (Blocki, 1993).

Hypercrosslinked polymeric adsorbents have found an increased application for removing VOCs from gas streams. Long et al., (2011) studied the effect of water vapor on adsorption of chlorinated VOCs onto the LC-1 polymeric adsorbent. They found that the humidity had an effect on adsorption capacity above 90% RH. Recently, Wang et al., (2015) reported that the presence of water vapors had little effect on the dynamic adsorption capacity and didn't change the adsorption breakthrough time of benzene on hypercrosslinked polymeric adsorbent (HCP=0.5). Jia and his colleagues (2017) also studied the adsorption kinetic behavior of water vapor on hypercrosslinked polymeric adsorbent HPA and compared it with granular activated carbon (GAC) and activated carbon fiber (ACF). They found that the kinetic rate constants follow the order HPA > ACF > GAC and is a function of surface functional groups.

In summary, the Dowex Optipore and high silica zeolite adsorbents exhibit excellent hydrophobicity, only adsorbing water at high relative humidity. Activated carbon is moderately hydrophobic, but exhibits a dramatic increase in its affinity for water at relative humidity over 50% (Schmidt, 1998).

3. CHAPTER THREE: MATERIALS AND METHODS

3.1 Adsorbent and adsorbate

The adsorbents used in this research are beaded activated carbon (BAC, G-70R, Kureha Corporation), ZEOCAT Z700, ZEOCAT F603, ZEOcat Z400 (ZEOCHEM) and OPTIPORE V503 (Dow Chemical). Table 3.1 shows relevant physical properties of these adsorbents.
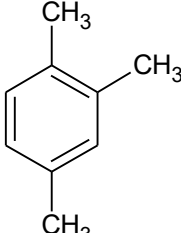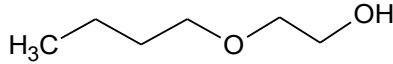
Table 3.1 Physical properties of tested adsorbents

Adsorbent name	Type	Si/Al ratio	Particle Size (mm)	Shape	BET surface area (m^2/g)	Micropore volume (cc/g)	Total pore volume (cc/g)
BAC G-70R	Activated carbon	-	0.7	beads	1,314	0.49	0.57
OPTIPORE V503	Hyper crosslinked	-	1	beads	1,262	0.29	0.90
ZEOcat Z700	USY	60	0.5-0.7	beads	553	0.16	0.43
ZEOcat F603	50/50, USY/ZSM-5	NA	0.5	beads	419	0.10	0.34
ZEOcat Z400	ZSM-5	NA	1.25	beads	280	0.02	0.24

The adsorbates tested in this study represent VOCs groups commonly present in automotive paint solvents. Single adsorbates as well as a solvent mixture were tested at an inlet concentration of 500 ppm$_v$. Two VOCs were tested individually as a single adsorbate; 1,2,4-trimethylbenzene (TMB) (nonpolar VOC) and 2-butoxyethanol (polar VOC). These two VOCs are commonly used in painting and surface coating operations (Hailin et al., 2013; Kim, 2011). TMB has a boiling point of 171 °C and kinetic diameter of 0.68 nm (Avhale et al., 2008; Gédéon et al., 2008). Its bulky structure promotes heel buildup and makes it easier to measure change in adsorption capacity and heel formation (Lashaki et al., 2016; Niknaddaf et al., 2016). 2-

butoxyethanol has similar boiling point to TMB, but is polar. The difference in polarity of these two compounds was used to investigate the effect of water vapor on VOC adsorption on zeolites. In addition to the two adsorbates, a solvent mixture, OAC-SST, was also tested. This mixture consists of a sample of condensate during the desorption of beaded activated carbon used to treat automotive painting booth air.

Table 3.2 Properties of tested adsorbates

Compounds	Structure	Boiling point (°C)*	Kinetic diameter (nm)	Molar mass (g/mol)
1,2,4-trimethylbenzene (TMB) (Fisher scientific p, >98%)		171	0.68	120.19
2-butoxyethanol (Acros Organic, >99%)		168	NA	118.17
OAC-SST	NA	NA	NA	115

3.2 Experimental setup and methods

Adsorption isotherm for TMB and 2-butoxyethanol on different adsorbents (BAC, Polymeric adsorbents and zeolites) were obtained using the dynamic column method (Seo, 2009). The present study examines the adsorption and desorption (five cycles) of a single and a mixture of adsorbate on the different adsorbent. Further, one cycle adsorption was used to examine the effect of polar and non-polar compounds on the selected zeolite adsorbent. Prior to

each experiment, pure and dry nitrogen was purged through the adsorption column for 3 h at 288ºC in order to remove the residual moisture and VOCs.

For adsorption at dry condition, the experimental setup (Figure 3.1) consists of an adsorption-regeneration tube, an adsorbate generation system, a gas detection system, a power application module, and a data acquisition and control system (DAC). The adsorption−regeneration tube consisted of a stainless-steel tube (1.44 cm inner diameter, 15.24 cm long) containing 4±0.1g of dry adsorbent except ZEOcat Z400 required to use 5±0.1g of dry adsorbent because of its' size. The adsorbent bed length was an average 4cm. Glass wool was used at the bottom and top of the reactor as a support for the adsorbent bed.

 Adsorbate was injected using a syringe pump (KD Scientific, KDS-220) into a 10 standard liter per minute (SLPM) at 1 atm and 25 °C of filtered air. A compressed air filter (Norman Filter Co.) was used to remove water and hydrocarbons from the air stream. The air flow rate was controlled at 10 SLPM using a mass flow controller (Alicat Scientific). The syringe pump injection rate was adjusted to maintain an inlet adsorbate concentration of 500 ppmv for all the experiments. The injection rate was calculated based on the ideal gas law using the adsorbates' density and molecular weight. The inlet and outlet organic concentrations were determined with a flame–ionization detector (FID) (Baseline Mocon, Series 9000). The FID used ultrahigh purity (grade 5.0) hydrogen gas with flow rate of 35 cc/min and compressed air as a combustion gas with flow rate of 175 cc/min. The FID was calibrated before each adsorption test using the same gas generation system. The VOC concentration at the adsorber's outlet stream was measured continuously during adsorption (1 min sampling frequency).

Regeneration was completed using thermal regeneration. Heating and insulation tapes (Omega) were wrapped around the adsorption tube during regeneration. A type K thermocouple

(1.6 mm outer diameter, ungrounded, Omega) was used to measure the temperature at the center of adsorber bed during adsorption and regeneration. The Data Acquisition and Control (DAC) system consisted of a LabVIEW program (National Instruments) and a data logger (National Instruments, Compact DAQ) equipped with analog input/output modules. The DAC was interfaced to the thermocouple to record temperature during adsorption/regeneration. Regeneration tests were performed for 3 hours by heating at 288 ºC which was chosen to simulate industrial operation (Kim, 2011; Lashaki et al., 2016), and allow for desorption of adsorbed species while minimizing potential damages to the structure of adsorbent as a result of exposure to high temperature (Salvador, 2015). However; DOWEX OPTIPORE V503 was regenerated at 200 ºC because exposure to high temperature can damage its structure (McCullough, 2003).

High purity (grade 4.8) nitrogen (1 SLPM) was used during regeneration to purge oxygen from the bed and carry desorbed compounds. Desorption tests were performed at 288 ºC for 3 h followed by 50 min cooling with continuous nitrogen purging of the bed.
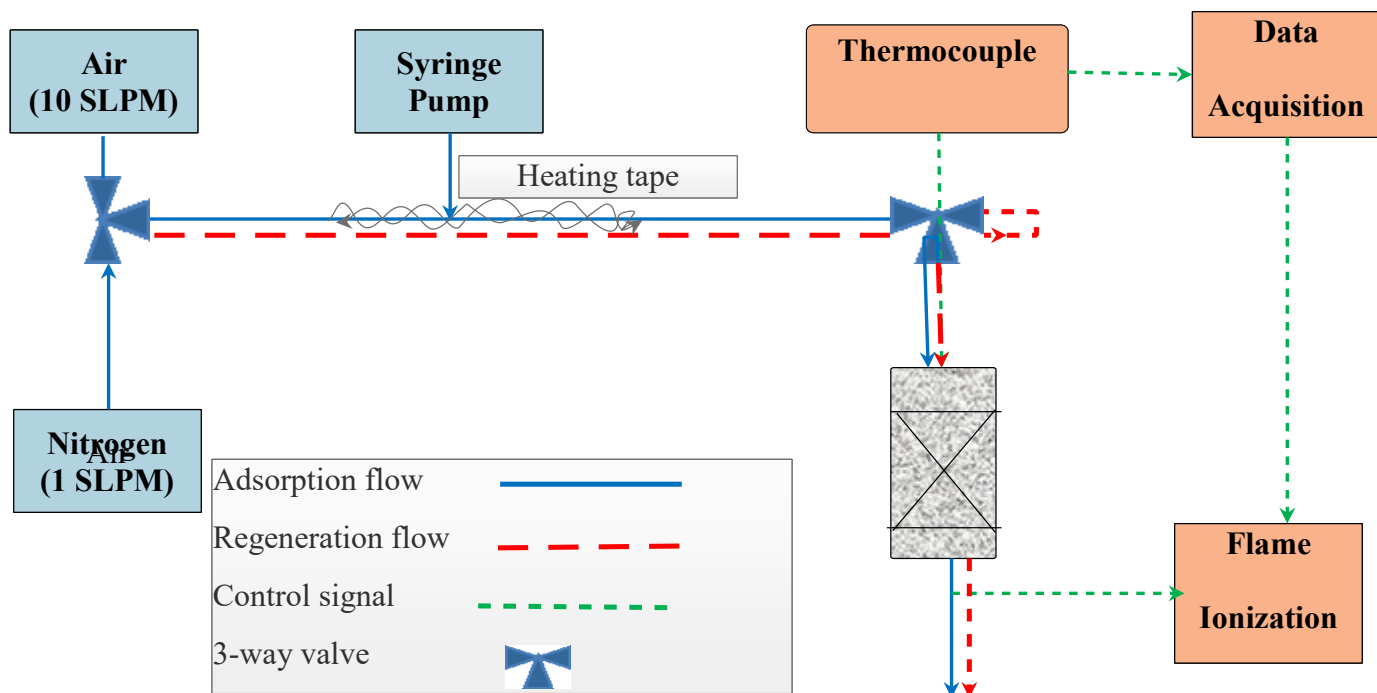
Figure 3.1 Schematic diagram of the experimental setup used for adsorption and regeneration

Adsorption and desorption amounts were determined using mass balances. The reactor was weighed using a balance (Mettler Toledo, MS603S) before and after adsorption to calculate the adsorption capacity of the adsorbent, as follows;

Adsorption capacity (%)

$$= \frac{\text{Adsorbent weight after adsorption} - \text{adsorbent weight before adsorption}}{\text{Weight of adsorbent}} \times 10$$

The difference in the reactor weight before an adsorption cycle and after the corresponding regeneration cycle represents the amount of heel built up during that cycle. Adsorption/regeneration experiments were completed in duplicates to assess testing reproducibility. The mass balance cumulative heel represents the total amount of heel build-up after five complete adsorption/regeneration cycles and is defined as follows:

Mass balance cumulative heel (%)

$$= \frac{\text{Adsorbent weight after last regeneration cycle} - \text{Adsorbent weight before 1st adsorption}}{\text{Weight of Adsorbent}} \times 100$$

For adsorption in presence of water vapor (Figure 3.2), a humidity generator and a relative humidity (RH) sensor were added to the setup. The humidity generator consisted of two water-filled impingers (1 L) with diffuser stones, connected in parallel. A parallel configuration of impingers provided a stable supply of required relative humidity levels. Dry air stream was humidified as it passed through the impingers. RH sensors (Vaisala HMT330) to measure the gas relative humidity. Two-point calibration of the FID was conducted with fresh air for zero and a steady state concentration of the adsorbate stream from the VOC-water vapor mixture generation system for span. Before the start of each adsorption test, the generated adsorbate gas stream was monitored using the FID and RH sensor and was used as a reference for monitoring effluent stream. Three operating relative humidity (RH=0%, 45% and 70%) and one VOC concentrations (500ppm) were tested in this study. After a steady concentration stream is achieved, the gas stream was directed into the inlet of the adsorber tube to start the adsorption. A slip stream from the effluent was directed to the FID for effluent concentration measurement. Adsorption was continued until the adsorbent was fully saturated, as indicted by stable effluent concentrations, equal to the influent concentrations, measured by the FID. The same amounts of adsorbent and glass wool were used for the humid condition as the dry condition experiment.
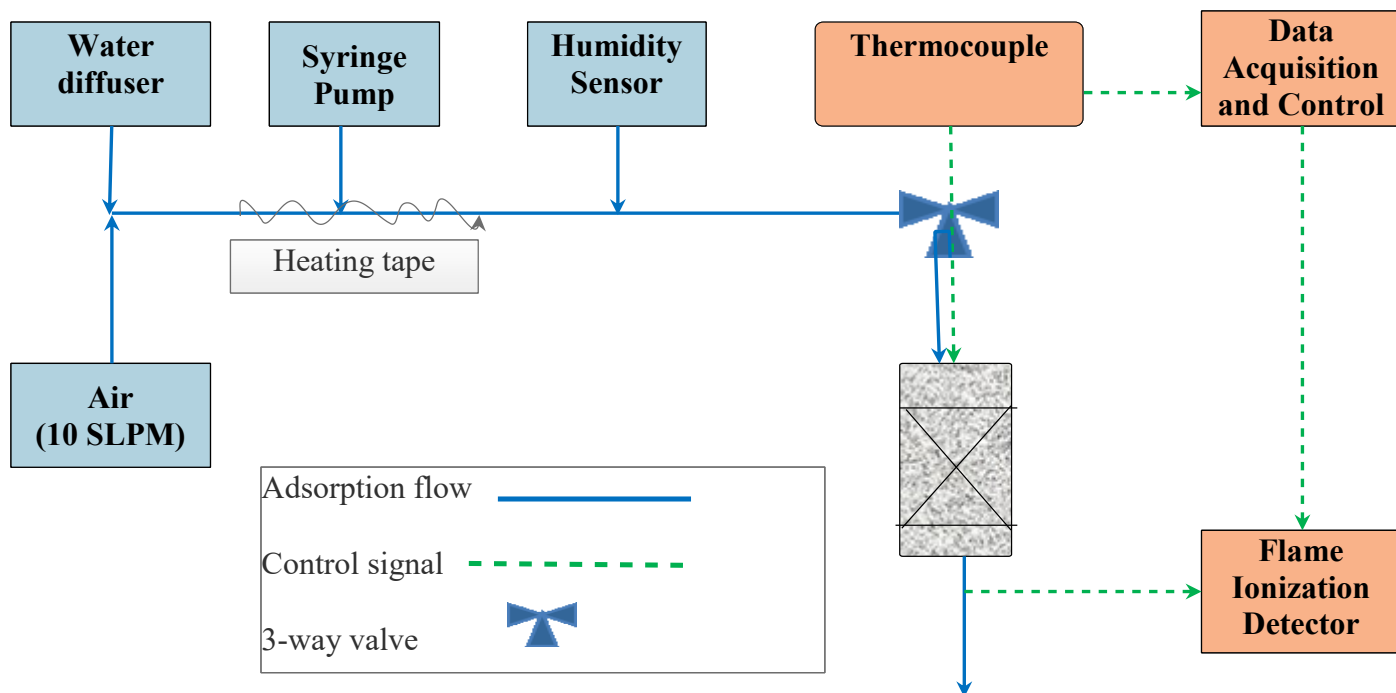
Figure 3.2. Experimental set up for measuring water and VOCs adsorption.

Data Analysis

The data obtained in the experiments described above were analyzed as follow: the experiments with zero RH, the difference in the weight of the adsorbent before and after the adsorption indicates the amount of VOC adsorbed. Hence, the VOC adsorption capacity at the 0% RH was obtained by dividing the weight of VOC adsorbed with the original weight of the adsorbent.

In case of VOC adsorption in the presence of water vapor, since VOCs measurement with FID is not affected by water vapor the amount of VOC adsorbed was calculated by integrating the area above the VOC breakthrough curve during VOC-water coadsorption. The net weight gain due to the co-adsorbates, VOC plus water, was determined by taking the difference of weight of adsorbents before adsorption from the weight of adsorbents after the coadsorption. Subtraction of the weight calculated using breakthrough from the net weight gain of the

adsorbates gave the total mass of water adsorbed. Henceforth, the water uptake was calculated as the ratio of water adsorbed to the original weight of the virgin adsorbent. One cycle adsorption on dry and humid condition was completed in duplicates to assess testing reproducibility for BAC, Optipore V503, ZEOcat Z700, and ZEOcat F603.

In addition, two different water vapor preconditioning cases were evaluated for ZEOcat Z700 and ZEOcat F603. The first case was carried out after the adsorbents were exposed to a flow of 45%RH air at 10 SLPM for 90 min, and the second case was performed after the adsorbent was exposed to a flow of 75% RH air at 10 SLPM for 90 min. After the completion of above mentioned preconditioning, 500ppm concentration of TMB and water vapor of 45% RH or 75% RH air streams were introduced into the adsorption column until adsorption equilibrium was reached for 45% RH or 75% preconditioned adsorbent, respectively.

3.3 Characterization tests
3.3.1 Thermogravimetric analysis (TGA)

Thermal stability of the virgin and regenerated samples were assessed using derivative thermogravimetric (DTG) analysis (TGA/DSC 1, Mettler Toledo). Samples were heated at a heating rate of 2°C/min to the temperature of 900°C and change of weight was measured. Desorbed species were purged with a stream of N_2 at a rate of 50 standard cubic centimeter per minute.

3.3.2 Micropore surface analysis

Virgin BAC, OPTIPORE V503 and ZEOcat Z700, ZEOcat F603 and ZEOcat Z400 samples were analyzed to determine Pore size distribution and BET surface area were obtained using a micropore surface analysis system (Autosorb iQ2MP, Quantachrome) with N_2 ($10^{-7} <$ P/P0 < 1) adsorption at -196 °C. 30-50 mg of sample was placed in a 6 mm cell and degassed for

5h at 150°C to remove any moisture. BET surface area and micropore volume were determined from relative pressures ranging from 0.01 to 0.07 and 0.2 to 0.4, respectively. V-t model was used to obtain micropore volume, and pore size distribution (PSD) was obtained using the quenched solid density functional theory (QSDFT).

3.3.3 Wheeler-Jonas Equation

The Wheeler-Jonas equation has been widely used for studying organic vapor adsorption breakthrough curves onto activated carbon (Abiko et al., 2016; Lodewyckx & Vansant, 2010). The equation is simple, and its input parameters are readily available. In this study, using the Wheeler-Jonas equation, rate coefficient (K_v), breakthrough curve and amount of adsorbent were predicted for TMB adsorption onto BAC, Optipore V503, ZEOcat Z700 and ZEOcat Z603 under dry conditions. The Wheeler Jonas equation is presented below (Wood & Moyer, 1989):

$$t_b = \frac{W_e.W}{Q.C_{in}} - \frac{\rho_b.W_e}{K_v.C_{in}} \ln(\frac{C_{in}}{C_{out}})$$

Where:

t_b = breakthrough time [min]
W_e = adsorption capacity of carbon [g/g-carbon]
W = carbon bed weight [g]
C_{in} = challenge vapor concentration [g/cm^3]
C_{out} = breakthrough concentration [g/cm^3]
Q = airflow rate [cm^3/min]
ρ_b = bulk density of carbon [g/cm^3]
k_v = adsorption rate coefficient [min^{-1}]

4. Chapter Four: RESULTS AND DISCUSSION

4.1 Adsorption Isotherms

Figure 4.1 indicates the adsorption isotherms for 1,2,4-trimethylbenzene (TMB) and 2-butoxyethanol on five adsorbents. Kureha BAC is highly microporous, Optipore V503 is highly mesoporous, and the tested zeolites (ZEOcat Z700, ZEOcat F603 and ZEOcat Z400) are moderately mesoporous adsorbents as shown in Table 3.1. There is a sharp increase in the highest uptake of VOCs at low concentrations for BAC. This could be attributed to the large volume of micropores, resulting in its high affinity toward VOCs. Micropores are primarily responsible for the adsorption of gases at low concentration (Bradley & Rand, 1995). On the other hand, Optipore V503 has a large volume of mesopores which are filled at higher concentrations. Hence, for BAC and zeolites the plateau in the isotherm might be due to the fact that most of the available pores are filled by TMB (Figure 4.1 (a)) or 2-butoxyethanol (Figure 4.1 (b)). Type I isotherms according to the IUPAC classification are found for both adsorbates on each adsorbent used in this study (Thommes et al., 2015). The steep adsorption at low concentration, a characteristic of type I isotherms, suggests that BAC could be a good candidate for adsorption of VOCs at the low concentrations typically found in paint booth air streams.

Overall BAC and Optipore V503 depicted better adsorption performance compared to zeolites, at all concentration levels. However, BAC is better than Optipore V503 at lower concentrations (<200 ppm) while Optipore V503 exhibits a better performance at higher concentrations (>200 ppm). The better performance at concentrations >200 ppm for Optipore V503 is mainly due to increased affinity of large micropores and mesopores at high concentration. Jacobs et al. (1981) reported that better organisation of molecules inside the pores of Optipore V503 at high concentrations contributes to the higher amount adsorbed.
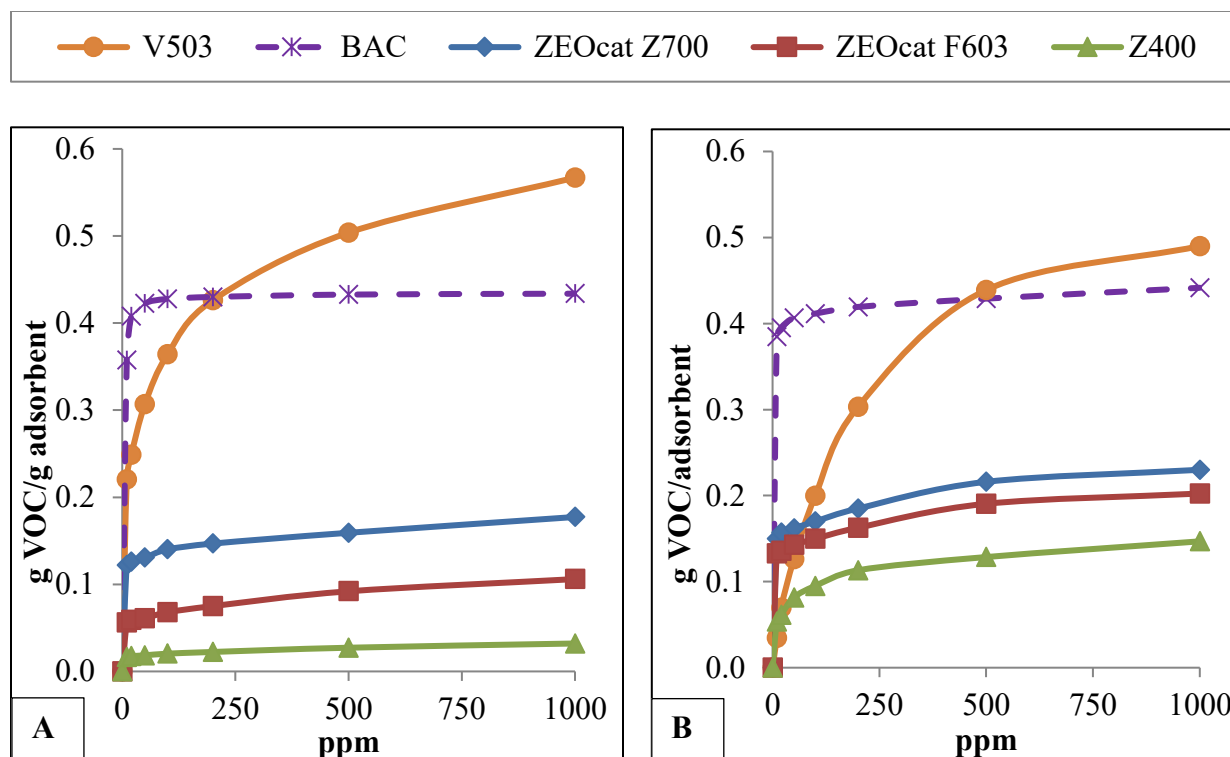
Figure 4.1 Adsorption isotherms at 22ºC: A) 1,2,4-trimethylbenzene, B) 2-butoxyethanol.

Figure 4.1 (b) shows a sharp increase in the uptake of 2-butoxyethanol at low concentrations for BAC, similar to the case of TMB. This could be attributed to the large volume of micropores, resulting in its high affinity toward 2-butoxyethanol at low concentration. On the other hand, Optipore V503 has a large volume of mesopores which are filled at higher concentrations. Overall BAC and Optipore V503 depicted better adsorption performance compared to zeolites, at all concentration levels.

Amongst the tested zeolites (ZEOcat Z700, ZEOcat F603, and ZEOcat Z400), ZEOcat Z700 (USY) depicted the best adsorption performance for all tested VOCs and concentrations (Figure 4.1). This is because ZEOcat Z700 has higher micropore volume than ZEOcat F603 and ZEOcat Z400 (Sun, 2012).

Figure 4.1 (b) shows the maximum adsorption capacity of for each zeolite is higher for 2-butoxyethanol compared to TMB. This can be due to three factors; 1) smaller kinetic diameter of 2-butoxyethanol (straight chain structure) compared to TMB (0.68 nm), which makes it easier for 2-butoxyethanol to reach the zeolite pores, 2) higher density of 2-butoxyethanol ($900kg/m^3$) compared to TMB ($876 \ kg/m^3$) and 3) stronger interaction charge on the surface of the adsorbent with 2-butoxyethanol. However, the increase in adsorption capacity between 2-butoxyethanol and TMB is greater for ZEOcat F603 and ZEOcat Z400 compared to ZEOcat Z700. This is because ZEOcat Z700 has higher Si/Al ratio than ZEOcat F603 and ZEOcat Z400, which loses a cation associated with the tetrahedrally coordinated aluminum (Wang et al., 2017). In fact, adsorption onto zeolites involves specific interaction between polar molecules and a cation which may be associated with the tetrahedrally coordinated aluminum. Therefore, the reason behind the smaller increase in adsorption capacity obtained for 2-butoxyethanol on ZEOcat Z700 compared with TMB is the influence of interaction of surface charge which is more prevalent than the kinetic diameter and density of the adsorbate. Li et al. 2010, as cited in Li et al., (2012) studied the impact of aromatic compound structure and property on adsorption capacity on ZSM-5 and found that the adsorbate polarity and molecular structure affected adsorption capacity. Indeed, TMB molecule (0.68nm kinetic diameter) is longer and larger than 2-butoxyethanol which has straight chain structure, results in $1.47x10^{-3}$ moles/g, $8.81x10^{-3}$ moles/g and $2.66x10^{-4}$ moles/g of TMB was adsorbed compared to $1.91x10^{-3}$ moles/g, $1.68x10^{-3}$ moles/g, and $1.24x10^{-3}$ moles/g 2-butoxyethanol on ZEOcat Z700, ZEOcat F603 and ZEOcat Z400, respectively. The adsorption of TMB corresponds to less number of molecule per pore intersection than 2-butoxyethanol adsorption. Similar results previously reported for adsorption of xylenes correspond to 1 molecule per pore intersection of HZSM-5 (Jacobs et al., 1981).

Amongst the three zeolites, ZEOcat Z400 (ZSM-5) depicted a very low adsorption capacity (0.032 g of TMB /g of ZEOcat Z400) at 1,000 ppm. This is because the adsorbate can only be adsorbed if its kinetic diameter is smaller than the pore diameter (Li et al., 2012). Hence, ZEOcat Z400 (pore-opening of 0.6 nm) does not allow molecules with higher kinetic diameter like TMB (0.68 nm) to pass. Whereas, with 2-butoxyethanol which has straight chain structure, the adsorption capacity increases to a maximum of 0.146 g/g for ZEOcat Z400.

4.2 Cyclic adsorption and regeneration

In order to investigate the performance of BAC, Optipore V503, ZEOcat Z700, ZEOcat F603, and ZEOcat Z400 adsorbents, adsorption and desorption experiments were carried out for five consecutive cycles. The results are discussed in terms of first cycle breakthrough curves (Section 4.2.1), adsorption capacities, and desorption performance (Section 4.2.2). To compare the adsorption performance of the five aforementioned adsorbents, adsorption cycles were completed in fixed bed configuration using single adsorbate TMB and a mixture of adsorbates (OAC SST). The detailed mass balances used to calculate the adsorption capacities, and heel buildups for each adsorbate after completing five cycle adsorption and desorption are presented in Appendix A.

4.2.1 Adsorption breakthrough curves

The term breakthrough curve refers to the response of an initially clean bed (i.e., free of adsorbate) to an influent stream of constant (i.e., time-independent) composition (Ralph T. Yang, 1987). A broader definition of the term includes a uniformly pre-saturated bed as well as an influent of changing concentration (Yang, 1987). Breakthrough curves depict the time emissions started (breakthrough time) and the time in which the adsorbent is fully saturated (saturation time). At the saturation time, the effluent concentration is the same as the influent concentration.

4.2.1.1 Single-component adsorption

The breakthrough time for adsorption of TMB was different for different adsorbents (Figure 4.2). The adsorbate effluent concentration reached 5% of its influent concentration for the first cycle adsorption at about 61, 57, 21, 12 and 0.1 minutes for BAC, Optipore V503, ZEOcat Z700, ZEOcat F603, and ZEOcat Z400, respectively. BAC showed longer breakthrough time due to its larger micropore volume compared to the other adsorbents used in this study. For a given concentration, the longer breakthrough time indicates a greater adsorption capacity (Huang et al., 2003). For zeolites, a shorter breakthrough time was expected because they have a smaller pore size in comparison with BAC and Optipore V503. For the same reason the saturation time for ZEOcat Z700, ZEOcat F603, and ZEOcat Z400 decreased to about 45, 25, and 14 minutes, respectively. Although Optipore V503 had a smaller breakthrough time compared to BAC, the saturation time of Optipore V503 was 45 minutes longer than that of BAC. This might be a result of the larger total pore volume of Optipore V503 compared to BAC.
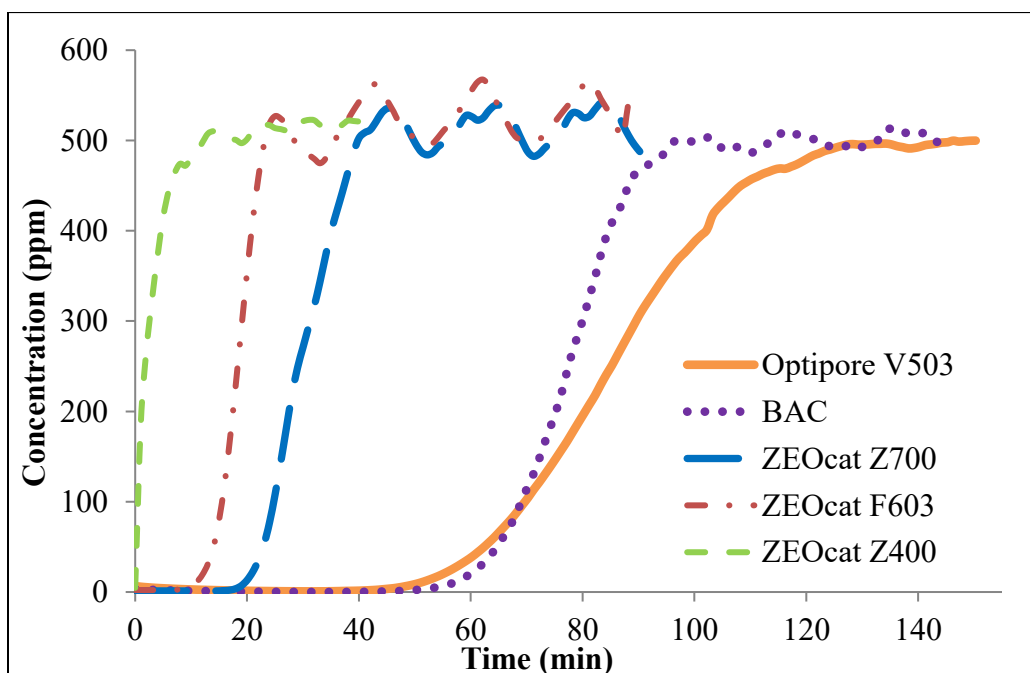

Figure 4.2. First cycle breakthrough curve for TMB adsorption.

Adsorption capacity of Optipore V503 (51%) seemed to be the highest as it adsorbed more TMB after the breakthrough time had passed up until it became saturated. The difference in the order of breakthrough time and saturation time led to the conclusion that after breakthrough time was reached for Optipore V503, there are still more pores available for VOCs adsorption until saturation time. This can be explained as the result of three factors: 1) Optipore V503 showed higher adsorption capacity due to a 61 % higher total pore volume than BAC (Long et al., 2009), 2) BAC had a longer and sharper breakthrough curve, possibly due to a higher affinity toward VOCs; and 3) Optipore V503 had predominant pore size distribution in the mesoporous region as compared to BAC, which had a significant proportion in the micropore region. Besides, Optipore V503 had shorter breakthrough time than BAC due to its larger average particle size (1mm) than BAC, which may cause some channeling.

Moreover, BAC showed a sharper breakthrough curve, which was attributed to having achieved a better mass transfer. This can be explained by calculating the throughput ratio (TPR) by using the breakthrough curves obtained for all adsorbents with the FID. TPR values ($TPR = \frac{t5\%}{t50\%}$, where $t_{5\%}$ and $t_{50\%}$ are the time required to achieve 5% and 50% breakthrough, respectively), measures how steep the breakthrough curve was during adsorption (Sullivan, et al., 2004). Higher TPR implies that transient mass-transfer limitations become less important in adsorption (Downarowicz, 2015). Table 4.1 shows that BAC has the highest TPR (0.79) due to its strong affinity for VOCs. Previous research also reported similar TPR values (0.74) for TMB adsorption onto BAC using fixed-bed configuration (Kamravaei et al., 2017).

Table 4.1 Breakthrough time and throughput ratio for TMB

Adsorbate and adsorbent type	Breakthrough time (min.)	Throughput ratio $TPR = \dfrac{t_{5\%}}{t_{50\%}}$
TMB on Optipore V503	57.9	0.67
TMB on BAC	61.0	0.79
TMB ZEOcat Z700	21.2	0.73
TMB ZEOcat F603	12.5	0.68
TMB ZEOcat Z400	0.1	0.06

4.2.1.2 Multicomponent adsorption

Most emissions from industrial sources, especially from paint booth, contain mixture of organic compounds covering wide range of functional groups and physical properties. A mixture of VOCs (OAC SST) was used to test adsorption and regeneration on the five different adsorbents.

The first cycle adsorption breakthrough profile for OAC SST on the five adsorbents is shown in Figure 4.3. The breakthrough times for the first adsorption cycle of OAC SST on BAC, Optipore V503, ZEOcat Z700, ZEOcat F603, and ZEOcat Z400 were recorded at about 64, 42, 22, 11, and 1 minutes, respectively. Optipore V503 breakthrough time was earlier than the breakthrough time for BAC, which may be because of Optipore V503 has lower micropore volume compared to BAC. This indicates that the mixture of VOCs during adsorption on Optipore V503 started penetrating at about 42 minutes, which is 10 minutes earlier than the breakthrough time need during TMB adsorption on V503. The difference in breakthrough time of TMB and OAC SST adsorption on V503 might be because of competitive adsorption,

whereby VOCs molecules with a lower affinity to strongly hydrophobic adsorbents like Optipore V503 start penetrating early from the adsorbent bed.
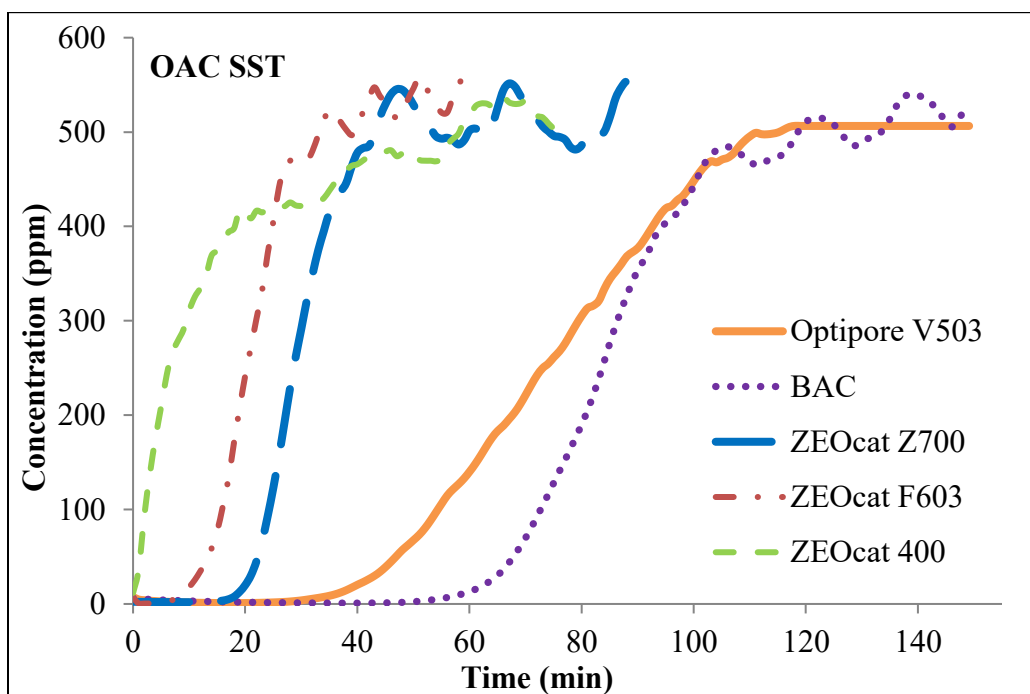
Figure 4.3 First cycle breakthrough curve for OAC SST adsorption**.**

Moreover, BAC showed a sharper breakthrough curve, which was attributed to achieving better mass transfer, as discussed in the previous section. Table 4.2 shows that BAC has highest TPR, due to its largest micropore followed by ZEOcat Z700, ZEOcat F603, Optipore V503, and ZEOcat Z400.

Table 4.2 Breakthrough time and throughput ratio for OAC-SST

Adsorbate and adsorbent type	Breakthrough time (min.)	Throughput ratio $TPR = \dfrac{t_{5\%}}{t_{50\%}}$
OAC-SST V503	41.6	0.57
OAC-SST BAC	63.9	0.76
OAC SST-ZEOcat 700	20.5	0.72
OAC SST-ZEOcat F603	11.0	0.54
OAC SST-ZEOcat Z400	1	0.09

The breakthrough time did not change considerably (less than 2% change) for TMB in all five cycles of adsorptions (Figure 4.4). This shows that the adsorbents maintain their adsorption capacity to a great extent throughout the five cycles, suggesting that adsorption is reversible, adsorption capacity can be completely recovered with thermal regeneration, and heel buildup is negligible. This is consistent with previous studies completed under similar conditions (Kamravaei et al., 2017; Salvador et al., 2015). On the other hand, for OAC-SST, the breakthrough time decresaed following the first adsorption cycle (Figure 4.4). This could be attributed to heel buildup that leads to a loss in adsorption capacity of the adsorbents over successive cycles and competitive adsorption among the constituents of of OAC-SST mixture.

A — TMB on BAC
B — OAC SST on BAC
C — TMB on V503
D — OAC SST on V503
E — TMB on ZEOcat Z700
F — OAC SST on ZEOcat Z700
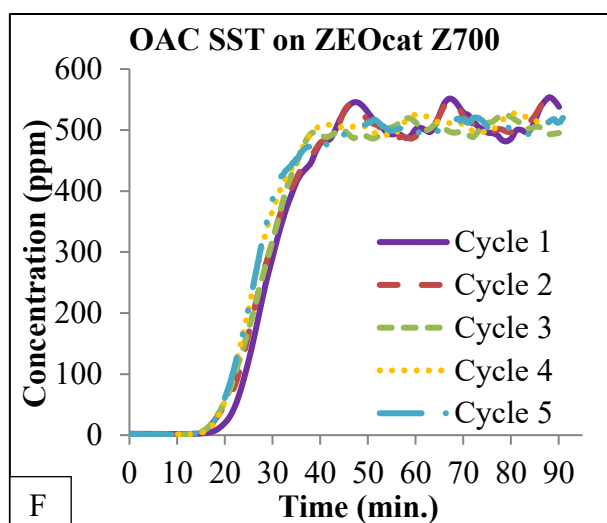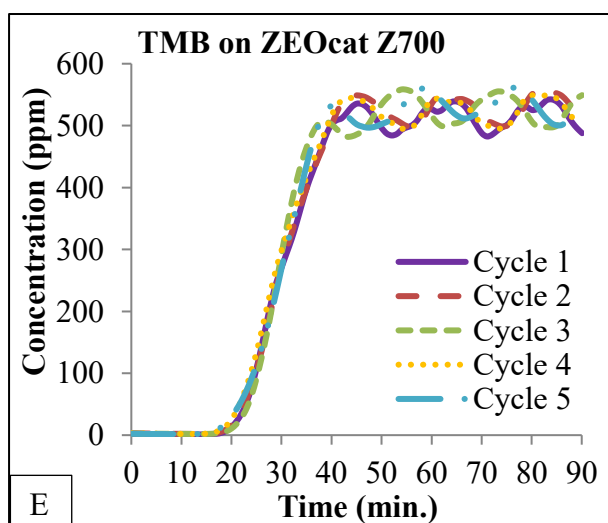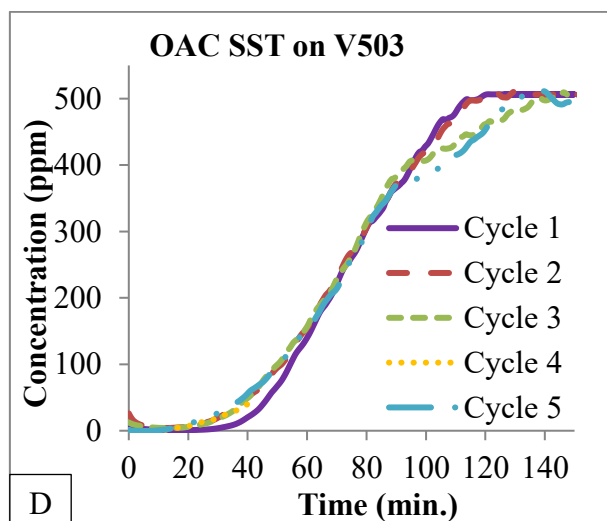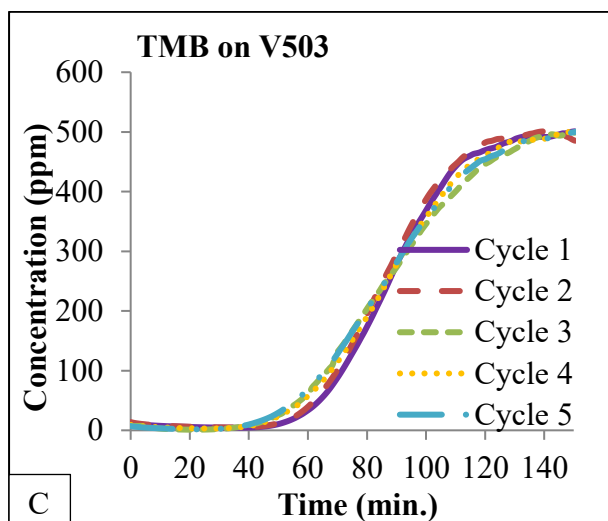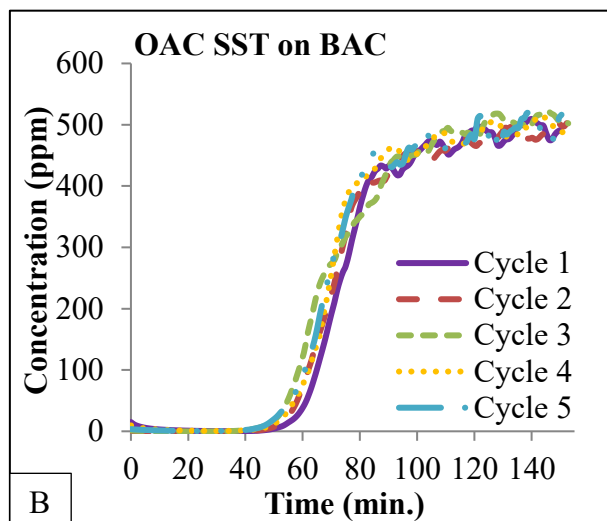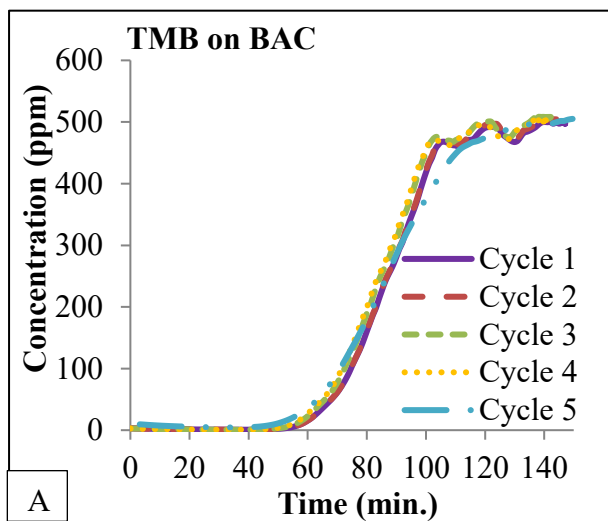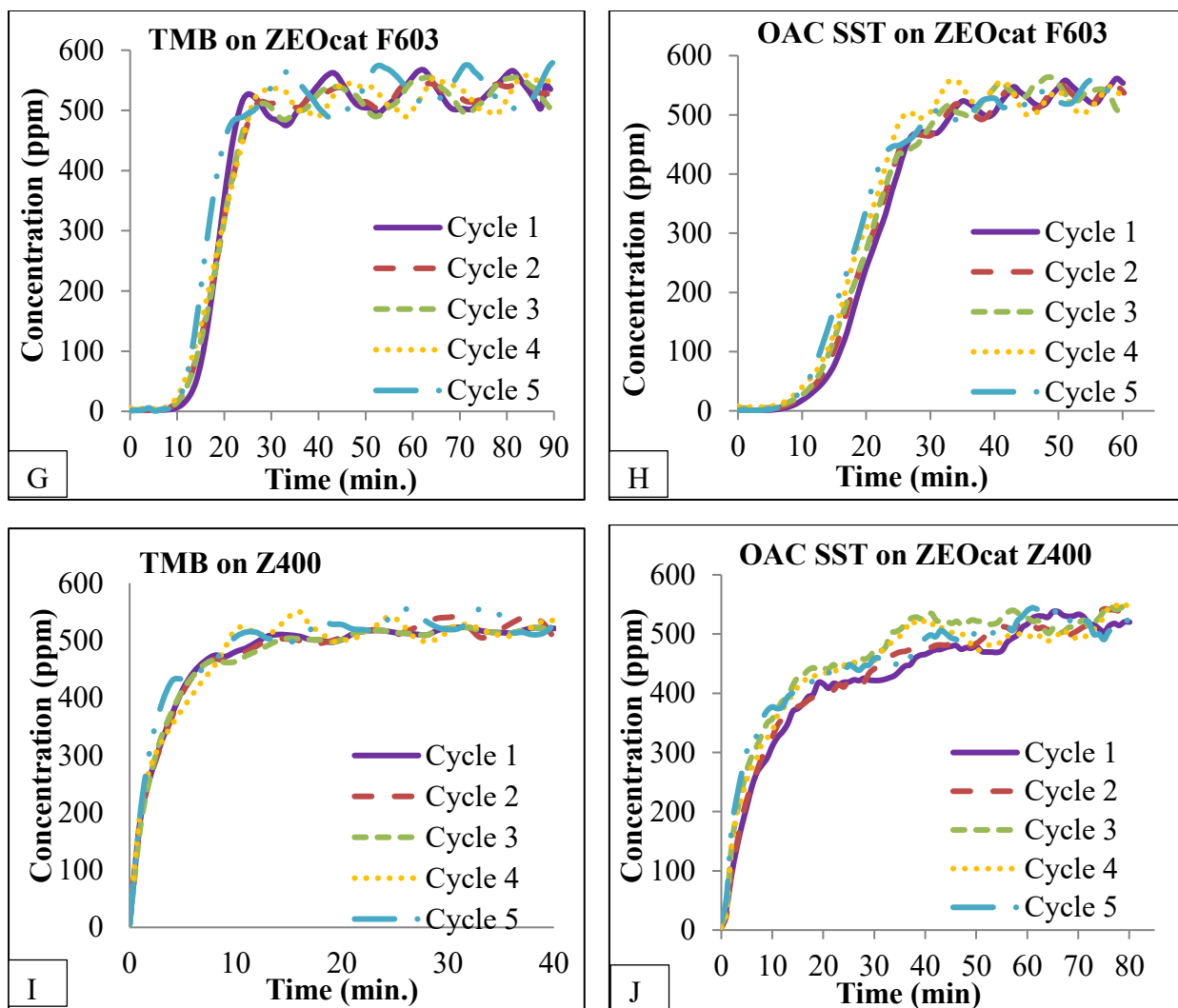
Figure 4.4 Breakthrough curves for five consecutive adsorption cyclesof TMB (A, C, E, G and I) and OAC-SST(B, D, F, H and J) on BAC, Optipore V503, ZEOcat Z700, ZEOcat F603 and ZEOcat 400.

4.2.2 Mass balance calculations
4.2.2.1 Adsorption capacity

The adsorption capacity of each cycle can be quantified by mass balance calculations before and after adsorption. Mass balance adsorption capacities for all five cycles are presented in Figure 4.5 (detailed results are presented in Appendix A). The results showed TMB first cycle adsorption capacities of 51% and 45.1% for Optipore V503 and BAC, respectively. The higher adsorption capacities for Optipore V503 could be attributed to a 60% larger total pore volume

compared to BAC (Long et al., 2009). Huang et al., (2003) showed higher surface area also resulted in higher adsorption capacity when the concentration was higher than 100 ppm for methyl ethyl ketone and benzene vapors adsorption on activated carbon fiber. Zeolites showed much lower adsorption capacities than Optipore V503 and BAC. Zeolites having the lowest adsorption capacity might be because of having the lowest total pore volume compared with BAC and Optipore V503. In contrast to first cycle adsorption of OAC-SST on ZEOcat Z700, ZEOcat F603 and ZEOcat Z400, Optipore V503 showed a lower first cycle adsorption capacity for OAC-SST than TMB. The lower adsorption capacity for OAC-SST on Optipore V503 might be due to pore obstructions by the first larger molecules adsorbed from the mixture, or the increased accessibility of pore size in zeolites.
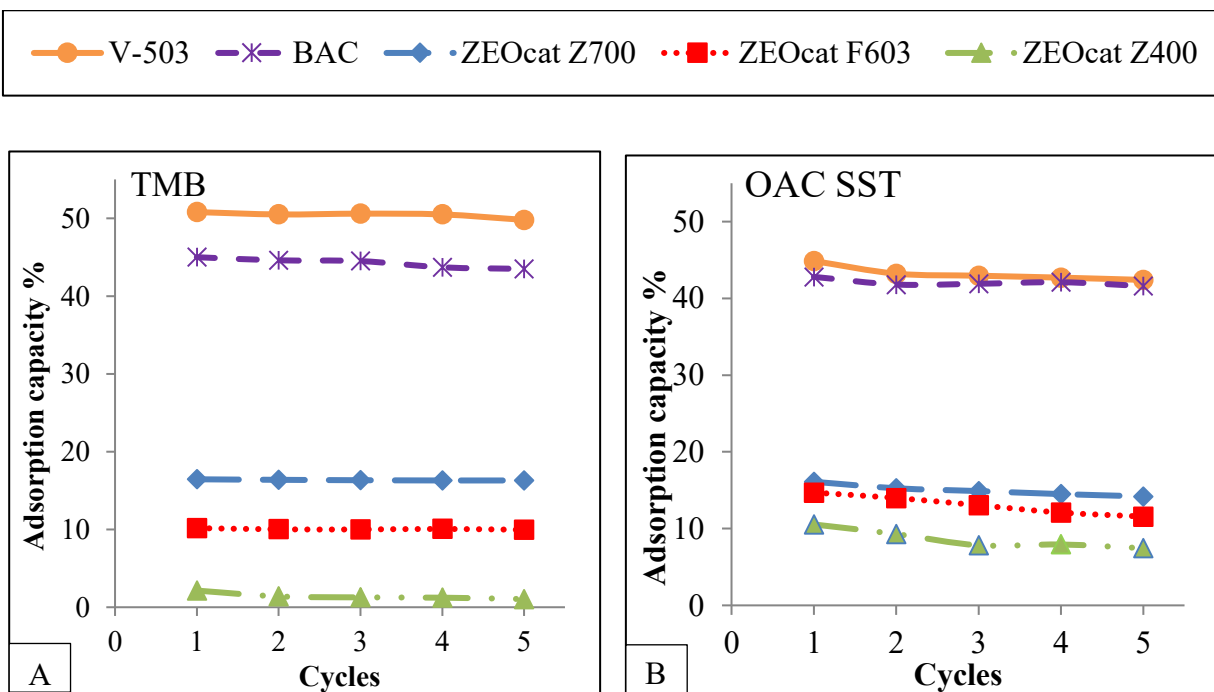
Figure 4.5 Adsorption capacity of different adsorbents for TMB (A) and OAC-SST (B)

Generally, the adsorption capacity gradually deteriorates if the adsorbent builds heel over successive adsorption/regeneration cycles. This heel build-up results in pore blockage and significantly reduces available adsorption sites (Lashaki et al., 2012). As accessible sites

decrease, adsorption capacity decreases. Therefore, for all tested adsorbents, the adsorption capacity during adsorption of OAC SST showed reduction over successive cycles, unlike the case of TMB. This might be attributed to the heel build up after each adsorption/regeneration cycle.

The adsorption capacity for the adsorbates mixture increased for ZEOcat F603 and ZEOcat Z400 but not for ZEOcat Z700. This might be because OAC-SST is mainly comprised of polar compounds which have less affinity towards the hydrophobic ZEOcat Z700 as compared to ZEOcat F603 and ZEOcat Z400. Additionally, for a given pore diameter distribution, the kinetic diameter of the adsorbate affects adsorption capacity. The adsorbate can be adsorbed only if the pore diameter (effective adsorbent pore diameter) is larger than the adsorbate kinetic diameter. However, if the pore diameter is significantly larger than the adsorbate kinetic diameter, the adsorption capacity is small due to the pore actually acts as a channel (Li et al., 2012; Tukur & Al-Khattaf, 2012). Therefore, TMB molecules having a kinetic diameter of (~0.68 nm) are more selectively adsorbed by USY ZEOcat Z700 (0.74 nm) than molecules having different sizes in a mixture of OAC-SST.

4.2.2.2 Regeneration efficiency

The heel buildup for different adsorbents used in this study to adsorb TMB and OAC-SST are presented in Figure 4.6. For both TMB and OAC SST, mass balance cumulative heel buildup for Optipore V503 is noticeably lower compared to the other adsorbents in this study, although the desorption temperature used for V503 was 80°C lower than the desorption temperature used for the other adsorbents. Along the same lines, Baya et al., (2000) also showed eight different VOCs desorbed at 210°C from polymeric adsorbents. Meng et al., (2014) proposed that this was related to the lower heat of adsorption for polymeric adsorbents. This

lower heat of adsorption also reduces the time required for desorbing the VOCs which reduces the nitrogen purge gas consumption, making the process more cost competitive. Previous literature also suggested short regeneration cycle times for activated carbon allow the process to be cost competitive (Sullivan et al., 2004). Mass balance heel buildup for five adsorption/regeneration cycles was also negligible for TMB on all adsorbents. Lashaki et al., (2016) demonstrated that heel formation was linearly correlated with BAC micropore volume.

Zeolites showed less than 1 % cumulative heel after five cycles of TMB adsorption and desorption which makes for cyclic adsorption/desorption. However, as discussed above, they have lower adsorption capacities than BAC and Optipore V503.
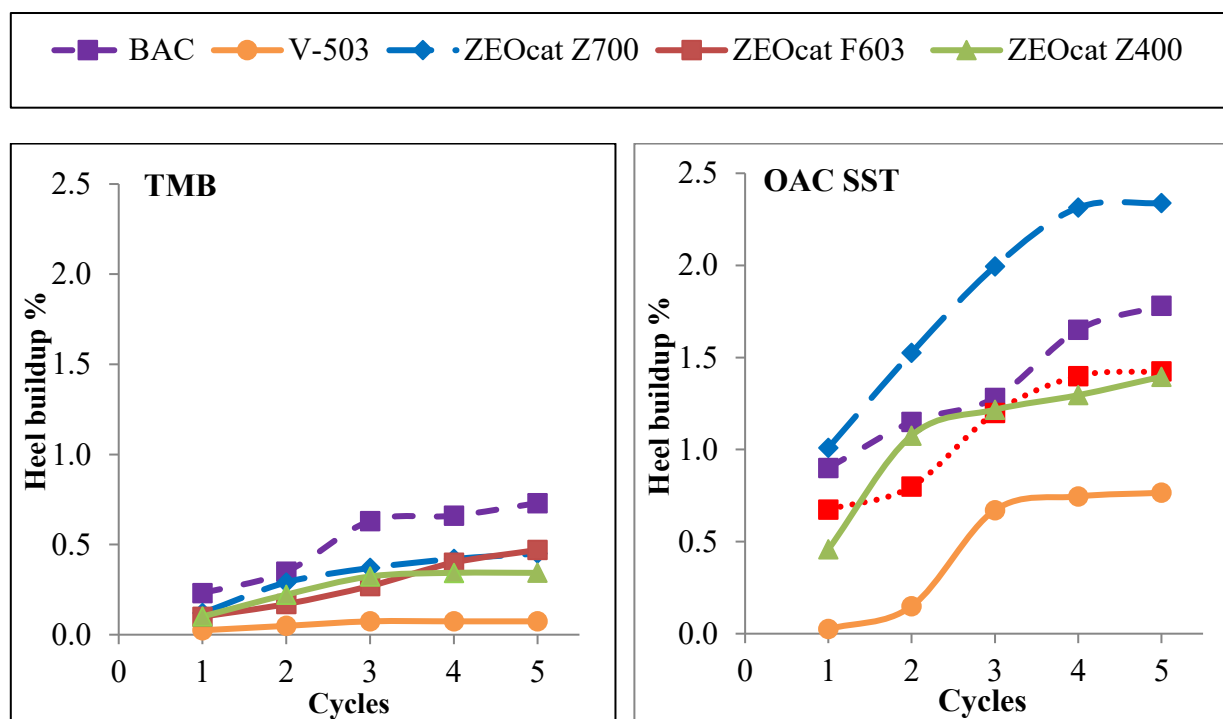
Figure 4.6 Mass balance heel build-up for different adsorbents.

In the case of OAC-SST, BAC, Optipore V503 and zeolites showed larger cumulative heel buildup compared to TMB. This might be due to strong interactions between high molecular weight compounds and the surface of adsorbents occurring after displacing the lighter molecules.

This leads to the conclusion that due to competition for a strong affinity for the surface, more energy is needed to remove adsorbed VOCs during regeneration (Kamravaei et al., 2017). Therefore, 288°C desorption temperature or 3 hours regeneration time might not be enough to remove OAC SST from BAC and zeolites.

4.2.3 Thermo-gravimetric analysis (TGA)

Adsorbents were analyzed with thermo-gravimetric methods before adsorption (virgin) as well as after five cycles of adsorption and regeneration of TMB and OAC SST for all adsorbents tested in this study. The adsorbent sample was heated up to 900°C in a TGA to desorb strongly adsorbed compounds from adsorbents. Based on the strength of interaction between adsorbent and adsorbate, the adsorbates will be desorbed at different temperatures. The sample weight loss with respect to temperature is demonstrated in Figure 4.7. Obtained results were sketched on the same figure for single and multicomponent adsorbates for each adsorbent for easier comparison.

TGA result in Figure 4.7 (a), (E), (G) and (I) depict more weight loss for OAC-SST than TMB for all adsorbents. However, Figure 4.7 (C) shows Optipore V503 loses 70% of weight due to its limited thermal stability at higher temperature as indicated by the weight loss of the virgin Optipore V503. Between 300-400ºC, OAC-SST loaded samples showed mass loss of approximately 2%, 2.5%.1.5% and 1.5% for BAC, ZEOcat Z700, ZEOcat Z400 and ZEOcat F603, respectively.

Multiple DTG peaks at different temperatures reflect the strength of adsorption and physisorption/chemisorption (Joly, 2006). Except for Optipore V503, the adsorbent used in this study showed very good thermal stability. The TGA results showed the capability of BAC to withstand temperature up to 700ºC and zeolite adsorbents up to 900ºC. Figure 4.7 (C) shows Optipore V503 loses 70% of weight due to its limited thermal stability between 350-500ºC as indicated by the weight loss of the virgin Optipore V503. This prevents further investigation of accumulated non-desorbed adsorbates on Optipore V503 at temperature higher than 350ºC due to material loss of the adsorbent itself.

The first peak which appeared at temperature lower than 100ºC in the DTG plot is related to water removal since some water vapor can be adsorbed before analysis (Popescu, 2003). Zeolites adsorbent showed more water adsorption compared to other adsorbents used in this study due to its higher affinity to adsorb humidity.
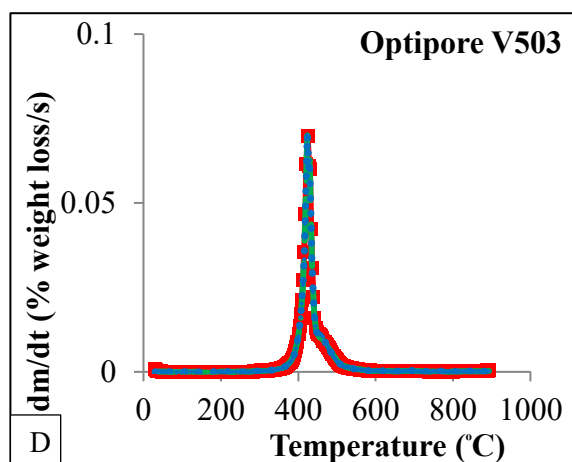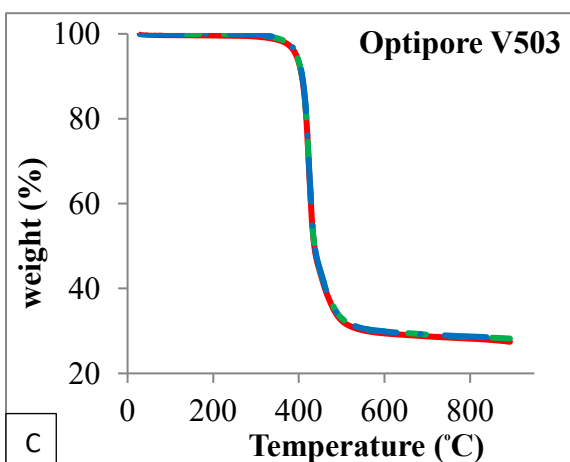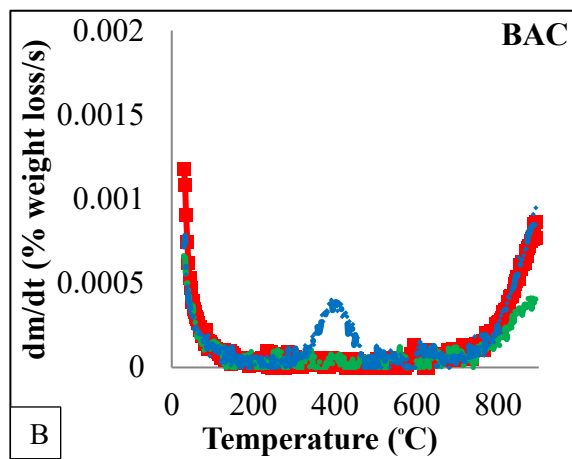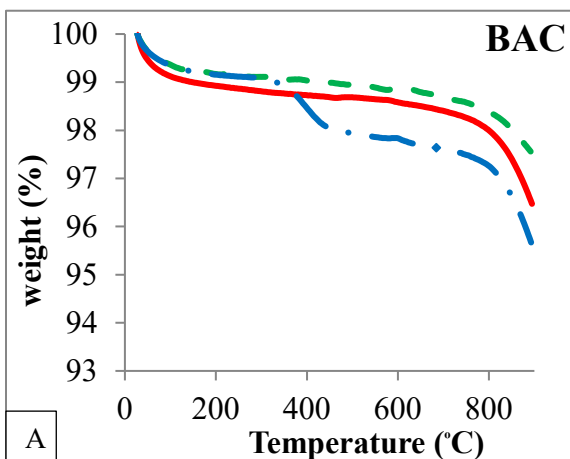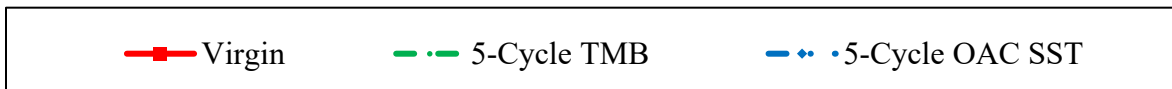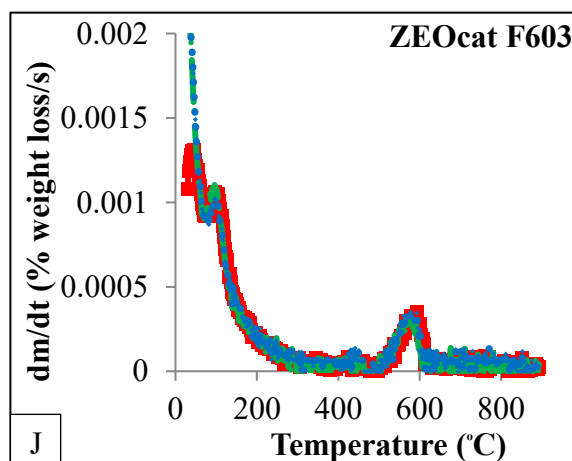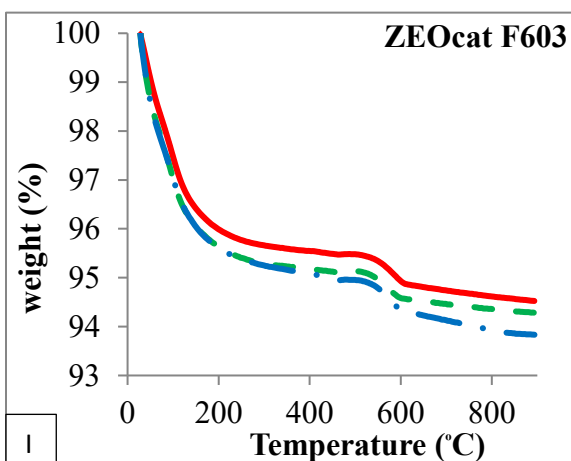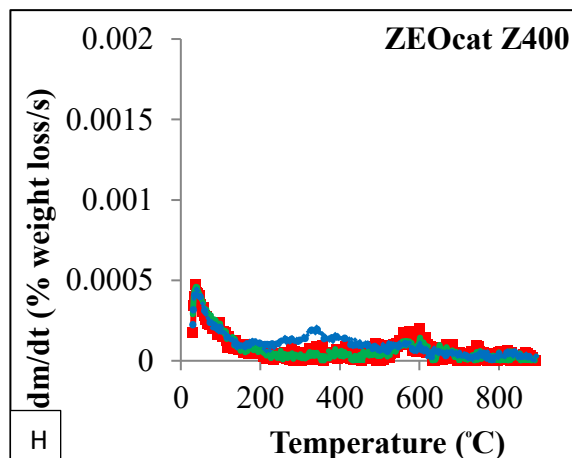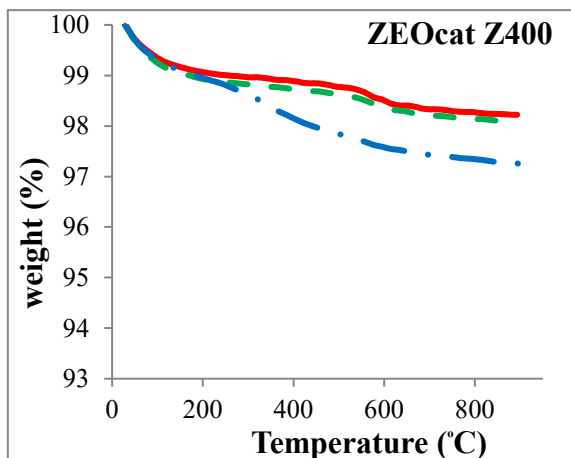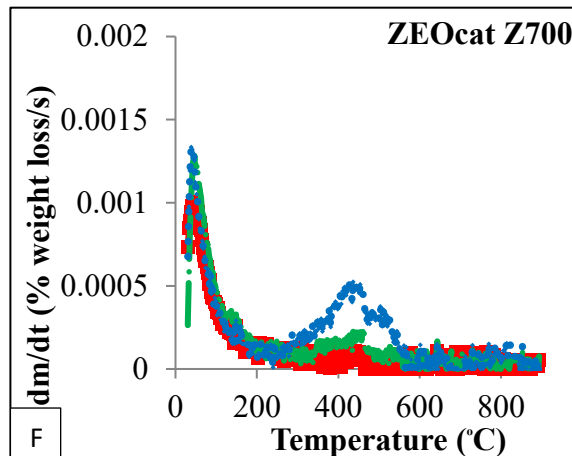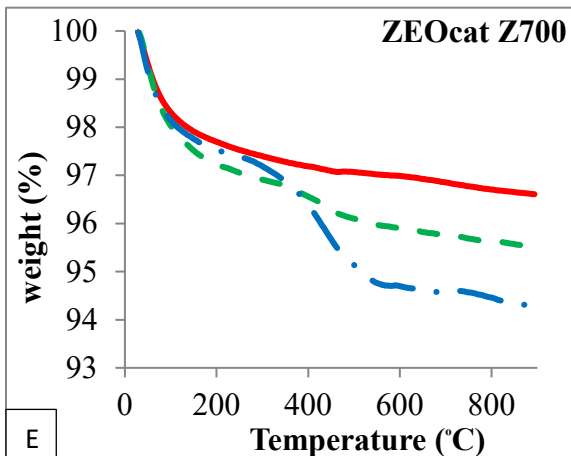
Figure 4.7 TGA (A, C, E,G, and I) and DTG (B,D,F,H and J) for adsorbents before (virgin) and after five adsorption/regeneration cycles.

Figure 4.7 also depicts higher weight loss between 300-400°C for BAC and ZEOcat Z700 compared to the other two zeolite, which can be attributed to the presence of more accumulated adsorbates with strong interactions that could not be desorbed at 288°C during regeneration. A higher temperature was needed to remove them from the adsorbents; this is because high boiling points and/or high molecular weights adsorbates have displaced lighter adsorbates and possibly form strong interaction with surface of the adsorbents. Previous researchers reported that heavier compounds have higher adsorption affinity on BAC than lighter compounds (Kamravaei et al., 2017; Wang et al., 2012).

4.2.4. Wheeler-Jonas analysis

The Wheeler-Jonas equation is commonly used to obtain rate constant for the adsorption process (Kv, min^{-1}) on activated carbon (Wood, 2002). In this study, Wheeler-Jonas equation is used to determine TMB adsorption rate constant K_v and fitting breakthrough curve as shown in Table 4.3 and Appendix D, respectively. BAC, ZEOcat Z700 and ZEOcat F603 shows higher Kv value than Optipore V503. The K_v value difference might be due to Kureha BAC is highly microporous and the tested zeolites (ZEOcat Z700, ZEOcat F603 and ZEOcat Z400) are moderately mesoporous whereas Optipore V503 is highly mesoporous. Lodewyckx (2002) as cited in (Lodewyckx, 2014), reported very small diameters and the large micropores surface of activated carbon fibres results in very high K_v values using the Wheeler-Jonas equation.

Table 4.3 TMB Adsorption rate constant based on the Wheeler-Jonas equation

Adsorbent	Adsorption rate coefficient (K_v) (min^{-1})
BAC	23,815
Optipore V503	10,525
ZEOcat Z700	23,251
ZEOcat F603	23,392

Kim (2011) reported a VOC concentration in the paint booth air of 50 to 200 ppmv. Assuming a VOC concentration of 100 ppmv as TMB, and a hypothetical flow rate of 1000 m^3/min, the Wheeler -Jonas equation was used with the adsorption rate coefficients (Table 4.3) to calculate the amount of adsorbent required to capture all of the VOCs from paint booth airstream for 24 hr. The amount of each adsorbent is shown in Table 4.4. Based on these calculations, using BAC would require the least amount of adsorbent to adsorb 100ppm of TMB as compared to the zeolites and polymeric adsorbents tested in this study.

Table 4.4 Amount of adsorbent required for TMB adsorption.

Adsorbent	Calculated adsorbent weight (kg)
BAC	1,991
Optipore V503	9,991
ZEOcat Z700	24,577
ZEOcat F603	53,031

4.3 Adsorption under dry and humid conditions

4.3.1 Water vapor adsorption isotherms

Figure 4.8 demonstrates water vapor adsorption isotherms on BAC, Optipore V503, ZEOcat Z700, ZEOcat F603, and ZEOcat Z400. For zeolites (ZEOcat Z700 and ZEOcat F603), Water vapor adsorption started from 10% of RH which suggests that water can compete with

both polar and non-polar solvents during coadsorption, which reduces VOC uptake. On the other hand, for BAC, adsorption of water vapor is negligible below 50% RH, and starts after 50% RH. After 60% RH, instead of adsorption capillary condensation starts, and more water molecules get into the pore to fill the space until it becomes saturated as shown in a plateau surface at the end of the isotherm (Brennan et al., 2001). For the other adsorbents also, the isotherms after 60% RH are concave upward which signals the commencement of capillary condensation (Chen, 1976). Kim et al., (2016) showed the same result after indistinct inflection; the adsorbed amount of water almost linearly increased with increasing relative pressure until it steeply increased by multilayer condensation. The water vapor adsorption isotherm was type V for BAC and type III for the zeolite and polymeric adsorbents used in this study (Figure 4.8). The mechanism of water vapor adsorption onto BAC begins with adsorption on the functional groups known as primary adsorption sites at the surface of the functional group of the adsorbent, followed by adsorption on the previously adsorbed water molecules, then pore filling and saturation at high relative humidity (Brennan et al., 2001). The observed trend for water vapor adsorption on BAC is consistent with the mechanism of physical adsorption at the surface and cluster formation between water molecules. In section 4.3.2, the effect of water vapor during co-adsorption with VOCs will be presented and compared to these results.
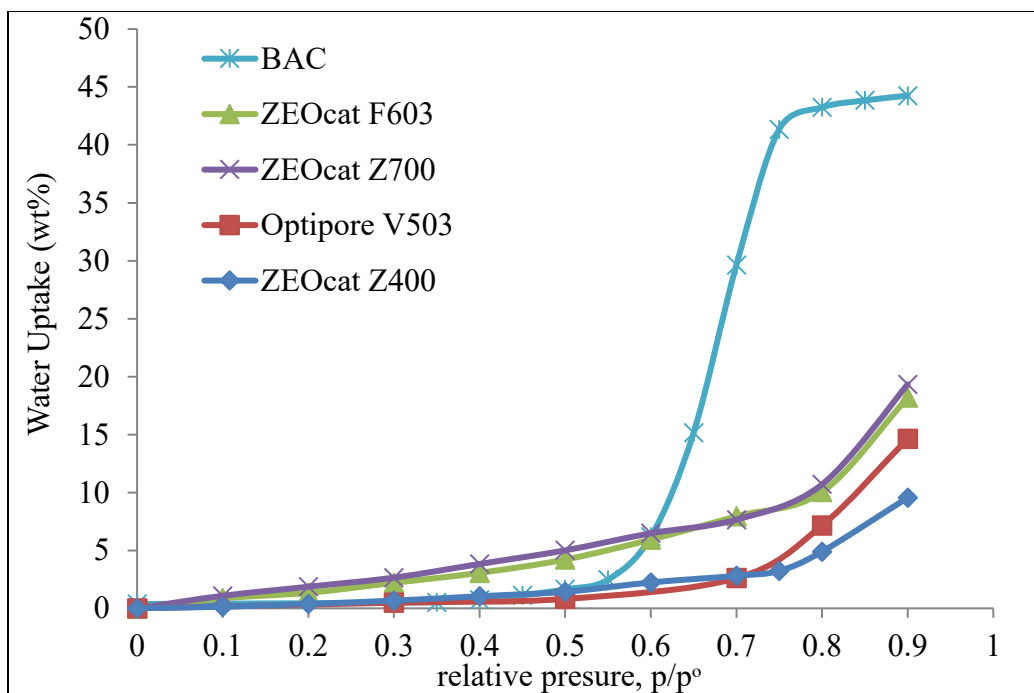
Figure 4.8. Water vapor adsorption isotherms at 25°C.

For Optipore V503, low moisture uptake was recorded even at high relative humidity such as 90% RH, which indicates that water is unlikely to compete with VOCs for the available adsorption sites. This low adsorption of water vapor contributes to lower energy requirement during regeneration since the energy needed is only that required to remove solvents from the adsorbent.

4.3.2 Effect of water vapor on VOCs adsorption

Adsorption breakthrough curves for TMB at dry and high relative humidity (75% RH) on BAC, Optipore V503, ZEOcat Z700, ZEOcat F603, and ZEOcatZ400 are shown in Figure 4.9 All the figures in these sections demonstrate the breakthrough curves of an initial concentration of TMB of 500 ppm. The effect of humidity on the adsorption breakthrough curve at the given relative humidity is almost negligible for BAC and Optipore V503. This is because BAC and Optipore V503 are hydrophobic adsorbents. Since water is a polar molecule; its affinity for a non-polar surface adsorbent such as activated carbon and the Optipore V503 used in this study is

much lower than TMB. Biron & Evans, (1998) showed that molecules with high affinity to the carbon surface, whether soluble or not, were less influenced by the presence of water. However, the effect of moisture on ZEOcat Z700 and ZEOcat F603 is noticeable and resulted in an earlier breakthrough because of coadsorption of humid with TMB. In the case of ZEOcat Z400 it seems that water vapor also has an influence on the breakthrough but because of the low adsorption capacity for TMB, the breakthrough comes early and the effect can't easily be shown from the breakthrough curve. But in general, all commonly known zeolites show strong affinity for water (Chen, 1976).
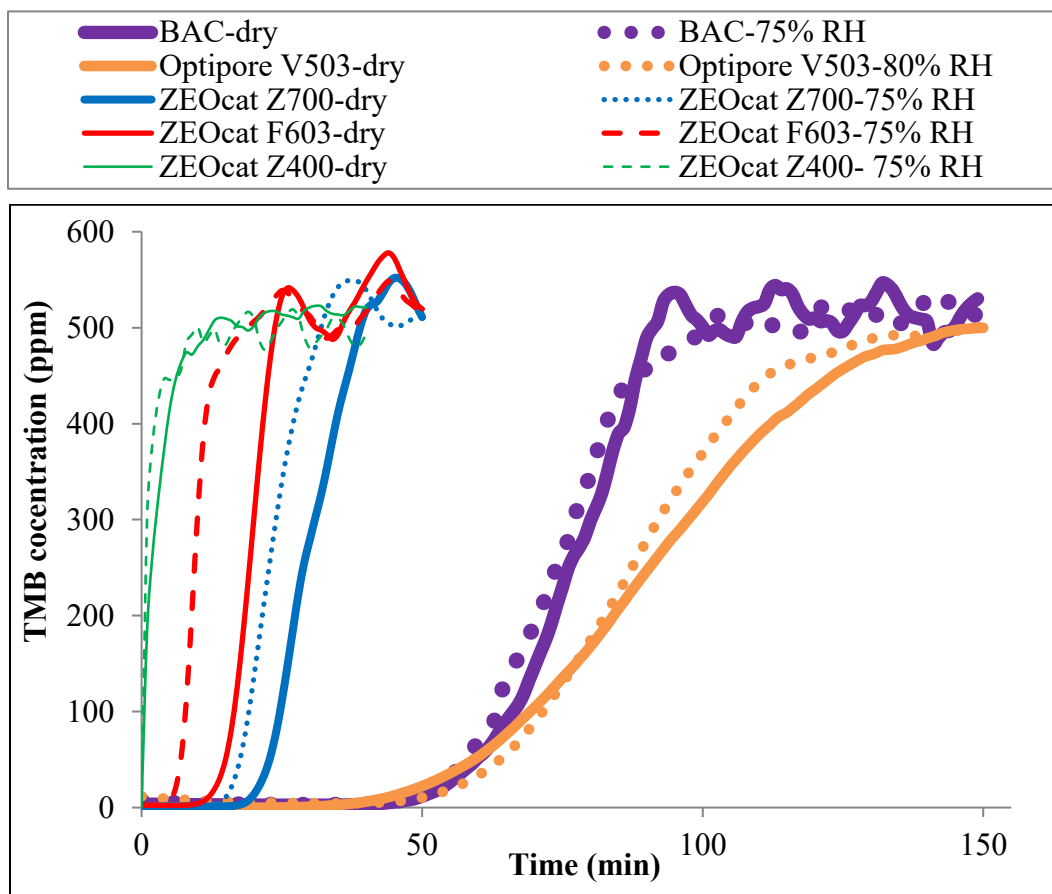
Figure 4.9. Adsorption of TMB at dry and humid condition

The mass balance results shown in Figure 4.10 indicates that at the RH used, the influence of humidity on TMB adsorption was neglegible (<2%) for BAC and Optipore V503,

but important for ZEOcat Z700 and ZEOcat F603(28% and 48%, respectively). This is because BAC and Optipore V503 are strong hydrophobic adsorbent. Therefore TMB is preferred over water vapor by both adsorbents. However, zeolites have a charge on their surface, which is the main reason for attracting water molecules, thus resulting in a reduction of adsorption capacity of TMB due to competitive adsorption of water vapor.
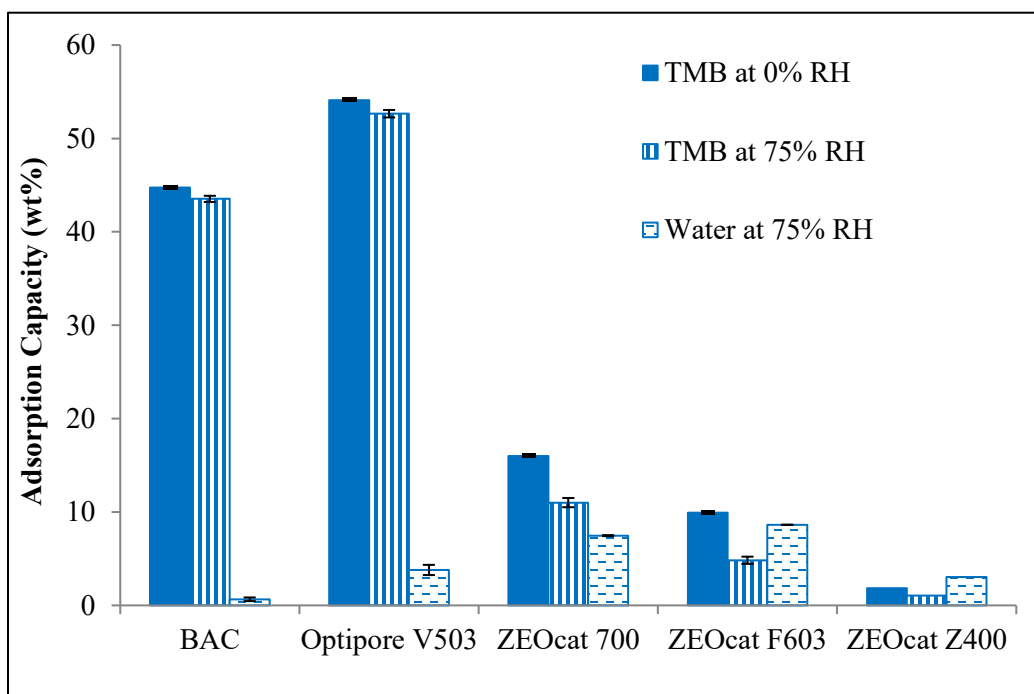
Figure 4.10. Mass balance for TMB and water vapor adsorption.

Based on the results discussed in this section, ZEOcatZ700 and ZEOcat F603 are considerably affected by humidity. Therefore, further investigation of the effect of humidity on VOC adsorption on these two zeolites was completed using breakthrough curve and uptake of polar and non-polar VOCs at three different relative humidity conditions.

4.3.3 Effect of water vapor on adsorption of polar and nonpolar VOC.

The adsorption breakthrough curves of TMB and 2-butoxyethanol onto ZEOcat F603 and ZEOcat Z700 under three relative humidity conditions are shown in Figure 4.11 and Figure 4.12,

respectively. The inlet VOC concentration was 500 ppm and the RH investigated were 0%, 45% and 75% RH. As shown in Figure 4.11, the breakthrough time of TMB on ZEOcat F603 decreased from 13.5 minutes in dry conditions to 8.6 and 6.2 minutes under 45% RH and 75% RH conditions, respectively. The breakthrough time at high humidity is less than that at low humidity (see Figure 4.11). Because the active sites of ZEOcat F603 may have been occupied by water molecules at higher humidity conditions, the entire mass transfer zone (MTZ) velocity increased, and consequently, the breakthrough time decreased with increasing relative humidity (Huang et al., 2003).
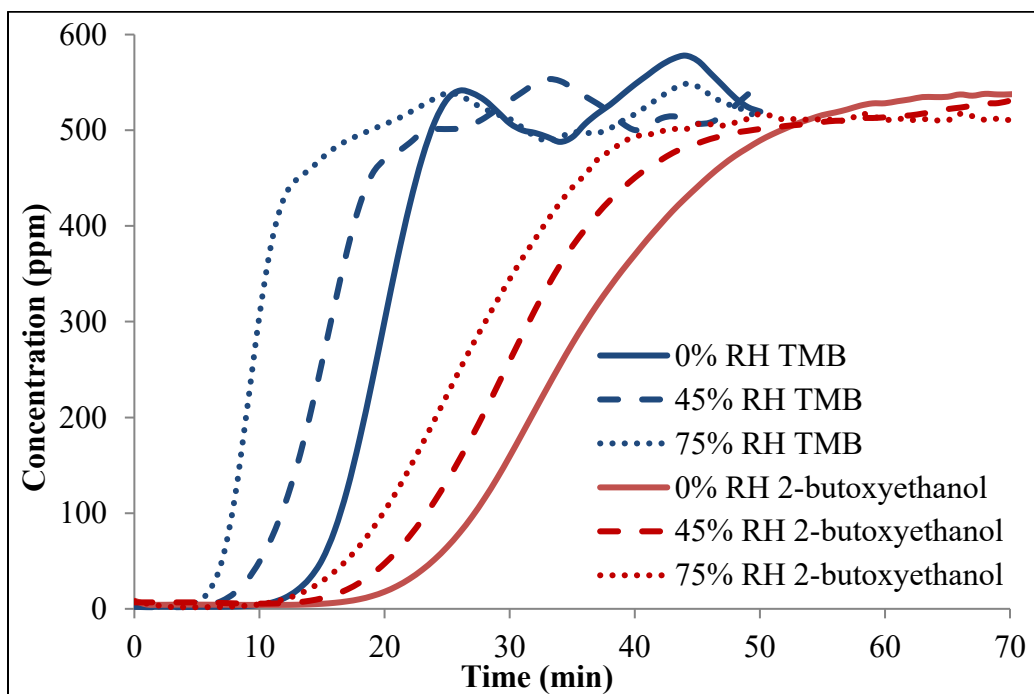
Figure 4.11 Adsorption breakthrough curves for TMB and 2-butoxyethanol onto ZEOcat F603 at different RH

In this study, comparison of breakthrough time was used to determine the performance of the adsorbents during VOC adsorption and the extent of humidity effect by calculating lead-time percentages (LPs). LPs are the extent of the early appearance of the breakthrough curve (Tao et al., 2004). Larger LP value means water vapor highly affect the breakthrough time of VOC

adsorption while smaller LP value indicates the effect of water vapor on VOC breakthrough time is low. Lps are defined as follows:

$$LP = (1 - t_{5\%H} / t_{5\%H=0}) * 100)$$

where $t_{5\%H}=$ is the breakthrough time (min) (at C/Co=0.05) of VOC adsorption in the presence of water vapor, and $t_{5\%H=0}$ is the breakthrough time (min) of the VOC adsorption without water.

As shown in Figure 4.11, the breakthrough time of ZEOcat F603 was strongly affected by humidity probably due to its lower Si/Al ratio (Stelzer et al., 1998). As a result of the charges on ZEOcat F603, it possibly has more affinity to attach polar adsorbate from a gas stream. This implies, during coadsorption of polar and non-polar compounds, water and TMB, the more strongly adsorbate water enter the pore than TMB to the surface of ZEOcat F603 (Lee et al., 2008). Additionally, the influence of water vapor is considerably higher than 2-butoxyethanol, probably because 50% of ZEOcat F603 being composed of ZSM-5. Consequently, TMB encounters a problem entering the pore-openings of ZEOcat F603 due to size exclusion. Furthermore, 2-butoxyethanol was relatively less affected by increasing the RH from 45% to 75 %RH compared to probably due to differences in polarity of TMB and 2-butoxyethanol which determines solubility in water. Similar results have been reported whereby the presence of moisture is also responsible for the promotion of adsorption of water-soluble vapors due to generation of a liquid film on activated carbon adsorbent (Okazaki et al., 1978).

Table 4.5 shows that, for ZEOcat F603, the LPs using TMB are higher than those obtained using 2-butoxyethanol, and there seems to be a tendency for LPs to increase with increasing relative humidity. When comparing LP values at low RH (45%) of TMB to the

highest RH (75%) of 2-butoxyethanol, TMB has 12.0% higher LP value than 2-butoxyethanol. This is probably due to the contribution of factors such as Si/Al ratio, kinetic energy distribution of the adsorbate molecules, shape of the adsorbate and size and pore path of the adsorbent (Gong & Keener, 1993b). Since adsorption of 2-butoxyethanol onto ZEOcat F603 has lower LP values even at 75% RH, it is probable that ZEOcat F603 is more suitable for polar VOC adsorption at high RH condition.

Table 4.5 Breakthrough properties of ZEOcat F603 at 0%, 45% and 75% RH

Adsorbates and adsorbent type	Breakthrough time (min.)	Throughput ratio (TPR)	Lead time percentage (%)
Dry TMB ZEOcat F603	13.5	0.70	-
45% RH TMB ZEOcat F603	8.6	0.58	35.80
75% RH TMB ZEOcat F603	6.2	0.66	53.98
Dry 2-butoxyethanol ZEOcat F603	21.2	0.63	-
45% RH 2-butoxyethanol ZEOcat F603	17.7	0.59	16.44
75% RH 2-butoxyethanol ZEOcat F603	14.5	0.56	31.37

The adsorption breakthrough curves for TMB and 2-butoxyethanol onto ZEOcat Z700 are presented in Figure 4.12 under the selected humidity conditions. The change in breakthrough time at 75 %RH was only 4 % earlier than breakthrough time at 45 %RH of the gas stream. The effect of humidity on VOC adsorption on ZEOcat Z700 is low compared to ZEOcat F603, probably due to the hydrophobicity of ZEOcat Z700 and its higher Si/Al ratio.
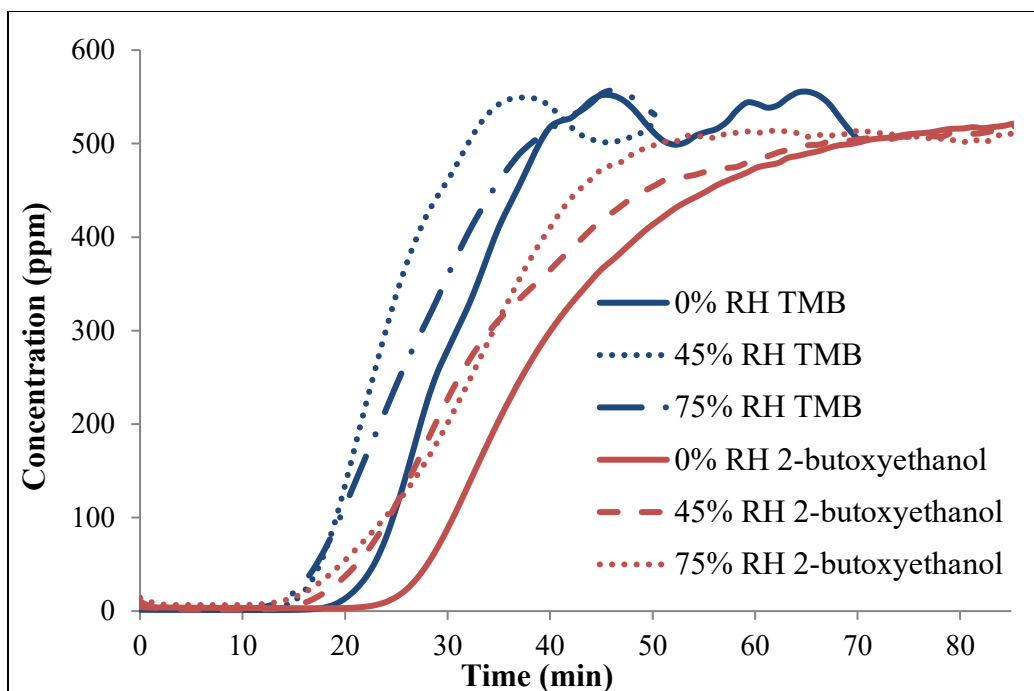
Figure 4.12 Adsorption breakthrough curves for TMB and 2-butoxyethanol onto
ZEOcat Z700 at different RH

Table 4.6 shows that for ZEOcat Z700, the values of LP using TMB are lower than those
for 2-butoxyethanol. The fundamental physical differences between the adsorbates may be used
to explain these differences. One significant difference between TMB and 2-butoxyethanol is
molecular polarity (Gong & Keener, 1993b). In physical adsorption, the forces bonding the
adsorbate molecules to the adsorbent surface are electrostatic in nature. Therefore, adsorption
can be hindered by the intermolecular forces of attraction between 2-butoxyethanol and water.

Table 4.6 Breakthrough properties of ZEOcat Z700 at 0%, 45% and 75% RH

Adsorbate and adsorbent type	Breakthrough time (min.)	Throughput ratio (TPR)	Lead time percentage (%)
Dry TMB ZEOcat Z700	21.2	0.73	-
45% TMB ZEOcat Z700	16.2	0.71	23.28
75% RH TMB ZEOcat Z700	15.5	0.61	26.95
Dry 2-butoxyethanol Z700	26.1	0.57	-
45% RH 2-butoxyethanol Z700	18.7	0.59	28.67
75% RH 2-butoxyethanol	16.8	0.52	35.84

4.3.4. Effect of water vapor on VOC uptake

In this section, the effect of water vapor on VOC uptake is discussed. VOC uptake for ZEOcat F603 and ZEOcat Z700 was calculated based on the breakthrough profiles. The integral area of FID breakthrough curve can be used to calculate the uptake of VOC in the presence of water vapor. Using this method, water vapor uptake was calculated by subtracting the calculated value of VOC uptake (from integrating area under VOC breakthrough profile) from the weight of the adsorbent after coadsorption (from mass balance). Calculating the uptake of VOCs using the area of the breakthrough for humid conditions has the benefit of determining the amount of adsorbed water vapor inside the adsorbent at a given relative humidity.

Figure 4.13 depicts uptake of TMB and 2-butoxyethanol during the first cycle of adsorption for ZEOcat Z700 and ZEOcat F603 under the selected humidity conditions. Although the adsorption capacities for both TMB and 2-butoxyethanol decreased with increases in relative humidity, the magnitude of the effect of water vapor on ZEOcat F603 was much higher than for ZEOcat Z700 during adsorption of TMB. TMB adsorption capacity of ZEOcat F603 decreased by 14.29% and 51% at 45% RH and 75% RH, respectively. On the other hand, ZEOcat Z700 decreased by 7.44% and 17.91% at 45% RH and 75% RH, respectively. Adsorption capacity decreased on both zeolites because adsorption properties of zeolite are closely related with the

charge transfer between the zeolite and the adsorbate, as a result, nonpolar adsorbate like TMB was less preferred than polar adsorbate like water vapor (Wang et al., 2017). Based on these results, it can be concluded that ZEOcat F603 has more hydrophilic sites than hydrophobic sites.
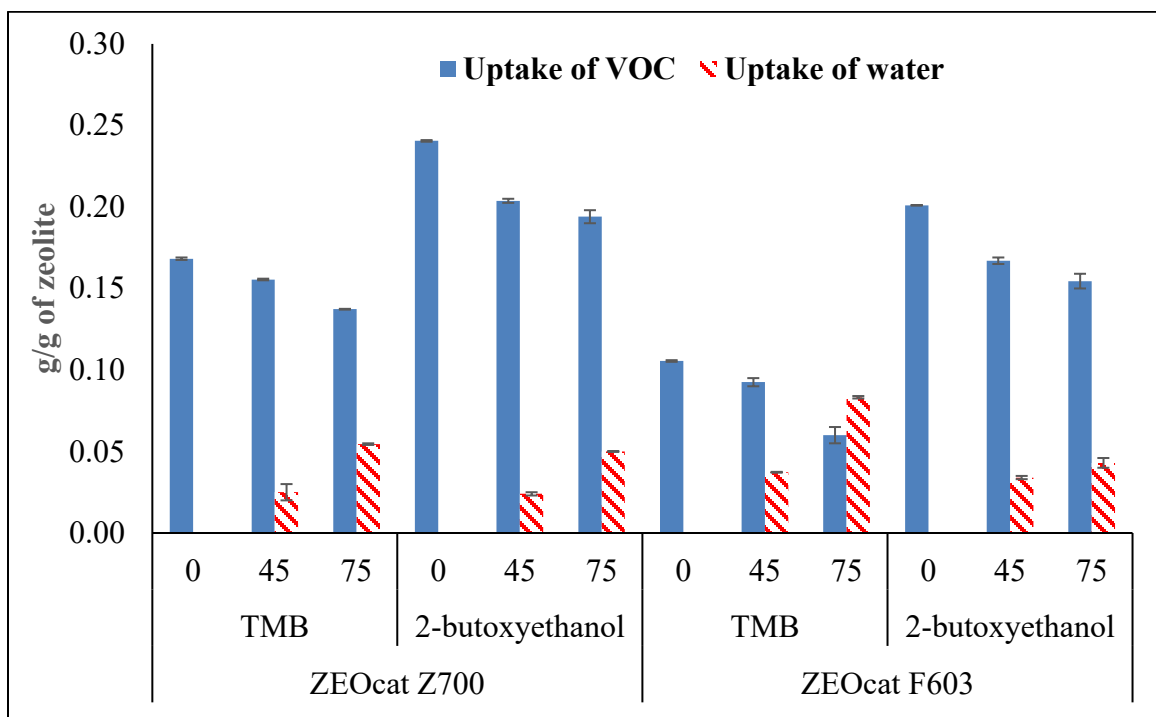
Figure 4.13 Mass balance for VOC and water vapor adsorption onto ZEOcat F603 and ZEOcat Z700

The values of TMB uptake without water vapor were 0.17 g/g and 0.10 g/g, for ZEOcat Z700 and ZEOcat F603, respectively. The higher adsorption capacity for ZEOcat Z700 at a given concentration could be attributed to 26% larger pore volume than ZEOcat F603. Therefore, ZEOcat Z700 is a favorable adsorbent for the tested VOC because of its high Si/Al ratio, large micropore and large total pore volume compared with ZEOcat F603 (Chen, 1976). Moreover, for the same cause, the adsorbed amount of 2-butoxyethanol at dry condition showed the highest value of 0.24g/g for ZEOcat Z700, while the corresponding value for ZEOcat F603 was 0.20 g/g. Furthermore, both ZEOcat Z700 and ZEOcat F603 demonstrated higher adsorption capacities for

2-butoxyethanol than TMB. This is due to the presence of polar charge on the surface of zeolites, as well as larger density and smaller kinetic diameter of 2-butoxyethanol.

Moreover, the comparison of the results obtained at dry and humid conditions demonstrated that the uptake of TMB (nonpolar VOC) decreased by 7.46% and 17.91% at 45% RH and 75% RH, respectively. However, the uptake for 2-butoxyethanol (polar VOC) decreased by 15.63% and 20.83% at 45 % RH and 75% RH, respectively. The higher effect of water vapor on 2-butoxyethanol adsorption can be due to the fundamental physical differences between the two adsorbates. One significant difference between TMB and 2-butoxyethanol is in their molecular polarity. The dipole moment of 2-butoxyethanol (2.10D) is larger than that of TMB (0.40D) and close to that of water (1.85D). Therefore, adsorption can be hindered by the intermolecular forces of attraction between water and 2-butoxyethanol in the gas stream. Orientation effects, dispersion effects, and induction effects are prevailing forces amongst gas molecules depending on the polarity of the relevant molecules. Out of these three effects, the orientation effect is strongest in magnitude followed by dispersion and induction effects (Gong & Keener, 1993b). Since water and 2-butoxyethanol are both polar molecules, the attractive force due to the orientation effect, is much greater than that between water and TMB due to the induction effect.

Adsorption onto a hydrophobic surface is due to the dispersion effect for non-polar adsorbate molecules while it is due to the induction effects for polar adsorbate molecules (Gong & Keener, 1993b). The bond energy for the orientation effect between water and 2-butoxyethanol in the gas phase is greater than the energy of the induction effects between 2-butoxyethanol and the hydrophobic zeolite ZEOcat Z700. The intermolecular forces of attraction are an accumulation of the forces exerted by the surrounding molecules; therefore, the effect of

water vapor on the adsorption of 2-butoxyethanol increases with increasing RH. For TMB however, the intermolecular forces in the gas phase, caused by induction effects between water and TMB molecules, are smaller than the dispersion forces on the surface of ZEOcat Z700 between the solid surface and TMB. Thus, the adsorption of TMB is less affected by water than 2-butoxyethanol (Gong & Keener, 1993b).

4.3.5 Effect of water vapor preconditioning on TMB adsorption.

In water vapor preconditioning test, zeolite is exposed to a 10 SLPM stream containing water vapor at 45% or 75 % RH for 90 minutes followed by coadsorption of TMB and water vapor at the same preconditioning RH until saturated with TMB. The effect of water vapor on the shape of breakthrough curves of organic vapors depends on the breakthrough order of water vapor and VOCs from the adsorbent bed. As it can be seen in Figure 4.14 and Figure 4.15, the effect of preconditioning with water vapor was higher for ZEOcat F603 than for ZEOcat Z700. This is due to the occupancy of water molecule over most of the available sites of ZEOcat F603 during water vapor preconditioning (Tao et al., 2004). Thus, the breakthrough time becomes shorter, implying that adsorption capacity decreased intensively during adsorption if water vapor was loaded onto ZEOcat F603 before coadsorption of VOCs and water vapor. In Table 4.7 and Table 4.8, the breakthrough time of TMB on preconditioned ZEOcat F603 was shorter, and the breakthrough curve was sharper than coadsorption of water vapor with VOC at the same RH.
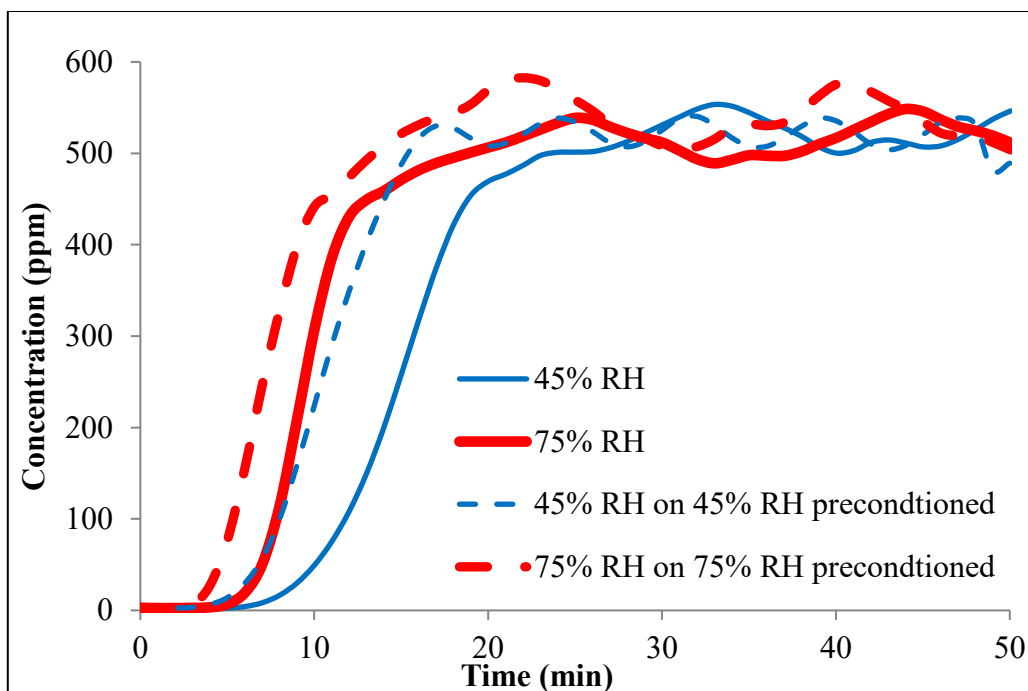
Figure 4.14 Effect of preconditioning ZEOcat F603 with water vapor on TMB adsorption

Table 4.7 Breakthrough time and throughput ratio for first cycle adsorption of TMB on ZEOcat F603

TMB	Breakthrough time (min.)	Throughput ratio $TPR = \dfrac{t_{5\%}}{t_{50\%}}$
45% RH	8.6	0.58
75% RH	6.2	0.66
45% RH on 45% RH preconditioned	5.7	0.55
75% RH on 75% RH preconditioned	3.9	0.55

Preconditioning of ZEOcat Z700 at 45% RH resulted in small effect on breakthrough time and almost no effect on uptake of TMB as shown in Table 4.8 and Appendix C, respectively. Negligible shift in breakthrough was observed as shown in Figure 4.15 and Table 4.8. However, 75% RH humidity in the adsorption gas stream and the water vapor at 75% RH that has been pre-adsorbed by ZEOcat Z700 can considerably influence the breakthrough curve and uptake of TMB as shown in Table 4.8 and Appendix C, respectively.

75
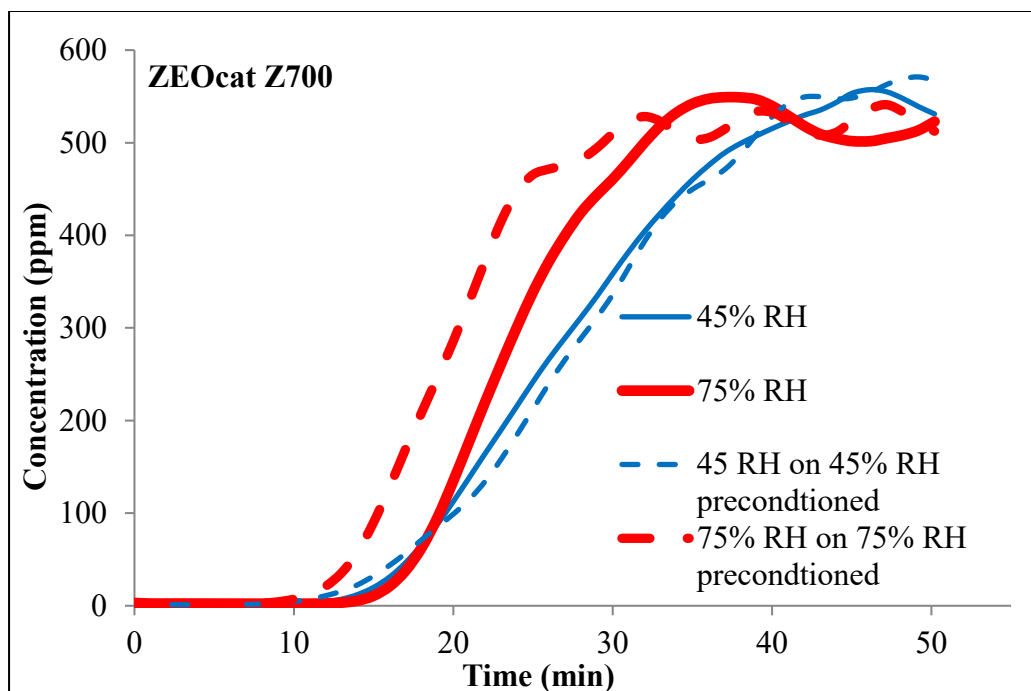
Figure 4.15 Effect of preconditioning ZEOcat Z700 with water vapor on TMB adsorption

Table 4.8 Breakthrough time and throughput ratio for first cycle adsorption of TMB on ZEOcat Z700.

TMB	Breakthrough time (min.)	Throughput ratio $TPR = \dfrac{t_{5\%}}{t_{50\%}}$
Dry	21.2	0.73
45% RH	15.5	0.61
75% RH	16.2	0.71
45% on 45% RH preconditioned	14.5	0.53
75% on 75% RH preconditioned	13.0	0.67

All the humid experiments were completed under the same conditions, with air as carrier gas with flow of 10 SLPM fixed bed configuration. The RH profile for coadsorption of VOCs with water vapor adsorption shows in Figure 4.16 shows nearly a constant value of relative humidity maintain until he adsorption completed.
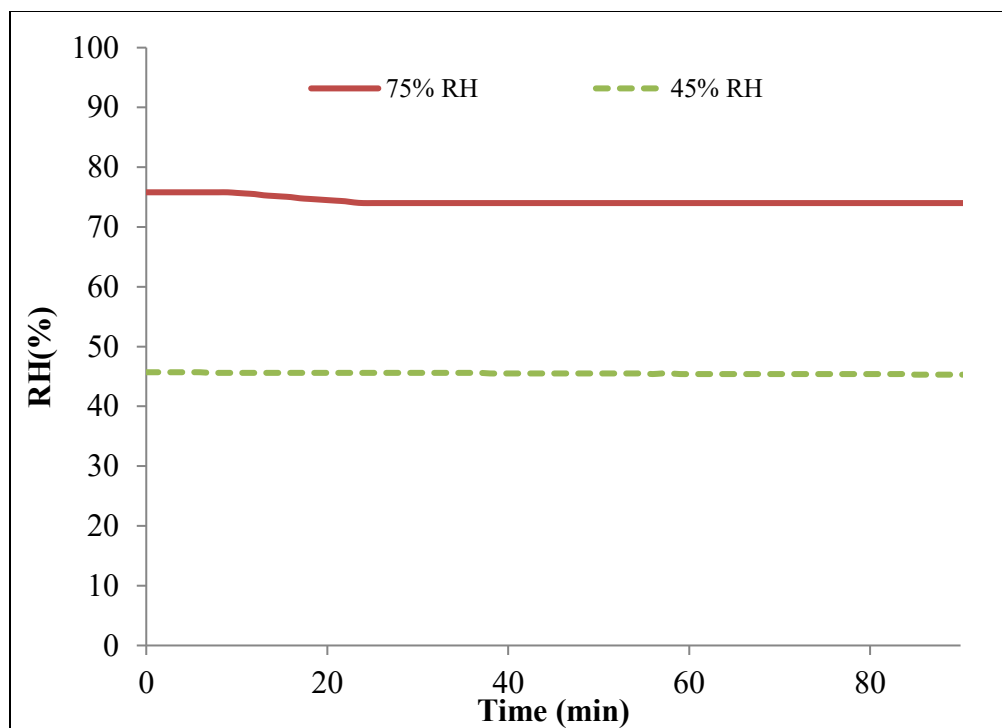
Figure 4.16 Relative humidity profile during coadsorption of VOCs with water vapor.

4.3.6 TGA analysis

Three samples of ZEOcat F603 were analyzed with thermogravimetric methods, a virgin sample and samples after one cycle adsorption of TMB and 2-butoxyethanol at different % RH. The samples' TGA and DTG results are demonstrated in Figure 4.17.

In Figure 4.17 (A) TGA results after one adsorption cycle showed approximately 8% and 13% mass loss for TMB and 2-butoxyethanol, respectively. These values correspond with the mass balance result discussed in section 4.3.2, in which ZEOcat F603 adsorbed more 2-butoxyethanol than TMB. Similarly, the weight loss percentage (1%) was obtained for all samples, including virgin ZEOcat F603, at 575°C. This weight loss is due to binders available from the original sample.
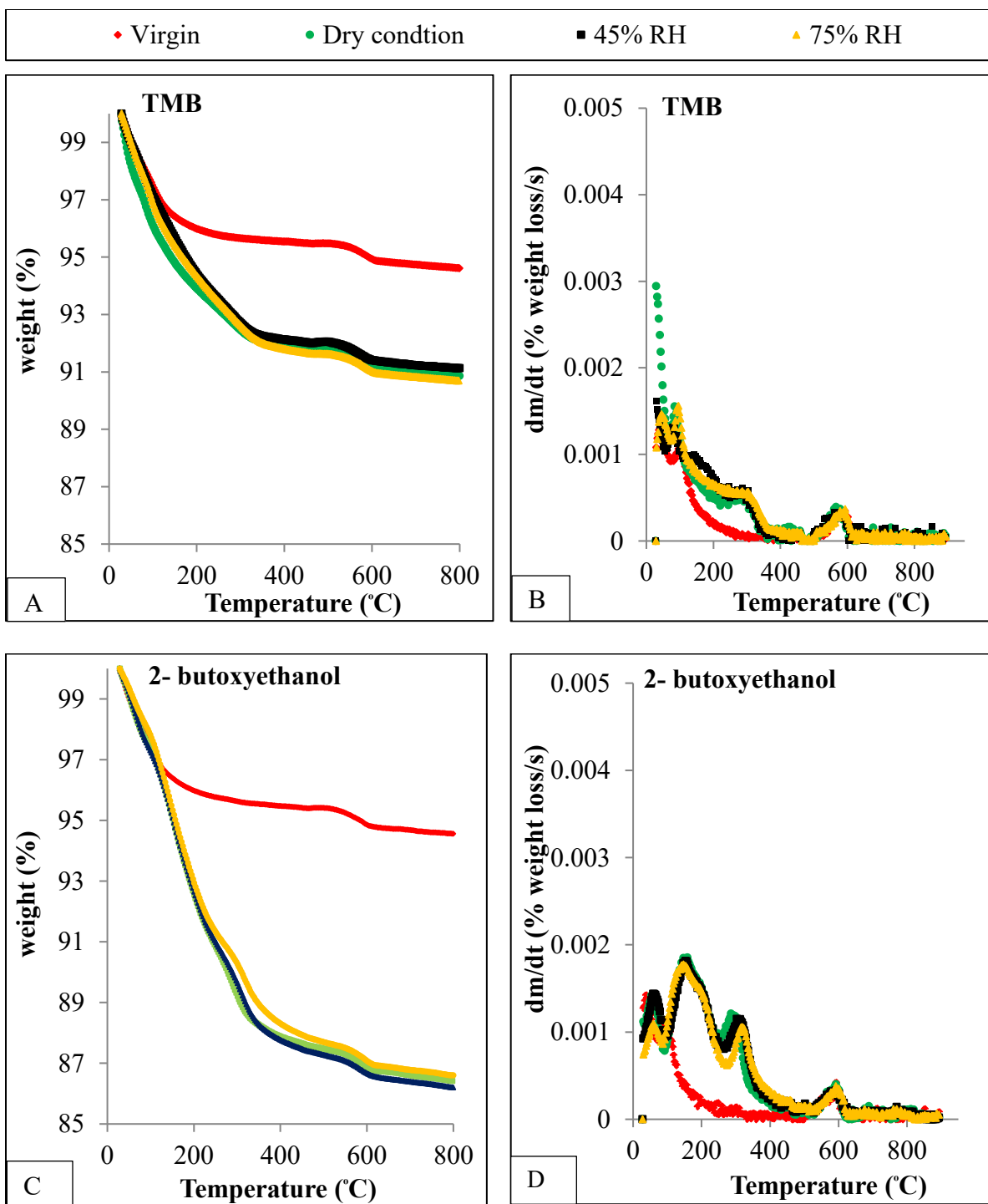
Figure 4.17 A and C) TGA and B and D) DTG results for ZEOcat F603

For TMB, one DTG peak was observed before the temperature reached to 350°C indicating that TMB was completely removed from the sample Figure 4.18. However, for 2-

butoxyethanol, two peaks are observed at 200°C and 320°C and desorption continued until the temperature reached 450°C. Multiple peaks at different temperatures are attributed to strength of adsorption (Joly, 2006). Based on the strength of interaction between adsorbent and adsorbate, the adsorbates will be desorbed at different temperatures. For example, chemisorbed adsorbates are desorbed at higher temperatures than physisorbed components because more energy is required to breakdown the bond formed between adsorbate and adsorbents. The first peak (at 200°C) is attributed to weak physisorption, and the second peak is probably attributed to the desorption of strongly bonded 2-butoxyethanol with surface charges on the adsorbent. Since 2-butoxyethanol has a polar charge pertaining to a hydroxyl group (-OH), it can form hydrogen bonds with the charged surfaces of adsorbents (Franz et al., 2000).

Similarly, samples containing virgin ZEOcat Z700 and one adsorption cycle of both TMB and 2-butoxyethanol were analyzed with thermogravimetric methods. The samples' TGA and DTG results are demonstrated in Figure 4.18 for better comparison.

From Figure 4.18 (a) and (b), TMB and 2-butoxyethanol loaded samples showed mass loss of 12% and 15%, respectively. This value again corresponds with the order of adsorption capacity obtained from mass balance and discussed in section 4.3.2. In summary, ZEOcat700 adsorbed more 2-butoxyethanol than TMB under all selected conditions.

From the DTG results, adsorbed TMB was completely removed from the ZEOcat700 before the temperature reached 300°C. However, 2-butoxyethanol showed two peaks at 165°C and 235°C and desorption continued until the temperature reached to 420°C. This is because 2-butoxyethanol has a polar charge that results in a strong affinity for the surface charge on ZEOcat Z700 compared with ZEOcat F603.
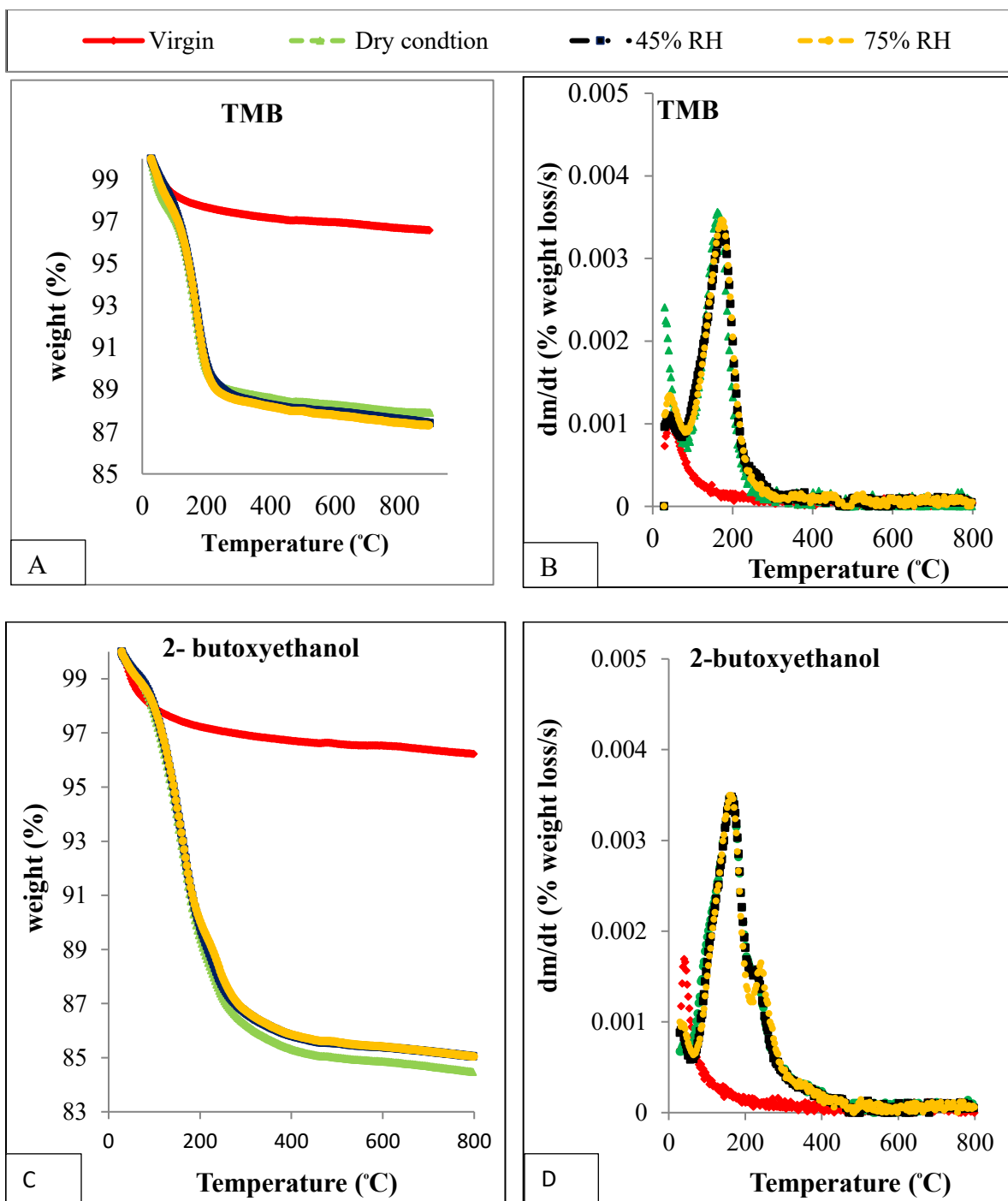
Figure 4.18 A and C) TGA, B and D) DTG results for ZEOcat Z700

5. Chapter Five: CONCLUSIONS AND RECOMMENDATIONS

5.1 Conclusions

This research has added to the understanding of the performance of activated carbon, polymeric adsorbent and zeolite for VOC adsorption. The experiments conducted on Optipore V503, ZEOcat Z700, ZEOcat F603 and ZEOcat Z400 adsorbents comprises the adsorption isotherms of 1,2,4-trimethylbenzene (TMB) and 2-butoxyethanol, the performance evaluation of 5-cycle adsorption/desorption of TMB and OAC SST, the effect of water vapor on breakthrough time and uptake of VOCs. Supporting characterization tests were also performed using thermo-gravimetric analysis (TGA). Important findings of this research are:

- Optipore V503 and BAC showed better adsorption performance for VOCs compared to the tested zeolites, at all concentration levels.

- Among the tested zeolites (ZEOcat Z700, ZEOcat F603, and ZEOcat Z400), ZEOcat Z700 (USY) showed better adsorption capacity for both polar and non-polar adsorbate.

- Longer breakthrough time and sharper breakthrough profile using BAC make this adsorbent desirable to obtain higher pollutants removal with near zero emission.

- Negligible (less than 1% by weight) cumulative heel formed in case of TMB adsorption for all adsorbents. Whereas, higher cumulative 5-cycle heel (1-2.5% by weight) was formed in case of OAC-SST adsorption for BAC and zeolites.

- All the zeolite used in this study showed high tendency to adsorb water vapor even at low relative humidity (10%). However, adsorption of water vapor was negligible below 50%

RH for BAC and below 90% RH for Optipore V503 indicating that Optipore V503 is the most suitable adsorbent for VOC removal from humid air streams.

- Coadsorption of TMB and water vapor on BAC and Optipore V503 showed negligible impact on adsorption capacity and breakthrough time up to 75 % RH. However, in case of ZEOcat Z700 and ZEOcat F603 competitive adsorption between water vapor and TMB was observed at lower RH level of 45 %. This is due to charge on the zeolite surface which results in inter-molecular forces leading to high affinity towards water adsorption.

- Based on the results obtained from the adsorption of 2-butoxyethanol (polar) and TMB (non-polar) in presence of water vapor, ZEOcat F603 showed higher tendency to adsorb polar compounds compared to ZEOcat Z700.

- The effect of preconditioning with water vapor was higher for ZEOcat F603 than for ZEOcat Z700 in case of TMB adsorption. This is due to the occupancy of water molecules over most of the available sites of ZEOcat F603.

This study showed that the adsorption VOC with/without presence of water vapor depends on the adsorbents properties and RH level. In this regard, zeolite showed less adsorption capacity for VOCs owing to lower surface area and pore volume compared to activated carbon and polymeric adsorbents. In addition, zeolite adsorption performance for VOC was observed to be noticeably affected in humid condition due to the surface charge. In terms of Regeneration efficiency for industrial application, polymeric adsorbent performed better in a 5-cycle adsorption/desorption than zeolite and activated carbon.

5.2 Recommendations

In this study, the performance of BAC, Optipore V503, ZEOcat 700, ZEOcat F603 and ZEOcat Z400 adsorbents was investigated by comparing the results obtained from adsorption isotherm, 5-cycle adsorption capacity, 5-cycle heel formation and effect of water vapor on VOCs adsorption. For further understanding of performance of adsorption capacity and desorption efficiency of aforementioned adsorbents, additional research should be conducted on the following topics

- The polymeric adsorbents seemed to be thermally unstable at high regeneration temperatures. Hence, modifying available polymeric adsorbents or producing new polymeric adsorbents that are more thermally stable is recommended.

- The effect of water vapor should to be investigated by considering multi-component adsorption. The VOCs mixture tested should inlcude different types of VOCs such as aliphatic hydrocarbon, aromatic hydrocarbon, polar VOCs.

- In this study zeolite shows high tendency to adsorb water due to charge on the surface. Modifying the hydrophilic sites of zeolite with alkyl groups would be interesting to investigate hydrophobicity of zeolite to increase uptake of VOCs in the presence of water vapor.

- Extend this study at different temperatures would be interesting for better understanding of the effect of water vapor.

Finally, the findings of this study suggest that for practical applications, using two or more adsorbents together can help controlling VOCs with wide range of functional group, molecular weight, polarity molecular size and concentration.

References:

Abiko, H., Furuse, M., & Takano, T. (2016). Estimation of Organic Vapor Breakthrough in Humidified Activated Carbon Beds: Application of Wheeler-Jonas Equation, NIOSH MultiVapor™ and RBT (Relative Breakthrough Time). *Journal of Occupational Health*, *58*(6), 570–581.

Aktaş, Ö., & Çeçen, F. (2006). Effect of type of carbon activation on adsorption and its reversibility. *Journal of Chemical Technology and Biotechnology*, *81*(1), 94–101.

Anand, S., & Howarth, J. (2013). Improving filtration in the automotive paint shop. *Filtration & Separation*, *50*(1), 22–26.

Ania, C. O., Parra, J. B., Menéndez, J. A., & Pis, J. J. (2005). Effect of microwave and conventional regeneration on the microporous and mesoporous network and on the adsorptive capacity of activated carbons. *Microporous and Mesoporous Materials*, *85*(1–2), 7–15.

Atkinson, R. (2000). Atmospheric chemistry of VOCs and NOx. *Atmospheric Environment*, *34*, 2063–2101.

Avhale, A., Kaya, D., Mabande, G. T. P., Selvam, T., Schwieger, W., Stief, T., & Dittmeyer, R. (2008). Defect-free zeolite membranes of the type BEA for organic vapour separation and membrane reactor applications. *Studies in Surface Science and Catalysis*, *174*, 669–672.

Aziz, A., & Kim, S. K. (2017). Adsorptive Volatile Organic Removal from Air onto

NaZSM-5 and HZSM-5: Kinetic and Equilibrium Studies. *Water Air Soil Pollut (2017)*, 228–319.

Bansal, R. C., & Goyal, M. (2005). *Activated carbon adsorptoon*. New York: Taylor & Francis.

Baya, M. P., Siskos, P. A., & Davankov, V. A. (2000). Evaluation of a hypercrosslinked polystyrene, MN-200, as a sorbent for the preconcentration of volatile organic compounds in air. *Journal of Association of Official Agricultural Chemists International*, *83*(3), 579–583.

Berenjian, A., Chan, N., & Malmiri, H. J. (2012). Volatile Organic Compounds Removal Methods: A Review. *American Journal of Biochemistry and Biotechnology Published Online*, *8*(84), 220–229.

Bingjun Pan, Pan, B., Zhang, W., Lv, L., Zhang, Q., & Zheng, S. (2009). Development of polymeric and polymer-based hybrid adsorbents for pollutants removal from waters. *Chemical Engineering Journal*, *151*(1–3), 19–29.

Biron, E., & Evans, M. J. B. (1998). Dynamic adsorption of water-soluble and insoluble vapours on activated carbon. *Carbon*, *36*(7–8), 1191–1197.

Blocki, S. W. (1993). Hydrophobic zeolite adsorbent: A proven advancement in solvent separation technology. *Environmental Progress*, *12*(3), 226–230.

Bradley, R. H., & Rand, B. (1995). On the physical adsorption of vapors by microporous carbons. *Journal of Colloid And Interface Science*.

Brennan, J. K., Bandosz, T. J., Thomson, K. T., & Gubbins, K. E. (2001). Water in porous carbons. *Colloids and Surfaces A: Physicochemical and Engineering Aspects*, (187–188), 539–568.

Burtch, N. C., Jasuja, H., & Walton, K. S. (2014). Water Stability and Adsorption in Metal−Organic Frameworks, *114*, 10575–10612.

Cal, M. P., Rood, M. J., & Larson, S. M. (1997). Gas Phase Adsorption of Volatile Organic Compounds and Water Vapor on Activated Carbon Cloth. *Energy & Fuels*, *11*, 311–315.

Canet, X., Gilles, F., Su, B.-L., De Weireld, G., Frère, M., & Mougin, P. (2007). Adsorption of Alkanes and Aromatic Compounds on Various Faujasites in the Henry Domain. 2. Composition Effect in X and Y Zeolites. *Journal of Chemical & Engineering*, *52*, 2127–2137.

Carratalá-Abril, J., Lillo-Ródenas, M. A., Linares-Solano, A., & Cazorla-Amorós, D. (2009). Activated carbons for the removal of low-concentration gaseous toluene at the semipilot scale. *Industrial and Engineering Chemistry Research*, *48*(4), 2066–2075.

Chakma, A., & Meisen, A. (1989). Activated carbon adsorption of diethanolamine, methyl diethanolamine and their degradation products. *Carbon*, *27*(4), 573–584.

Chang, C., & Lee, C. (2002). Assessment of the strategies for reducing volatile organic compound emissions in the automotive industry in Taiwan, *34*, 117–128.

Chen, N. Y. (1976). Hydrophobic properties of zeolites. *The Journal of Physical*

Chemistry, *80*(1), 60–64.

Chiang, H.-L., Huang, C. P., & Chiang, P. C. (2002). The surface characteristics of activated carbon as affected by ozone and alkaline treatment. *Chemosphere*, *47*, 257–265.

Chiang, Y. C., Chiang, P., & Chang, E. . (2001). Effect of surface characteristics of activated carbon on VOC adsorption. *Journal of Environmental Engineering*, *54*, 54–62.

Choung, J.-H., Lee, Y.-W., Choi, D.-K., & Kim, S.-H. (2001). Adsorption Equilibria of Toluene on Polymeric Adsorbents. *Journal of Chemical & Engineering*, *46*, 954–958.

Chun, Y. C., Chi, P. C., & Pao, C. (2001). Effects of pore structure and temperature on VOC adsorption on activated carbon. *Carbon*, *39*, 523–534.

Cooper, C. D., & Alley, F. C. (2002). *Air pollution control : a design approach* (3rd ed.). Prospect Heights, Ill. : Waveland Press.

Daems, I., Leflaive, P., Méthivier, A., Baron, G. V, & Denayer, J. F. M. (2006). Influence of Si:Al-ratio of faujasites on the adsorption of alkanes, alkenes and aromatics. *Microporous and Mesoporous Materials*, *96*, 149–156.

DAVANKOV, V. A., & TSYURUPA, M. P. (2011). Hypercrosslinked Polymeric Networks and Adsorbing Materials: Synthesis, Properties, Structure, and Applications (Vol. 56, pp. 315–358). Elsevier B.V.

Dĕdeček, J., Sklenak, S., Li, C., Wichterlová, B., Gábová, V., Brus, J., … Sauer, J. (2009).

Effect of Al-Si-Al and Al-Si-Si-Al Pairs in the ZSM-5 Zeolite Framework on the Al NMR Spectra. A Combined High-Resolution Al NMR and DFT/MM Study. *Journal of Physical Chemistry*, *113*(4), 1447–1458.

Delage, F., Pre, P., & Cloirec, C. (1999). Effects of moisture on warming of activated carbon bed during voc adsorption. *Journal of Environmental Engineering*, *125*, 1160–1167.

Deosarkar, S. P., & Pangarkar, V. G. (2004). Adsorptive separation and recovery of organics from PHBA and SA plant effluents. *Separation and Purification Technology*, *38*, 241–254.

Díaz, E., Ordóñez, S., Vega, A., & Coca, J. (2005). Comparison of adsorption properties of a chemically activated and a steam-activated carbon, using inverse gas chromatography. *Microporous and Mesoporous Materials*, *82*(1–2), 173–181.

Downarowicz, D. (2015). Adsorption characteristics of propan-2-ol vapours on activated carbon Sorbonorit 4 in electrothermal temperature swing adsorption process. *Adsorption Journal of The International Adsorption Society*, *21*, 87–89. https://doi.org/10.1007/s10450-015-9652-1

Ejka, J. Č., Kotrla, J., Krejčí, A., & Heyrovsk, J. (2004). Disproportionation of trimethyl benzenes over large pore zeolites: catalytic and adsorption study. *Applied Catalysis*, *277*, 191–199.

Environment and Climate Change. (2016). Volatile organic compound emissions. Retrieved January 29, 2018, from https://www.canada.ca/en/environment-climate-

change/services/environmental-indicators/air-pollutant-emissions/volatile-organic-compound-emissions.html

Ferreira, A., Mittelmeijer-Hazeleger, M., Bergh, J., Aguado, S., Jansen, J., Rothenberg, G., … Kapteijn, F. (2013). Adsorption of hexane isomers on MFI type zeolites at ambient temperature: Understanding the aluminium content effect. *Microporous and Mesoporous Materials 170*, *170*, 26–35.

Franz, M., Arafat, H. a, & Pinto, N. G. (2000). Effect of chemical surface heterogeneity on the adsorption mechanism of dissolved aromatics on activated carbon. *Carbon*, *38*, 1807–1819.

Gédéon, A., Massiani, P., & Babonneau, F. (2008). *Zeolites and related materials. Part A : trends, targets and challenges : proceedings of the 4th International FEZA Conference*. Paris, France: Elsevier.

Gong, R., & Keener, T. (1993a). A Qualitative Analysis of the Effects of Water Vapor on Multi-Component Vapor-Phase Carbon Adsorption. *Air & Waste Air Waste Manage. Assoc*, *436*(43).

Gong, R., & Keener, T. C. (1993b). A Qualitative Analysis of the Effects of Water Vapor on Multi-Component Vapor-Phase Carbon Adsorption. *Air & Waste Air Waste Manage. Assoc*, *43*, 864–872.

Gregg, S. J., & Sing, K. S. W. (1982). *Adsorption, Surface Area and Porosity* (2ed ed.). London: Academic press inc.

Guth, J.-L., & Kessler, H. (1999). *Synthesis of Aluminosilicate Zeolites and Related Silica-Based Materials*. New York in: Springer.

Hailin, W., Lie, N., Jing, L., Yufei, W., Gang, W., Junhui, W., & Zhengping, H. (2013). Characterization and assessment of volatile organic compounds (VOCs) emissions from typical industries. *Environmental Chemistry March*, *58*(7), 724–730.

Han, X., Wang, L., Li, J., Zhan, X., Chen, J., & Yang, J. (2011). Tuning the hydrophobicity of ZSM-5 zeolites by surface silanization using alkyltrichlorosilane. *Applied Surface Science*, *257*(22), 9525–9531.

Hashisho, Z., Emamipour, H., Rood, Mark, J., K.James, H., Kim, Byung, J., & Thurston, D. (2008). Concomitant Adsorption and Desorption of Organic Vapor in Dry and Humid Air Streams using Microwave and Direct Electrothermal Swing Adsorption. *Environmental Science & Technology*, *42*, 9317–9322.

Herná, N. M. A., Corona, L., Gonzá, A. I., Rojas, F., Lara, V. H., & Silva, F. (2005). Quantitative Study of the Adsorption of Aromatic Hydrocarbons (Benzene, Toluene, and p-Xylene) on Dealuminated Clinoptilolites. *Industrial & Engineering Chemistry Research*, *44*, 2908–2916.

Huang, M., Chou, C. H., & Teng, H. (2002). Pore-size effects on activated-carbon capacities for volatile organic compound adsorption. *American Institute of Chemical Engineers Journal*, *48*(8), 1804–1810.

Huang, Z. H., Kang, F., Liang, K. M., & Hao, J. (2003). Breakthrough of methyethylketone and benzene vapors in activated carbon fiber beds. *Journal of Hazardous Materials*,

98(1–3), 107–115.

IUPAC-Recommendation. (1985). *Reporting physisorption data for gas/solid systems with special reference to the determination of surface area and porosity. Pure and Applied Chemistry* (Vol. 57). International Union of Pure and Applied Chemistry.

Jacobs, P. A., Beyer, H. K., & Valyon, J. (1981). Properties of the end members in the Pentasil-family of zeolites: characterization as adsorbents. *Zeolites*, *1*(3), 161–168.

Jahandar Lashaki, M., Atkinson, J. D., Hashisho, Z., Phillips, J. H., Anderson, J. E., Nichols, M., & Misovski, T. (2016). Effect of desorption purge gas oxygen impurity on irreversible adsorption of organic vapors. *Carbon*, *99*, 310–317.

Jha, B., & Singh, D. N. (2016). Basics of Zeolites (pp. 5–31). Springer, Singapore.

Jia, L., Yao, X., Ma, J., & Long, C. (2017). Adsorption kinetics of water vapor on hypercrosslinked polymeric adsorbent and its comparison with carbonaceous adsorbents. *Microporous and Mesoporous Materials*, *241*, 178–184.

Joly, J. P. (2006). Regeneration of Activated Carbons With Chlorophenols Exhausted. *Environmental Engineering and Management Journal*, *5*(2), 203–212.

Jonas, L.A., Sansone, E.B., Farris, T. S. (1985). The effect of moisture on the adsorption of chlororm by Actvated Carbon. *American Industrial Hygiene Association Journal*, *46*(1), 20–23.

Kampa, M., & Castanas, E. (2008). Human health effects of air pollution. *Environmental Pollution*, *151*(151), 362–367.

Kamravaei, S., Shariaty, P., Lashaki, M. J., Atkinson, J. D., Hashisho, Z., Phillips, J. H., …
Nichols, M. (2017). Effect of Beaded Activated Carbon Fluidization on Adsorption of
Volatile Organic Compounds. *Industrial & Engineering Chemistry Research*, *56*,
1297–1305.

Kawasaki, N., Kinoshita, H., Oue, T., Nakamura, T., & Tanada, S. (2004). Study on
adsorption kinetic of aromatic hydrocarbons onto activated carbon in gaseous flow
method. *Journal of Colloid and Interface Science*, *275*, 40–43.

Khan, F. I., & Ghoshal, A. K. (2000). Removal of Volatile Organic Compounds from
polluted air. *Journal of Loss Prevention in the Process Industries*, *13*, 527–545.

Khan, F. I., & Kr. Ghoshal, A. (2000). Removal of Volatile Organic Compounds from
polluted air. *Journal of Loss Prevention in the Process Industries*, *13*(6), 527–545.

Kim, B. R. (2011). VOC Emissions from Automotive Painting and Their Control: A
Review. *Environmental Engineering Research*, *16*(1), 1–9.

Kim, B. R., Adams, J. A., Klaver, P. R., Kalis, E. M., Contrera, M., Griffin, M., … Pastick,
T. (2000). Biological removal of gaseous vocs from automotive painting operations.
Journal of Environmental Engineering, *126*(8), 145–153.

Kim, B. R., Kalis, E. M., Dewulf, T., Andrews, K. M., Kim, B. R., Kalis, E. M., …
Andrews, K. M. (2000). Henry â€™ s Law Constants for Paint Solvents and Their
Implications on Volatile Organic Compound Emissions from Automotive Painting,
72(1), 65–74.

Kim, J. H., Ryu, Y. K., Haam, S., Lee, C. H., & Kim, W. S. (2001). Adsorption and steam regeneration of n- hexane, mek, and toluene on activated carbon fiber. *Separation Science and Technology*, *36*, 263–281.

Kim, K.-M., Oh, H.-T., Lim, S.-J., Ho, K., Park, Y., & Lee, C.-H. (2016). Adsorption Equilibria of Water Vapor on Zeolite 3A, Zeolite 13X, and Dealuminated Y Zeolite. *Journal of Chemical & Engineering*, *61*, 1547–1554.

Kolade, M. A., Kogelbauer, A., & Alpay, E. (2009). Adsorptive reactor technology for VOC abatement. *Chemical Engineering Science*, *64*, 1197–1177.

Lashaki, M. J., Atkinson, J. D., Hashisho, Z., Phillips, J. H., Anderson, J. E., & Nichols, M. (2016). The role of beaded activated carbon's surface oxygen groups on irreversible adsorption of organic vapors. *Journal of Hazardous Materials*, *317*(317), 284–294.

Lashaki, M. J., Fayaz, M., Wang, H., Hashisho, Z., Philips, J. H., Anderson, J. E., & Nichols, M. (2012). Effect of Adsorption and Regeneration Temperature on Irreversible Adsorption of Organic Vapors on Beaded Activated Carbon. *American Chemical Society*, *46*, 4083–4090.

Lee, S. W., Park, H. J., Lee, S. H., & Lee, M. G. (2008). Comparison of adsorption characteristics according to polarity difference of acetone vapor and toluene vapor on silica-alumina fixed-bed reactor. *Journal of Industrial and Engineering Chemistry*, *14*, 10–17.

Leng, C., & Pinto, N. (1997). Effects of surface properties of activated carbons on adsorption behavior of selected aromatics. *Carbon*, *35*(9), 1375–1385.

Li, L., Sun, Z., Li, H., & Keener, T. C. (2012). Effects of activated carbon surface

    properties on the adsorption of volatile organic compounds. *Journal of the Air &*

    Waste Management Association, *6210*(10), 1096–2247.

Lillo-Ró Denas, M. A., Cazorla-Amoró, D., Linares-Solano, A., Lillo-Ródenas, M. A.,

    Cazorla-Amorós, D., & Linares-Solano, A. (2005). Behaviour of activated carbons

    with different pore size distributions and surface oxygen groups for benzene and

    toluene adsorption at low concentrations. *Carbon*, *43*(8), 1758–1767.

Lin, C. L., Cheng, Y. H., Liu, Z. S., & Chen, J. Y. (2013). Adsorption and oxidation of high

    concentration toluene with activated carbon fibers. *Journal of Porous Materials*,

    20(4), 883–889.

Liu, P., Long, C., Li, Q., Qian, H., Li, A., & Zhang, Q. (2009). Adsorption of

    trichloroethylene and benzene vapors onto hypercrosslinked polymeric resin. *Journal*

    of Hazardous Materials, *166*, 46–51.

Lodewyckx, P. (2014). Adsorption of Volatile Organic Vapours. *Green Carbon Materials:*

    Advances and Applications Edited, 978–981.

Lodewyckx, P., & Vansant, E. F. (2010). American Industrial Hygiene Association Journal.

    American Industrial Hygiene Association, (March 2013), 37–41.

Long, C., Li, A., Wu, H., & Zhang, Q. (2009). Adsorption of naphthalene onto

    macroporous and hypercrosslinked polymeric adsorbent: Effect of pore structure of

    adsorbents on thermodynamic and kinetic properties. *Colloids and Surfaces A:*

    Physicochemical and Engineering Aspects, *333*(1–3), 150–155.

Long, C., Li, Q., Li, Y., Liu, Y., Li, A., & Zhang, Q. (2010). Adsorption characteristics of benzene-chlorobenzene vapor on hypercrosslinked polystyrene adsorbent and a pilot-scale application study. *Chemical Engineering Journal*, *160*(2), 723–728.

Long, C., Li, Y., Yu, W., & Li, A. (2012). Adsorption characteristics of water vapor on the hypercrosslinked polymeric adsorbent. *Chemical Engineering Journal*, *180*, 106–112.

Long, C., Liu, P., Li, Y., Li, A., & Zhang, Q. (2011). Characterization of Hydrophobic Hypercrosslinked Polymer as an Adsorbent for Removal of Chlorinated Volatile Organic Compounds. *Environmental Science & Technology*, *45*(10), 4506–4512.

Lowell, S., & Shields, J. E. (1984). Adsorption isotherms. In *Powder Surface Area and Porosity* (pp. 11–13). Dordrecht: Springer Netherlands.

Lu, H.-F., Cao, J., Zhou, Y., Zhan, D., & Chen, Y. (2013). Novel hydrophobic PDVB/R-SiO2 for adsorption of volatile organic compounds from highly humid gas stream. *Journal of Hazardous Materials*, *262*, 83–90.

Lu, Q., & Sorial, G. A. (2009). A comparative study of multicomponent adsorption of phenolic compounds on GAC and ACFs. *Journal of Hazardous Materials*, *167*(1–3), 89–96.

Marcus, Cormier, B. K., & William E. (1999). Going green with Zeolites. *Chemical Engineering Progress*, *95*(6), 47–54.

Matthew McCullough. (2003). Method for achieving ultra-low emission limits in VOC control.

Meng, Q. B., Yang, G.-S., & Lee, Y.-S. (2013). Preparation of highly porous hypercrosslinked polystyrene adsorbents: Effects of hydrophilicity on the adsorption and microwave-assisted desorption behavior toward benzene, *181*, 222–227.

Meng, Q. B., Yang, G.-S. S., & Lee, Y.-S. S. (2014). Sulfonation of a hypercrosslinked polymer adsorbent for microwave-assisted desorption of adsorbed benzene. *Journal of Industrial and Engineering Chemistry*, *20*(4), 2484–2489.

Mohan, N., Kannan, G. K., Upendra, S., Subha, R., & Kumar, N. S. (2009). Breakthrough of toluene vapours in granular activated carbon filled packed bed reactor. *Journal of Hazardous Materials*, *168*, 777–781.

Monneyron, P., Manero, M.-H., & Jean-Noel, F. (2003). Measurement and Modeling of Single- and Multi-Component Adsorption Equilibria of VOC on High-Silica Zeolites. *Environ. Sci. Technol.*, *37*(11), 2410–2414.

Nevskaia, D. M., Fuertes, A. B., & Marban, G. (2003). A dsorption of volatile organic compounds by means of activated carbon fibre-based monoliths, *41*, 87–96.

Nguyen, V. T., Horikawa, T., Do, D. D., & Nicholson, D. (2014). Water as a potential molecular probe for functional groups on carbon surfaces. *Carbon*, *67*, 72–78.

Niknaddaf, S., Atkinson, J. D., Shariaty, P., Lashaki, M. J., Hashisho, Z., Phillips, J. H., … Nichols, M. (2016). Heel formation during volatile organic compound desorption from activated carbon fiber cloth. *Carbon*, *96*, 131–138.

Okazaki, M., Tamon, H., & Toei, R. (1978). Prediction of binary adsorption equilibria of

solvent and water vapor on activated carbon. *Journal of Chemical Engineering of Japan*, *11*(3), 209–215.

Pariselli, F., Sacco, M. G., Ponti, J., & Rembges, D. (2009). Effects of toluene and benzene air mixtures on human lung cells (A549). *Experimental and Toxicologic Pathology*, *61*(4), 381–386.

Park, E. J., Seo, H. O., & Kim, Y. D. (2017). Influence of humidity on the removal of volatile organic compounds using solid surfaces. *Catalysis Today*, *295*, 3–13.

Parmar, G. R., & Rao, N. N. (2009). *Emerging control technologies for volatile organic compounds*. *Critical Reviews in Environmental Science and Technology* (Vol. 39).

Pina-Salazar, E. Z., & Kaneko, K. (2015). Adsorption of water vapor on mesoporosity-controlled singe wall carbon nanohorn. *Colloids and Interface Communication*, *5*, 8–11.

Popescu, M., Joly, J. P., Carre, J., & Danatoiu, C. (2003). Dynamical adsorption and temperature-programmed desorption of VOCs (toluene, butyl acetate and butanol) on activated carbons. *Carbon*, *41*, 739–748.

Qi, N., Appel, W. S., Levan, M. D., & Finn, J. E. (2006). Adsorption Dynamics of Organic Compounds and Water Vapor in Activated Carbon Beds. *Industrial & Engineering Chemistry Research*, *45*, 2303–2314.

Salvador, F., & Jiménez, C. S. (1996). A new method for regenerating activated carbon by thermal desorption with liquid water under subcritical conditions. *Carbon*, *34*(4), 511–

516.

Salvador, F., Martin-Sanchez, N., Sanchez-Hernandez, R., Sanchez-Montero, M. J., &
Izquierdo, C. (2015). Regeneration of carbonaceous adsorbents. Part I: Thermal
Regeneration. *Microporous and Mesoporous Materials*, *202*, 259–276.

Schmidt, D. W. P. and P. S. (1998). VOC Recovery through Microwave Regeneration of
Adsorbents: Process Design Studies. *J. Air & Waste Manage*, *48*, 1135–1145.

Schnelle, K. B., & Brown, C. A. (2002). Air Pollution Control Technology Handbook. In
The Mechanical Engineering Handbook Series. Boca Raton: CRC Press:

Scholz, M., & Martin, R. J. (1998). Control of bio-regenerated granular activated carbon by
spreadsheet modelling. *Journal of Chemical Technology and Biotechnology*, *71*(3),
253–261.

Sheintuch, M. (1999). Comparison of catalytic processes with other regeneration methods
of activated carbon. *Catalysis Today*, *53*(1), 73–80.

Silvestre-Albero, A., Ramos-Ferná Ndez, J. M., Martínez-Escandell, M., Sepú Lveda-
Escribano, A., Silvestre-Albero, J., & Rodríguez-Reinoso, F. (2009). High saturation
capacity of activated carbons prepared from mesophase pitch in the removal of volatile
organic compounds. *Carbon*, *48*, 548–556.

Singh, K. P., Mohan, D., Tandon, G. S., & Gupta, G. S. D. (2002). Vapor-Phase Adsorption
of Hexane and Benzene on Activated Carbon Fabric Cloth: Equilibria and Rate
Studies. *Industrial & Engineering Chemistry Research*, *41*, 2480–2486.

Stelzer, J., Paulus, M., Hunger, M., & Weitkamp, J. (1998). Hydrophobic properties of all-silica zeolite beta1. *Microporous and Mesoporous Materials*, *22*, 1–8.

Sullivan, P. D., Rood, M. J., Dombrowski, K. D., & Hay, K. J. (2004). Capture of organic vapors using adsorption and electrothermal regeneration. *Journal of Environmental Engineering*, *130*(3), 258–267.

Suzukthe, M. (1990). *Adsorption Engineering* (25th ed.). Japan: Kodansha LTd.

Tamon, H., Atsushi, M., & Okazaki, M. (1996). On irreversible adsorption of electron-donating compounds in aqueous solution. *Journal of Colloid and Interface Science*, *177*(2), 384–390.

Tao, W.-H., Yang, T. C.-K., Chang, Y.-N., Chang, L.-K., & Chung, T.-W. (2004). Effect of Moisture on the Adsorption of Volatile Organic Compounds by Zeolite 13×. *Journal of Environmental Engineering*, *130*(10), 1210–1216.

Tchobanoglous, G., Burton, F. L., & Stensel, H. D. (2003). *Wastewater Engineering, Treatment and Reuse* (4th ed.). New York, NY, USA.: McGraw-Hill Edition.

Thommes, M., Kaneko, K., Neimark, A. V, Olivier, J. P., Rodriguez-Reinoso, F., Rouquerol, J., & Sing, K. S. W. (2015). IUPAC Technical Report Physisorption of gases, with special reference to the evaluation of surface area and pore size distribution (IUPAC Technical Report). *Pure Applied Chemistry*, *87*(910), 1051–1069.

Tipnis, P. R., & Harriott, P. (1986). Thermal regeneration of activated carbons. *Chemical Engineering Communications*, *46*(1–3), 11–28.

Tsai, J. H., Chiang, H. M., Huang, G. Y., & Chiang, H. L. (2008). Adsorption characteristics of acetone, chloroform and acetonitrile on sludge-derived adsorbent, commercial granular activated carbon and activated carbon fibers. *Journal of Hazardous Materials*, *154*(1–3), 1183–1191.

Tsyurupa, M. P., & Davankov, V. A. (2006). Porous structure of hypercrosslinked polystyrene: State-of-the-art mini-review. *Reactive and Functional Polymers*, *66*, 768–779.

Tukur, N. M., & Al-Khattaf, S. (2012). Catalytic Transformation of 1 , 3 , 5-Trimethylbenzene over a USY Zeolite Catalyst. *Energy*, (4), 2499–2508.

Vidic, R. ., Suidan, M. T., & Brenner, R. C. (1993). Oxidative Coupling of Phenols on Activated Carbon: Impact on Adsorption Equilibrium. *Environmental Science and Technology*, *27*(10), 2079–2085.

Vidic, R. ., Tessmer, C. H., & Uranowski, L. J. (1997). Impact of surface properties of activated carbons on oxidative coupling of phenolic compounds. *Carbon*, *35*(9), 1349–1359.

Vidic, R., & Suidan, M. T. (1991). Role of Dissolved Oxygen on the Adsorptive Capacity of Activated Carbon for Synthetic and Natural Organic Matter. *Environmental Science and Technology*, *25*(9), 1612–1618. https://doi.org/10.1021/es00021a013

Villacañas, F., Pereira, M. F. R., Órfão, J. J. M., & Figueiredo, J. L. (2006). Adsorption of simple aromatic compounds on activated carbons. *Journal of Colloid and Interface Science*, *293*(1), 128–136.

WANG, F., WANG, W., HUANG, S., TENG, J., & XIE, Z. (2007). Experiment and

    Modeling of Pure and Binary Adsorption of n-Butane and Butene-1 on ZSM-5

    Zeolites with Different Si/Al Ratios. *Chinese Journal of Chemical Engineering*, *15*(3),

    376–386.

Wang, H., Jahandar Lashaki, M., Fayaz, M., Hashisho, Z., Philips, J. H., Anderson, J. E., &

    Nichols, M. (2012). Adsorption and desorption of mixtures of organic vapors on

    beaded activated carbon. *Environmental Science and Technology*, *46*(15), 8341–8350.

Wang, L., & Balasubramanian, N. (2009). Electrochemical regeneration of granular

    activated carbon saturated with organic compounds. *Chemical Engineering Journal*,

    155(3), 763–768.

Wang, W. Q., Wang, J., Chen, J. G., Fan, X. S., Liu, Z. T., Liu, Z. W., … Hao, Z. (2015).

    Synthesis of novel hyper-cross-linked polymers as adsorbent for removing organic

    pollutants from humid streams. *Chemical Engineering Journal*, *281*, 34–41.

Wang, Y., Yang, C., Liu, Y., Feng, X., Fu, H., & Shan, H. (2017). Molecular Simulation

    Effect of Si/Al ratio on tetralin adsorption on Y zeolite: a DFT study Effect of Si/Al

    ratio on tetralin adsorption on Y zeolite: a DFT study. *Molecular SiMulation*, *43*(12),

    945–952.

Wood, G. O. (2002). A review of the effects of covapors on adsorption rate coefficients of

    organic vapors adsorbed onto activated carbon from flowing gases. *Carbon*, *40*, 685–

    694.

Wood, G. O., & Moyer, E. (1989). A Review of the Wheeler Equation and Comparison of

Its Applications to Organic Vapor Respirator Cartridge Breakthrough Data. *American Industrial Hygiene Association Journal*.

Yahia, M., Torkia, Y., Knani, S., Hachicha, M., Khalfaoui, M., & Lamine, A. (2013). Models for Type VI Adsorption Isotherms from a Statistical Mechanical Formulation. *Adsorption Science & Technology*, *31*(4), 341–358.

Yang, R. T. (1987). Adsorber Dynamics: Bed Profiles and Breakthrough Curves. In *Gas Separation by Adsorption Processes* (pp. 141–200).

Yang, R. T. (1987a). CHAPTER 2 – Adsorbents and Adsorption Isotherms. In *Gas Separation by Adsorption Processes* (pp. 9–48).

Yang, R. T. (1987b). *Front Matter*. Gas Separation by Adsorption Processes. Boston: London: Imperial college press.

Yang, R. T. (1987). *Gas separation by adsorption processes*. London: Imperial college press.

Yang, R. T., & Yang, R. T. (1987). Rate Processes in Adsorbers. In *Gas Separation by Adsorption Processes* (pp. 101–139).

Yun, J.-H., Hwang, K.-Y., & Choi, D.-K. (1998). Adsorption of Benzene and Toluene Vapors on Activated Carbon Fiber at 298, 323, and 348 K. *Journal of Chemical & Engineering*, *43*, 843–845.

Zaitan, H., Manero, M. H., & Valdés, H. (2015). Application of high silica zeolite ZSM-5 in a hybrid treatment process based on sequential adsorption and ozonation for VOCs

elimination. *Journal of Environm Ental Sciences*, *41*, 59–68.

Zhao, Z., Wang, S., Yang, Y., Li, X., Li, J., & Li, Z. (2015). Competitive adsorption and selectivity of benzene and water vapor on the microporous metal organic frameworks (HKUST-1). *Chemical Engineering Journal*, (259), 79–89.

Zhu, Z., Xu, H., Jiang, J., Wu, H., & Wu, P. (2017). Hydrophobic Nanosized All-Silica Beta Zeolite: Efficient Synthesis and Adsorption Application. *American Chemical Society Applied Materials & Interfaces*, *9*, 27273–27283.

APPENDICES

APPENDIX A

Mass balance for five-cycle adsorption and desorption

Adsorption of 1,2,4-trimethylbenzene (TMB)

Table A-1. Mass balance for 5-cycle adsorption/desorption test of TMB on Beaded activated carbon (BAC)

Cycle	BAC[1] (g)	Before Adsorption[2] (g)	After Adsorption[3] (g)	Adsorbed Adsorbate[4] (g)	Adsorption Capacity[5] (%)	After Regeneration[6] (g)	Heel[7] (g)	Total Heel[8] (g)	Total Heel[9] (%)	Adsorption Time (min)
				Mass balance						
1	4.012	332.972	334.751	1.779	45.1	332.981	0.009	0.009	0.23	150
2	-	332.981	334.751	1.770	44.6	332.986	0.005	0.014	0..35	150
3	-	332.986	334.779	1.793	44.5	332.997	0.011	0.025	0.63	150
4	-	332.997	334.781	1.784	43.7	332.998	0.001	0.026	0..66	150
5	-	332.998	334.779	1.781	43.5	333.001	0.003	0.029	0.73	150

[1]Weight of dry BAC

[2]Weight of full reactor before adsorption

[3]Weight of full reactor after adsorption

[4]Weight of adsorbed adsorbate=
 After Adsorption - Before Adsorption

[5]Adsorption capacity = (Mass adsorbed/Mass of BAC) ×100

[6]Weight of full reactor after regeneration

[7]Weight of adsorbate remaining on the BAC after regeneration=
(After Regeneration- Before Adsorption)

[8]Total Heel = weight of reactor after this regeneration test - weight of reactor before any adsorption

[9]Total heel (%) = (Total heel/mass of BAC) ×100

Table A-2 Mass balance for 5-cycle adsorption/desorption test of TMB on Optipore V503

| Cycle | Mass balance | | | | | | | | | Adsorption Time (min) |
	V503[1] (g)	Before Adsorption[2] (g)	After Adsorption[3] (g)	Adsorbed Adsorbate[4] (g)	Adsorption Capacity[5] (%)	After Regeneration [6] (g)	Heel[7] (g)	Total Heel[8] (g)	Total Heel[9] (%)	
1	4.072	336.337	338.330	2.073	50.9	336.269	0.002	0.002	0.049	150
2	-	336.269	338.336	2.067	50.8	336.260	0.001	0.003	0.074	150
3	-	336.260	338.335	2.065	50.7	336.360	0.000	0.003	0.074	150
4	-	336.260	338.329	2.062	50.6	336.260	0.000	0.003	0.074	150
5	-	336.260	338.292	2.035	49.9	336.260	0.000	0.003	0.074	150

[1]Weight of dry Optipore V503

[2]Weight of full reactor before adsorption

[3]Weight of full reactor after adsorption

[4]Weight of adsorbed adsorbate =
 After Adsorption - Before Adsorption

[5] Adsorption capacity = (Mass adsorbed/Mass of Optipore V503) *100

[6]Weight of full reactor after regeneration

[7]Weight of adsorbate remaining on Optipore V503 after regeneration =
After Regeneration - Before Adsorption

[8]Weight of reactor after this regeneration test - weight of reactor before any adsorption

[9]Total heel (%) = (Total heel/mass of Optipore V503) ×100

Table A-1. Mass balance for 5-cycle adsorption/desorption test of TMB on ZEOcat Z700

| Cycle | Mass balance | | | | | | | | | Adsorption Time (min) |
	ZEOcat Z700[1] (g)	Before Adsorption[2] (g)	After Adsorption[3] (g)	Adsorbed Adsorbate[4] (g)	Adsorption Capacity[5] (%)	After Regeneration [6] (g)	Heel[7] (g)	Total Heel[8] (g)	Total Heel[9] (%)	
1	4.006	330.140	330.804	0.664	16.452	330.145	0.005	0.005	0.124	90
2	-	330.145	330.806	0.666	16.378	330.155	0.010	0.015	0.372	90
3	-	330.155	330.814	0.674	16.328	330.155	0.000	0.015	0.372	90
4	-	330.155	330.813	0.673	16.303	330.157	0.002	0.017	0.421	90
5	-	330.157	330.157	0.675	16.303	330.158	0.001	0.018	0.446	90

[1]Weight of dry ZEOcat Z700

[2]Weight of full reactor before adsorption

[3]Weight of full reactor after adsorption

[4]Weight of adsorbed adsorbate =
 After Adsorption - Before Adsorption

[5]Adsorption capacity = (Mass adsorbed/Mass of Z700) ×100)

[6]Weight of full reactor after regeneration

[7]Weight of adsorbate remaining on the ZEOcat Z700 after regeneration =
After Regeneration - Before Adsorption

[8]Weight of reactor after this regeneration test - weight of reactor before any adsorption

[9]Total heel (%) = (Total heel/mass of ZEOcat Z700) ×100

Table A-2. Mass balance for 5-cycle adsorption/desorption test of TMB on ZEOcat F603

| Cycle | ZEOcat F603[1] (g) | Mass balance | | | | | | | | | Adsorption Time (min) |
		Before Adsorption[2] (g)	After Adsorption[3] (g)	Adsorbed Adsorbate[4] (g)	Adsorption Capacity[5] (%)	After Regeneration[6] (g)	Heel[7] (g)	Total Heel[8] (g)	Total Heel[9] (%)	
1	4.022	336.827	337.827	0.409	10.169	336.831	0.004	0.004	0.099	90
2	-	336.831	337.234	0.403	10.020	336.832	0.001	0.005	0.124	90
3	-	336.832	337.234	0.402	9.995	336.838	0.006	0.011	0.273	90
4	-	336.838	337.243	0.405	10.070	336.843	0.003	0.016	0.398	90
5	-	336.843	337.243	0.400	9.945	336.846	0.001	0.019	0.472	90

[1]Weight of dry ZEOcat F603

[2]Weight of full reactor before adsorption

[3]Weight of full reactor after adsorption

[4]Weight of adsorbed adsorbate=
 After Adsorption - Before Adsorption

[5]Adsorption capacity = (Mass adsorbed/Mass of ZEOcat F603) ×100

[6]Weight of full reactor after regeneration

[7]Weight of adsorbate remaining on the ZEOcat F603 after regeneration=
(After Regeneration- Before Adsorption)

[8]Weight of reactor after this regeneration test - weight of reactor before any adsorption

[9]Total heel (%) = (Total heel/mass of ZEOcat F603) ×100

Table A-3. Mass balance for 5-cycle adsorption/desorption test of TMB on ZEOcat Z400

| Cycle | BAC[1] (g) | Mass balance | | | | | | | | Adsorption Time (min) |
		Before Adsorption[2] (g)	After Adsorption[3] (g)	Adsorbed Adsorbate[4] (g)	Adsorption Capacity[5] (%)	After Regeneration[6] (g)	Heel[7] (g)	Total Heel[8] (g)	Total Heel[9] (%)	
1	4.956	330.450	330.556	0.106	2.14	330.455	0.005	0.005	0.101	40
2	-	330.455	330.524	0.069	1.39	330.461	0.006	0.011	0.222	40
3	-	330.461	330.524	0.063	1.27	330.466	0.005	0.016	0.323	40
4	-	330.466	330.527	0.061	1.23	330.467	0.001	0.017	0.343	40
5	-	330.467	330.519	0.052	1.05	330.467	0.000	0.017	0.343	40

[1]Weight of dry ZEOcat Z400

[2]Weight of full reactor before adsorption

[3]Weight of full reactor after adsorption

[4]Weight of adsorbed adsorbate=
 After Adsorption - Before Adsorption

[5]Adsorption capacity = (Mass adsorbed/Mass of ZEOcat Z400) ×100

[6]Weight of full reactor after regeneration

[7]Weight of adsorbate remaining on the ZEOcat Z400 after regeneration=
(After Regeneration- Before Adsorption)

[8]Weight of reactor after this regeneration test - weight of reactor before any adsorption

[9]Total heel (%) = (Total heel/mass of ZEOcat Z400) ×100

Adsorption of OAC-SST

Table A-6. Mass balance for 5-cycle adsorption/desorption test of OAC-SST on BAC

Cycle	BAC[1] (g)	Before Adsorption[2] (g)	After Adsorption[3] (g)	Adsorbed Adsorbate[4] (g)	Adsorption Capacity[5] (%)	After Regeneration[6] (g)	Heel[7] (g)	Total Heel[8] (g)	Total Heel[9] (%)	Adsorption Time (min)
				Mass balance						
1	4.02	330.241	332.660	1.684	41,9	331.016	0.040	0.040	1.0	150
2	-	332.660	332.690	1.680	41.8	331.030	0.014	0.054	1.3	150
3	-	332.690	332.654	1.676	41.7	331.032	0.002	0.056	1.4	150
4	-	332.654	332.677	1.660	41.3	331.037	0.005	0.061	1.5	150
5	-	332.677	332.677	1.652	41.1	331.039	0.002	0.063	1.6	150

[1]Weight of dry BAC

[2]Weight of full reactor before adsorption

[3]Weight of full reactor after adsorption

[4]Weight of adsorbed adsorbate=

 After Adsorption - Before Adsorption

[5]Adsorption capacity = (Mass adsorbed/Mass of BAC) ×100

[6]Weight of full reactor after regeneration

[7]Weight of adsorbate remaining on the BAC after regeneration=

(After Regeneration- Before Adsorption)

[8]Weight of reactor after this regeneration test - weight of reactor before any adsorption

[9]Total heel (%) = (Total heel/mass of BAC) ×100

Table A-7. Mass balance for 5-cycle adsorption/desorption test of OAC-SST on Optipore V503

Cycle	V503[1] (g)	Mass balance								Adsorption Time (min)
		Before Adsorption[2] (g)	After Adsorption[3] (g)	Adsorbed Adsorbate[4] (g)	Adsorption Capacity[5] (%)	After Regeneration[6] (g)	Heel[7] (g)	Total Heel[8] (g)	Total Heel[9] (%)	
1	4.026	335.133	336.939	1.806	44.86	335.134	0.001	0.025	0.025	150
2	-	335.134	336.874	1.740	43.23	335.139	0.006	0.149	0.149	150
3	-	335.139	336.868	1.729	42.95	335.160	0.027	0.671	0.671	150
4	-	335.160	336.879	1.719	42.69	335.160	0.003	0.745	0.745	150
5	-	335.163	336.872	1.709	42.45	335.167	0.004	0.845	0.845	150

[1]Weight of dry Optipore V503

[2]Weight of full reactor before adsorption

[3]Weight of full reactor after adsorption

[4]Weight of adsorbed adsorbate =
 After Adsorption- Before Adsorption

[5] Adsorption capacity = (Mass adsorbed/Mass of Optipore V503) *100

[6]Weight of full reactor after regeneration

[7]Weight of adsorbate remaining on Optipore V503 after regeneration =
After Regeneration - Before Adsorption

[8]Weight of reactor after this regeneration test - weight of reactor before any adsorption

[9]Total heel (%) = (Total heel/mass of Optipore V503) ×100

Table A-8. Mass balance for 5-cycle adsorption/desorption test of OAC-SST on ZEOcat Z700

| Cycle | Mass balance | | | | | | | | | Adsorption Time (min) |
	ZEOcat Z700[1] (g)	Before Adsorption[2] (g)	After Adsorption[3] (g)	Adsorbed Adsorbate[4] (g)	Adsorption Capacity[5] (%)	After Regeneration[6] (g)	Heel[7] (g)	Total Heel[8] (g)	Total Heel[9] (%)	
1	4.063	331.103	331.757	0.654	16.096	331.144	0.041	0.041	1.009	90
2	-	331.144	331.764	0.620	15.260	331.165	0.062	0.021	1.529	90
3	-	331.165	331.770	0.605	14.890	331.184	0.019	0.019	1.994	90
4	-	331.184	331.773	0.589	14.497	331.197	0.013	0.013	2.314	90
5	-	331.197	331.774	0.577	14.201	331.198	0.001	0.095	2.338	90

[1] Weight of dry ZEOcat Z700

[2] Weight of full reactor before adsorption

[3] Weight of full reactor after adsorption

[4] Weight of adsorbed adsorbate = After Adsorption - Before Adsorption

[5] Adsorption capacity = (Mass adsorbed/Mass of Z700) ×100)

[6] Weight of full reactor after regeneration

[7] Weight of adsorbate remaining on the ZEOcat Z700 after regeneration = After Regeneration - Before Adsorption

[8] Weight of reactor after this regeneration test - weight of reactor before any adsorption

[9] Total heel (%) = (Total heel/mass of ZEOcat Z700) ×100

Table A-9. Mass balance for 5-cycle adsorption/desorption test of OAC-SST on ZEOcat F603

| Cycle | ZEOcat F603[1] (g) | Mass balance | | | | | | | | Adsorption Time (min) |
		Before Adsorption[2] (g)	After Adsorption[3] (g)	Adsorbed Adsorbate[4] (g)	Adsorption Capacity[5] (%)	After Regeneration[6] (g)	Heel[7] (g)	Total Heel[8] (g)	Total Heel[9] (%)	
1	4.003	329.673	330.261	0.588	14.69	329.700	0.027	0.027	0.674	70
2		329.700	330.260	0.560	13.99	329.705	0.005	0.032	0.799	70
3		329.705	330.227	0.522	13.04	329.721	0.016	0.048	1.199	70
4		329.721	330.205	0.484	12.09	329.729	0.008	0.056	1.399	70
5		329.729	330.192	0.463	11.57	3297.30	0.001	0.057	1.424	70

[1]Weight of dry ZEOcat F603

[2]Weight of full reactor before adsorption

[3]Weight of full reactor after adsorption

[4]Weight of adsorbed adsorbate =
 After Adsorption - Before Adsorption

[5]Adsorption capacity = (Mass adsorbed/Mass of ZEOcat F603) ×100

[6]Weight of full reactor after regeneration

[7]Weight of adsorbate remaining on the ZEOcat F603 after regeneration=
(After Regeneration- Before Adsorption)

[8]Weight of reactor after this regeneration test - weight of reactor before any adsorption

[9]Total heel (%) = (Total heel/mass of ZEOcat F603) ×100

Table A-10. Mass balance for 5-cycle adsorption/desorption test of OAC-SST on ZEOcat Z400

| Cycle | Mass balance | | | | | | | | | Adsorption Time (min) |
	ZEOcat Z400[1] (g)	Before Adsorption[2] (g)	After Adsorption[3] (g)	Adsorbed Adsorbate[4] (g)	Adsorption Capacity[5] (%)	After Regeneration[6] (g)	Heel[7] (g)	Total Heel[8] (g)	Total Heel[9] (%)	
1	4.99	336.348	336.897	0.549	10.484	336.391	0.043	0.043	0.86	80
2	-	336.391	336.857	0.466	9.323	336.422	0.031	0.074	1.48	80
3	-	336.422	336.815	0.393	7.863	336.429	0.007	0.081	1.62	80
4	-	336.429	336.827	0.398	7.963	336.433	0.004	0.085	1.70	80
5	-	336.433	336.807	0.374	7.483	336.438	0.005	0.090	1.80	80

[1]Weight of dry ZEOcat Z400
[2]Weight of full reactor before adsorption
[3]Weight of full reactor after adsorption
[4]Weight of adsorbed adsorbate=
 After Adsorption - Before Adsorption

[5]Adsorption capacity = (Mass adsorbed/Mass of ZEOcat Z400) ×100
[6]Weight of full reactor after regeneration
[7]Weight of adsorbate remaining on the ZEOcat Z400 after regeneration=
(After Regeneration- Before Adsorption)
[8]Weight of reactor after this regeneration test - weight of reactor before any adsorption
[9]Total heel (%) = (Total heel/mass of ZEOcat Z400) ×100

APPENDIX B

Mass balance for one cycle adsorption of TMB and 2-butoxyethanol in dry and humid condition

ZEOcat F603

Table B-4. Adsorption capacity from breakthrough curve curve and mass balance for adsorption of 500 ppm$_v$ TMB on ZEOcat F603 at dry, 45% and 75% relative humidity (RH) conditions

Condition	Total amount adsorbed, from mass balance	TMB adsorbed, from breakthrough curve		Water adsorbed, by difference	
	g	g	%	g	%
TMB at 0% RH	0.40	0.40	9.87	0	0
TMB at 45% RH	0.51	0.36	8.98	0.15	3.82
TMB at 75% RH	0.56	0.22	5.62	0.33	8.25

Table B- 2. Mass balance for adsorption of 500 ppm$_v$ **TMB** on ZEOcat F603 at **dry, 45% RH** and **75% RH** conditions

Test	Mass balance (g)					Ads. Time (min)
	ZEOcat F603[1]	B. Ad.[2]	A. Ad.[3]	Ads.[4]	Ads. %[5]	
TMB at 0% RH	4.09	337.18	337.53	0.40	9.80	50
TMB at 45% RH	3.99	337.14	337.65	0.51	12.80	50
TMB at 75% RH	4.00	336.81	337.37	0.56	13.87	50

Adsorption flow: Air, 10 SLPM
[1]Weight of dry ZEOcat F603
[2]Weight of full reactor before adsorption
[3]Weight of full reactor after adsorption
[4]Weight of adsorbed adsorbate = (A.Ad.- B.Ad.)
[5] Adsorbed percentage = (Ads./Weight of dry ZEOcat F603)×100

Table B-3. Adsorption capacity from Breakthrough curve curve and mass balance for adsorption of 500 ppm$_v$ 2-butoxyethanol on ZEOcat F603 at dry, 45% RH and 75% RH conditions

Condition	Total amount adsorbed, from mass balance	TMB adsorbed, from breakthrough curve		Water adsorbed, by difference	
	g	g	%	g	%
2-butoxyethanol at 0% RH	0.77	0.81	19.97	0	0
2-butoxyethanol at 45% RH	0.80	0.66	16.72	0.14	3.64
2-butoxyethanol at 75% RH	0.76	0.60	15.07	0.16	4.05

Table B- 4. Mass balance for adsorption of 500 ppm$_v$ 2-butoxyethanol on ZEOcat F603 at 45% RH and 0% RH

Test	Mass balance (g)					Ads. Time (min)
	ZEOcat F603[1]	B. Ad.[2]	A. Ad.[3]	Ads.[4]	Ads. %[5]	
2-butoxyethanol at 0% RH	4.05	337.30	338.07	0.77	19.02	50
2-butoxyethanol at 45% RH	3.92	336.96	337.76	0.80	20.36	50
2-butoxyethanol at 75% RH	3.96	335.54	336.29	0.76	19.13	50

Adsorption flow: Air, 10 SLPM
[1]Weight of dry ZEOcat F603
[2]Weight of full reactor before adsorption
[3]Weight of full reactor after adsorption
[4]Weight of adsorbed adsorbate = (A.Ad.- B.Ad.)
[5] Adsorbed percentage = (Ads./Weight of dry ZEOcat F603)×100

ZEOcat Z700

Table B-5. Adsorption capacity from Breakthrough curve curve and mass balance for adsorption of 500 ppm$_v$ TMB on ZEOcat Z700 at dry, 45% RH and 75% RH conditions

Condition	Total amount adsorbed, from mass balance	TMB adsorbed, from breakthrough curve		Water adsorbed, by difference	
	g	g	%	g	%
TMB at 0% RH	0.65	0.64	15.91	0	0
TMB at 45% RH	0.73	0.62	15.45	0.12	2.88
TMB at 75% RH	0.77	0.55	10.29	0.22	5.49

Table B- 6. Mass balance for adsorption of 500 ppm$_v$ 2-butoxyethanol on ZEOcat Z700 at 45% RH and 0% RH

Test	Mass balance (g)					Ads. Time (min)
	ZEOcat F603[1]	B. Ad.[2]	A. Ad.[3]	Ads.[4]	Ads. %[5]	
TMB at 0% RH	4.05	330.15	330.80	0.65	16.19	50
TMB at 45% RH	4.00	330.03	330.76	0.73	18.33	50
TMB at 75% RH	4.04	330.22	330.99	0.77	19.01	50

Adsorption flow: Air, 10 SLPM
[1]Weight of dry ZEOcat Z700
[2]Weight of full reactor before adsorption
[3]Weight of full reactor after adsorption
[4]Weight of adsorbed adsorbate = (A.Ad.- B.Ad.)
[5] Adsorbed percentage = (Ads./Weight of dry ZEOcat Z700)×100

Table B-7. Adsorption capacity from Breakthrough curve and mass balance for adsorption of 500 ppm$_v$ 2-butoxyethanol on ZEOcat Z700 at dry, 45% RH and 75% RH conditions

Condition	Total amount adsorbed, from mass balance	2-butoxyethanol adsorbed, from breakthrough curve		Water adsorbed, by difference	
	g	g	%	g	%
2-butoxyethanol at 0% RH	0.94	0.96	23.74	0	0
2-butoxyethanol at 45% RH	0.91	0.81	20.31	0.10	2.44
2-butoxyethanol at 75% RH	0.95	0.76	18.84	0.20	4.90

Table 8. Mass balance for adsorption of 500 ppm$_v$ 2-butoxyethanol on ZEOcat Z700 at 45% RH and 0% RH

Test	Mass balance (g)					Ads. Time (min)
	ZEOcat Z700[1]	B. Ad.[2]	A. Ad.[3]	Ads.[4]	Ads. %[6]	
2-butoxyethanol at 0% RH	4.04	330.59	331.52	0.94	23.13	50
2-butoxyethanol at 45% RH	4.01	329.99	330.99	0.91	22.75	50
2-butoxyethanol at 75% RH	4.04	330.59	331.52	0.94	23.13	50

Adsorption flow: Air, 10 SLPM
[1]Weight of dry ZEOcat Z700
[2]Weight of full reactor before adsorption
[3]Weight of full reactor after adsorption
[4]Weight of adsorbed adsorbate = (A.Ad.- B.Ad.)
[5] Adsorbed percentage = (Ads./Weight of dry ZEOcat Z700)×100

Preconditioned ZEOcat F603

Table B-9. Adsorption capacity from Breakthrough curve and mass balance for adsorption of 500 ppm$_v$ TMB on ZEOcat F603 at 45% RH and 75% RH with and without preconditioned with water vapor.

Condition	Total amount adsorbed, from mass balance	TMB adsorbed, from breakthrough curve		Water adsorbed, by difference	
	g	g	%	g	%
TMB at 45% RH	0.51	0.36	8.98	0.15	3.82
TMB at 45% RH, 45% preconditioned	0.44	0.24	6.16	0.23	5.31
TMB at 75% RH	0.56	0.22	5.62	0.33	8.25
TMB at 75% RH on 75% RH preconditioned	0.56	0.17	4.31	0.38	9.47

Table B- 10. Mass balance for adsorption of 500 ppm$_v$ TMB on ZEOcat F603 at 45% RH and 75% RH with and without preconditioned with water vapor.

Test	Mass balance (g)					Ads. Time (min)
	ZEOcat F603[1]	B. Ad.[2]	A. Ad.[3]	Ads.[4]	Ads. %[6]	
TMB at 45% RH	3.99	337.14	337.65	0.51	12.80	50
TMB at 45% RH, 45% preconditioned	3.94	336.55	337.00	0.44	11.22	55
TMB at 75% RH	4.00	336.81	337.37	0.56	13.87	50
TMB at 75% RH on 75% RH preconditioned	4.04	336.21	336.76	0.56	13.77	50

Adsorption flow: Air, 10 SLPM
[1]Weight of dry ZEOcat F603
[2]Weight of full reactor before adsorption
[3]Weight of full reactor after adsorption
[4]Weight of adsorbed adsorbate = (A.Ad.- B.Ad.)
[5] Adsorbed percentage = (Ads./Weight of dry ZEOcat F603)×100

Preconditioned ZEOcat Z700

Table B-11. Adsorption capacity from Breakthrough curve and mass balance for adsorption of 500 ppm$_v$ TMB on ZEOcat Z700 at 45% RH and 75% RH with and without preconditioned with water vapor.

Condition	Total amount adsorbed, from mass balance	TMB adsorbed, from breakthrough curve		Water adsorbed, by difference	
	g	g	%	g	%
TMB at 45% RH	0.73	0.62	15.45	0.12	2.88
TMB at 45% RH, 45% preconditioned	0.72	0.63	15.76	0.08	2.69
TMB at 75% RH	0.77	0.55	10.29	0.22	5.49
TMB at 75% RH on 75% RH preconditioned	0.77	0.46	11.37	0.31	7.69

Table B- 12. Mass balance for adsorption of 500 ppm$_v$ TMB on ZEOcat Z700 at 45% RH and 75% RH with and without preconditioned with water vapor

Test	Mass balance (g)					Ads. Time (min)
	ZEOcat F603[1]	B. Ad.[2]	A. Ad.[3]	Ads.[4]	Ads. %[6]	
TMB at 45% RH	4.00	330.03	330.76	0.73	18.33	50
TMB at 45% RH, 45% preconditioned	4.03	331.01	331.73	0.72	17.85	50
TMB at 75% RH	4.04	330.22	330.99	0.77	19.01	50
TMB at 75% RH on 75% RH preconditioned	4.02	330.42	331.19	0.77	19.06	50

Adsorption flow: Air, 10 SLPM

[1]Weight of dry ZEOcat Z700

[2]Weight of full reactor before adsorption

[3]Weight of full reactor after adsorption

[4]Weight of adsorbed adsorbate = (A.Ad.- B.Ad.)

[5] Adsorbed percentage = (Ads./Weight of dry ZEOcat Z700)×100

APPENDIX C

Breakthrough curve fitting using the Wheeler-Jonas equation
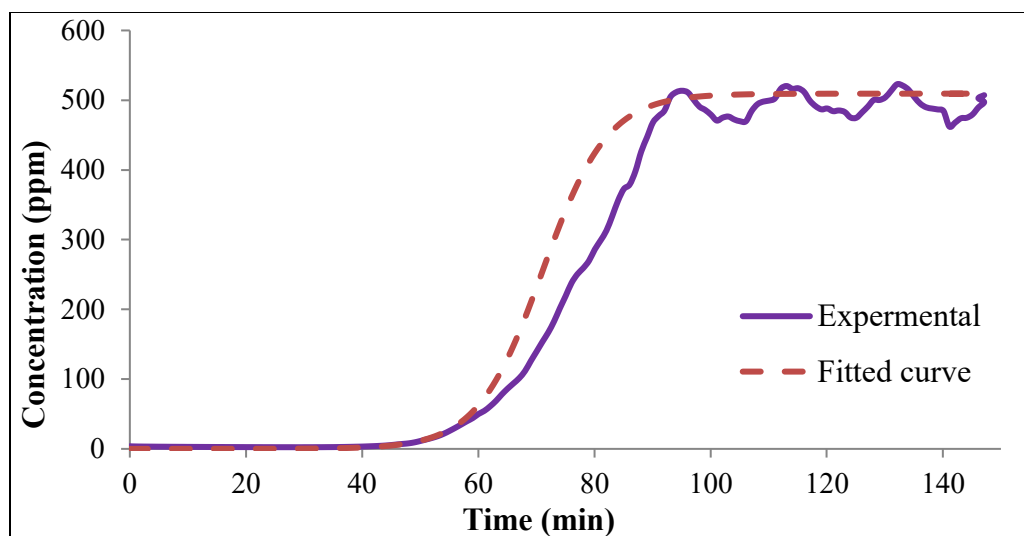
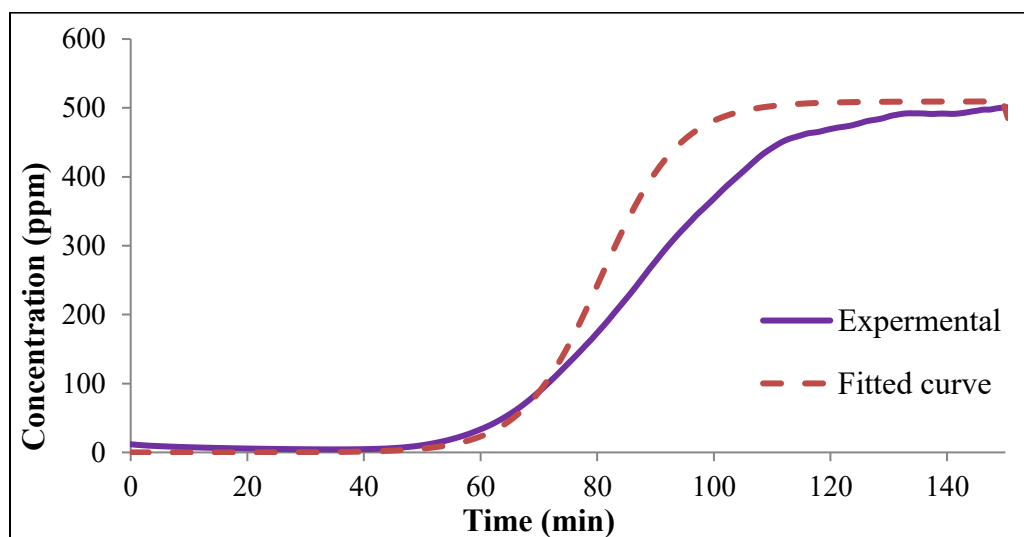Figure C-1. Breakthrough curve of TMB on BAC

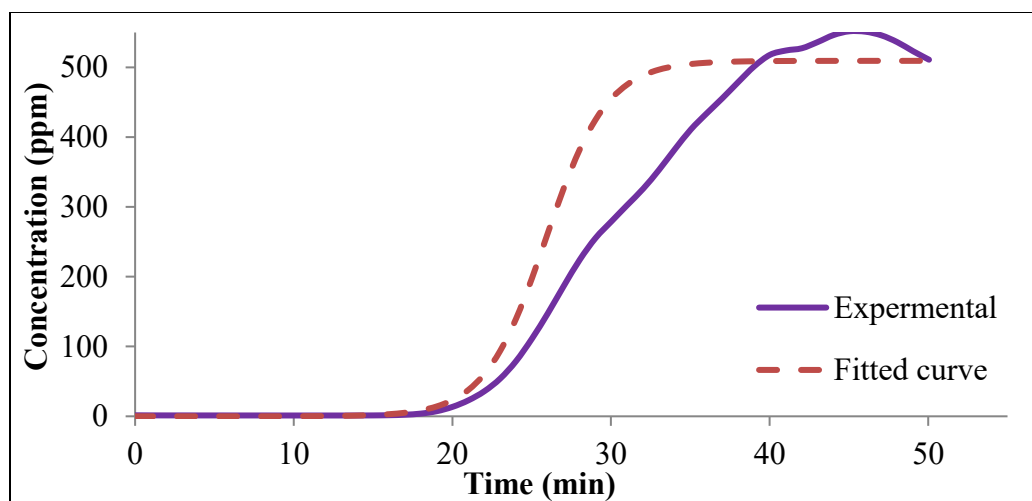Figure C-2. Breakthrough curve of TMB on Optipore V503
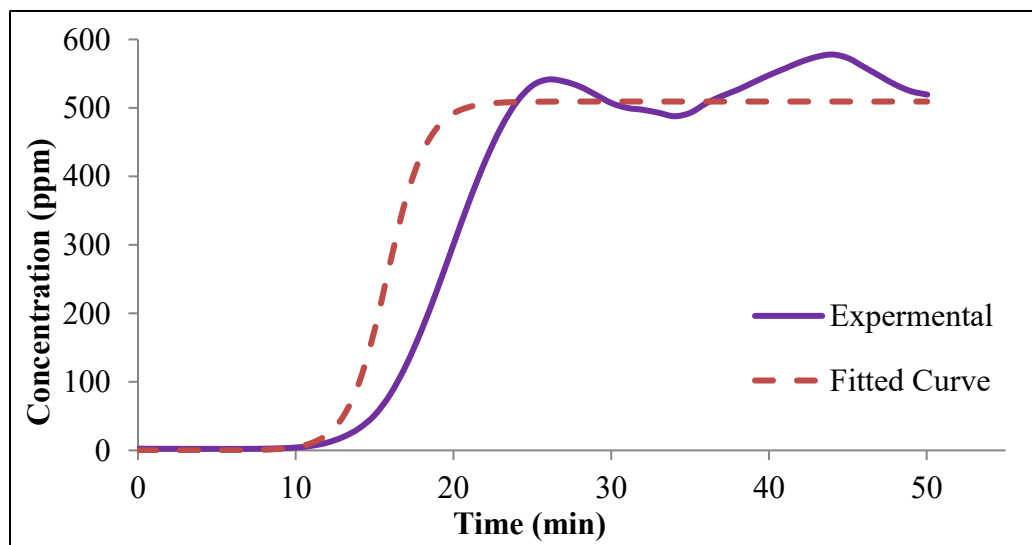
Figure C-3. Breakthrough curve of TMB on Z700

Figure C-4. Breakthrough curve of TMB on ZEOcat F603